


November 2015

## Utilizing in Silico and/or Native ESI Approaches to Provide New Insights on Haptoglobin/Globin and Haptoglobin/Receptor Interactions

Ololade Fatunmbi  
*University of Massachusetts - Amherst*

Follow this and additional works at: [https://scholarworks.umass.edu/dissertations\\_2](https://scholarworks.umass.edu/dissertations_2)

 Part of the [Analytical Chemistry Commons](#), [Biochemistry, Biophysics, and Structural Biology Commons](#), [Bioinformatics Commons](#), and the [Computational Biology Commons](#)

---

### Recommended Citation

Fatunmbi, Ololade, "Utilizing in Silico and/or Native ESI Approaches to Provide New Insights on Haptoglobin/Globin and Haptoglobin/Receptor Interactions" (2015). *Doctoral Dissertations*. 532.  
[https://scholarworks.umass.edu/dissertations\\_2/532](https://scholarworks.umass.edu/dissertations_2/532)

This Open Access Dissertation is brought to you for free and open access by the Dissertations and Theses at ScholarWorks@UMass Amherst. It has been accepted for inclusion in Doctoral Dissertations by an authorized administrator of ScholarWorks@UMass Amherst. For more information, please contact [scholarworks@library.umass.edu](mailto:scholarworks@library.umass.edu).

**UTILIZING IN SILICO AND/OR NATIVE ESI APPROACHES TO PROVIDE NEW  
INSIGHTS ON HAPTOGLOBIN/GLOBIN AND  
HAPTOGLOBIN/RECEPTOR INTERACTIONS**

A Dissertation Presented

by

OLOLADE FATUNMBI

Submitted to the Graduate School of the  
University of Massachusetts Amherst in partial fulfillment  
of the requirements of the degree of

DOCTOR OF PHILOSOPHY

September 2015

Chemistry

© Copyright by Ololade Fatunmbi 2015  
All Right Reserved

**UTILIZING IN SILICO AND/OR NATIVE ESI APPROACHES TO PROVIDE NEW  
INSIGHTS ON HAPTOGLOBIN/GLOBIN AND  
HAPTOGLOBIN/RECEPTOR INTERACTIONS**

A Dissertation Presented

by

OLOLADE FATUNMBI

Approved as to style and content by:

---

Igor A. Kaltashov, Chair

---

Anne Gershenson, Co-Chair

---

Scott Auerbach, Member

---

Richard W. Vachet, Member

---

Craig Martin Department Head  
Department of Chemistry

## DEDICATION

To my loving and supportive family: My father, Dr. Hafeez Fatunmbi, my mother, Mrs.

Kemi Fatunmbi, my older brother, Mr. Bukola Fatunmbi, and my younger sister,

Miss Bisola Fatunmbi

To my friend, Miss Safaa Mohammed and my Godson, Mr. Daniel Simmons.

To my friend, Mr. Robert Lee Sanders III, may his soul rest in peace

## ACKNOWLEDGEMENTS

I am so blessed that my quest for a doctoral degree in chemistry at the University of Massachusetts Amherst was not a solitary journey. God has certainly blessed me with the greatest team of advisors, mentors, supporters, collaborators, and friends. My advisors, Prof. Igor Kaltashov and Prof. Anne Gershenson were simply phenomenal. Prof. Kaltashov's confidence in me was and still is a tremendous compliment. He has driven me to lead new areas of research and design novel methodologies beyond my imagination. My introduction into combining bioinformatics and mass spectrometry methods in research probably would not have been possible without him. The encouragement and the freedom he gave me with my research made my doctoral process enthralling and worthwhile. Prof. Gershenson has been such an outstanding mentor and supporter. I have to acknowledge her for her valuable literary discussions, software tutorials, and continuous edits on my work. I appreciate her patience with me so much because I really used to make some embarrassing mistakes, but she has always made me feel like I am capable and I belong here in this scientific realm. This alone was vital for my confidence as a young scientist. My committee members, Prof. Scott Auerbach and Prof. Richard Vachet also played an instrumental role to my success, even at my early stages. I appreciate Prof. Auerbach for reciting lectures about "particle in a box" for me in my first year, and allowing me to collaborate with him in my final year. Prof. Vachet has consistently been there for me in the forefront and behind the scenes to edit my work and encourage me. Thank you.

My labmates Gunabo, Shunhai, Burcu, Son, Muneer, Hanwei, Yunglong, Sheng-Sheng, Jake, Chengfeng, Honglin, and postdoctoral fellow Grégoire have been wonderful people to have around me. In my early stages, my then postdoctoral mentors (which now have advance titles), Drs. Abzalimov and Bobst, have been generous in

helping me design experiments and learn different instruments. I would like to thank Qinfang Sun for our collaborations and Angela Miguez for her thoughtful discussions.

I thank God for my family. My father is my hero, the most charming, hardworking, intelligent scientist I have ever known. Ever since I could remember, I wanted to be just like him. I have a forever-praying-over-loving-investigative mother that will always listen to my fears and uncertainties. I simply do not know where I would be without her prayers. My brother, Bukola, has helped me so much. He taught me linux commands, assisted me with classes, provided me with the software I needed, and fixed so many items for me. My sister has been there to listen to my concerns and celebrate victories..

Two women that started my graduate journey with me have been so critical to my success, Dr. Joelle Labistide and (soon to be doctor) Anesia Auguste. I really don't know what I could have done without either of you two! Thank you both for every paper of mine you ever edited, every presentation you ever listened to, every word of encouragement you have ever gave me, and every tear you turned into laughter. Joelle, I have grown so much through our conversations about women issues to light scattering. I appreciate you letting your mother help me. I am overjoyed to have you both in my lives as sisters and I pray we continue to grow spiritually, academically, and professionally.

During my tenure at Amherst, I met a plethora of friends that have become so important to me. I was blessed to meet the some of the most wonderful sorority members from Rho Kappa and Xi Xi Omega: Tynesia, Jasmine, Eden, Brianna, Sonia, Debra, Ms. Tracey, and Ashley. I have to give a special thank you to my best friend, Tynesia. She has continuously been there for me in so many ways I can honestly write a 5-page acknowledgement section on her alone. She is always there when I call and always on time. I also met some really great people from my fraternity, Richard, Sam, Tony, Cameron, Obi, Jason, Mo, Lino, Sy, and Otis. In addition, I am thankful for my wonderful friends and mentees I have met or has been there for me through these years

of graduate school Safaa, Jamal, Chinomso, Shaynah, Regan, Iman, Rose, Vernaldi, Melissa, Luc, Idriys, Tammy, Kyle, Chris, Camille, Francis, Prince, Marwan, Sade, Nair, Helen, Monique, Anita, Akin, Kunle, Dan, Angele, Dina, Ms. Hannah, Orf, and Chibueze.

Thank you to my line sister, soon-to-be doctor, and best friend, Lenora Codrington. We are finally accomplishing the things we always said we would do!!! We have gone through so much together and I thank God for placing us in each other's lives. Thank you, line sisters, for our hilarious group chats Ashley, Nicole, and Lenora. Thank you, Chrisonne and Tasha, I love you both and my nephews so much. Chrisonne, your spiritual e-mails were everything. Thank you to my neo babies Chalwe, Evanna, Monique, and Jasmine for keeping me sane. I have to also give a special thank you to Soror Alisa Drayton for her consistent support and love. I also thank my friend Jonathan for being there for me through this past year because I could not have made it through this process with out your love, support, and prayers. Miss Kasey, my lovely mentee, I am coming for your defense lady, so keep on pushing! Our late night conversations and too comfortable moments will be missed. Miss Sarah, you keep on pushing too.

I end my acknowledgements with plenty more people to thank. Thank you, Dr. John Chikwem, Dr. Derrick Swinton, Dr. Takeyce Whittingham, Dr. Robert Langley, Dr. Carl Walton, and Dr. Amar Tung for being my amazing professors and mentors at Lincoln University. Thank you, Prof. Julian Tyson and Prof. Paul Lahti, for giving me the opportunity to conduct research in your labs at UMass during the summers of 2007 and 2010, respectively. Thank you, Ms. Patricia Lehouillier, Ms. Carolyn Gardner, Dr. Heyda Martinez and all the other wonderful people that helped me within NEAGEP. Thank you Prof. Nathaniel Whitaker for your advice and help through these years. Thank you, Dr. Takiya Ahmed for your role in preparing me as a young scientist.

Last but not least, thank you, Prof. Sandra Peterson. I never met anyone in the world can remind me of my mom until I met Ms. Sandy. Thank you.



## ABSTRACT

UTILIZING IN SILICO AND/OR NATIVE ESI APPROACHES TO PROVIDE NEW  
INSIGHTS ON HAPTOGLOBIN/GLOBIN AND  
HAPTOGLOBIN/RECEPTOR INTERACTIONS

SEPTEMBER 2015

OLOLADE FATUNMBI, B.S., LINCOLN UNIVERSITY

PH.D., UNIVERSITY OF MASSACHUSETTS AMHERST

Directed by: Professor Igor A. Kaltashov

Haptoglobin (Hp), an acute phase protein, binds free hemoglobin (Hb) dimers in one of the strongest non-covalent interactions known in biology. This interaction protects Hb from causing potentially severe oxidative damage and limiting nitric oxide bioavailability. Once Hb/Hp complexes are formed, they proceed to bind CD163, a cell surface receptor on macrophages leading to complex internalization and catabolism. Myoglobin, (Mb) a monomeric protein, that is normally found in the muscle but can be released into the blood in high concentrations during myocardial injury, is homologous to Hb and shares many conserved Hb/Hp interface residues. Both monomeric Hb and Mb species present potential risks, yet their interactions with Hp have not been extensively studied or are a matter of controversy, respectively. To predict possible interactions of monomeric globins with Hp, we employed a variety of cost and time effective molecular modeling approaches. Native electrospray ionization mass spectrometry (ESI MS) experiments confirm the modeling results and show that monomeric Hb and Mb bind Hp with a stoichiometry of two globin monomers per Hp tetramer.

The ESI MS results also demonstrate the success of our computational approaches to Mb/Hp interactions, motivating us to model Hb/Hp/CD163 complexes. Both CD163 bound  $\text{Ca}^{2+}$  and specific CD163 acidic residues are known to be essential for binding specific Hp basic residues resulting in Hb/Hp/CD163 complex formation, but

the structural details of Hb/Hp/CD163 interactions are unknown. We therefore constructed experimentally driven molecular models of Hb/Hp/CD163 complexes using molecular docking. In order to understand the role of  $\text{Ca}^{2+}$  in Hp/CD163 interactions and dynamics, all-atom molecular dynamics (MD) simulations were conducted for CD163 models in the presence and absence of  $\text{Ca}^{2+}$ . The molecular models of Hb/Hp/CD163 suggest that Hp basic residues R252 and K262 each interact with a conserved acidic triad (E27, E28, D94) in CD163 domains 2 and 3. A calcium ion is postulated to stabilize this CD163 acidic cluster facilitating Hp recognition. Consistent with this, MD simulations on isolated CD163 domains suggest that  $\text{Ca}^{2+}$  bound at a specific site in CD163 preserves the arrangement of the acidic triad and protein structural stability. Our studies demonstrate how molecular modeling and molecular dynamics aided/correlated with mass spectrometry experiments can elucidate the structural basis and dynamics of interactions between Hp, globins and/or CD163. This approach may be useful for designing therapeutics that utilizes the Hb/Hp/CD263 endocytosis pathway and unraveling novel avenues for possible Hp-therapy administration for diseases or complications arising from Mb toxicity.

## TABLE OF CONTENTS

|   | Page |
|---|------|
| ACKNOWLEDGEMENTS.....   | v    |
| ABSTRACT.....   | viii |
| LIST OF TABLES.....   | xii  |
| LIST OF FIGURES.....  | xiii |
| LIST OF ABBREVIATIONS.....  | xv   |
| CHAPTER   |      |
| 1. INTRODUCTION.....  | 1    |
| 1.1. Haptoglobin.....   | 1    |
| 1.1.1. Function.....  | 1    |
| 1.1.2. Other Functions.....   | 4    |
| 1.1.3. Structural Features.....   | 5    |
| 1.1.4. Haptoglobin and its potential as a drug carrier and<br>therapeutic.....                                | 6    |
| 1.2. In silico methods to characterize protein structure, interactions and/or<br>dynamics.....                | 7    |
| 1.2.1. Homology modeling.....   | 7    |
| 1.2.2. Macromolecular docking.....  | 9    |
| 1.2.3. Molecular dynamics.....  | 10   |
| 1.3. Experimental methods to characterize protein structure, interactions.....                                | 11   |
| 1.3.1. Conventional Methods.....  | 11   |
| 1.3.2. Mass Spectrometry.....   | 13   |
| 1.4. Objectives.....  | 15   |
| 2. COMBINED COMPUTATIONAL MODELING AND MASS SPECTROMETRY<br>STUDY OF HP AND GLOBIN INTERACTIONS.....          | 16   |
| 2.1. Introduction.....  | 16   |
| 2.2. Materials and methods.....   | 19   |
| 2.2.1. Homology modeling and molecular docking.....   | 19   |
| 2.2.2. Structural Comparisons of Mb/Hp models with the Hb $\alpha$ and Hb $\beta$<br>binding sites on Hp..... | 20   |
| 2.2.3. Identification of critical Hb interface residues.....  | 20   |
| 2.2.4. Materials and HPLC separation of Hb chains.....  | 20   |

|   |    |
|---|----|
| 2.2.5. Mass Spectrometry.....   | 21 |
| 2.3. Results and Discussion.....  | 22 |
| 2.3.1. Construction and Evaluation of the Mb/Hp Model.....  | 22 |
| 2.3.2. Analysis of the Mb/Hp model interface.....   | 27 |
| 2.3.3. Further Identification of Residues Important for Binding.....  | 31 |
| 2.3.4. Native ESI MS of Hb/Hp and Hba/Hp Complexes.....   | 34 |
| 2.4. Conclusions.....   | 40 |
| 3. MOLECULAR MODELS OF THE HEMOGLOBIN-HAPTOGLOBIN COMPLEX<br>DOCKED TO CD163 DOMAIN 2 AND/OR DOMAIN 3 AND<br>CALCIUM-INDUCED DYNAMICS REVEALED BY<br>MOLECULAR DYNAMICS ..... | 41 |
| 3.1. Introduction .....   | 41 |
| 3.2. Materials and Methods.....   | 46 |
| 3.2.1. Homology Modeling of CD163 domain 2 and 3.....   | 46 |
| 3.2.2. Molecular Docking of Hb/Hp/CD163 .....   | 46 |
| 3.2.3. Molecular Dynamics .....   | 48 |
| 3.3. Results and Discussion .....   | 49 |
| 3.3.1. Homology Models of Domains 2 and 3 .....   | 49 |
| 3.3.2. Molecular Dynamics CD163 domain 2 and 3 .....  | 52 |
| 3.3.3. Molecular Docking of Hb/Hp complex to CD163 domain 2 or 3 or<br>both .....   | 58 |
| 3.3.4. Molecular Dynamics of Hp loop and CD163 .....  | 63 |
| 3.4. Conclusions.....   | 70 |
| 4. SUMMARIES AND FUTURE OUTLOOK.....  | 73 |
| BIBLIOGRAPHY.....   | 76 |

## LIST OF TABLES

| Table  | Page |
|--|------|
| 2.1. Comparisons of Hb/Hp and Mb/Hp molecular interactions.....  | 29   |
| 2.2. Comparisons of globin-globin hydrogen bond interactions in human Hb $\alpha$ / $\beta$ or Mb <sub>2</sub> dimers in complex with Hp.....                                | 30   |
| 3.1. Summary of interaction restraints used in protein-protein dockings and scores.....  | 47   |
| 3.2. Distance comparisons of the calcium-binding sites in the domains 2 and 3 molecular models to various X-ray crystallographic structures with calcium-binding sites ..... | 52   |
| 3.3. Comparisons of the distances between acidic and basic residues in calcium-dependent, electrostatic receptor-ligand interactions .....                                   | 72   |

## LIST OF FIGURES

| Figure  | Page |
|---|------|
| 1.1. Reactions associated with the generation of reactive oxygen specie .....   | 1    |
| 1.2. Schematic representation of Hb/Hp complex uptake by macrophages via CD163-mediated endocytosis.....  | 3    |
| 1.3. Structure of human haptoglobin .....   | 6    |
| 2.1. Sequence alignments of human Mb to the human and porcine Hb $\alpha$ or Hb $\beta$ subunits and structural super-positions of human Mb, Hb $\alpha$ , and Hb $\beta$ crystal structures..... | 23   |
| 2.2. Structure of porcine Hb/Hp complex superimposed on the human Mb/Hp models.....   | 24   |
| 2.3. Ramachandran plot prepared by “Procheck” for the Mb2/Hp homology model shown in Figure 2A.....   | 25   |
| 2.4. RMSD per residue in angstroms for structural alignments of Hb/Hp structures and Mb/Hp models as calculated by VMD .....  | 26   |
| 2.5. RMSD per residue in angstroms for structural alignments of Hb/Hp structures and Mb/Hp models as calculated by VMD .....  | 27   |
| 2.6. Schematic overview of porcine Hp/Hb interactions and the corresponding interactions in the human Mb/Hp homology models.....  | 28   |
| 2.7. Predicted effects of alanine substitutions on the binding energy of the Hb/Hb structures and Mb/Hp models by the DrugScorePPI Web server in kcal/mole.....                                   | 33   |
| 2.8. ESI-MS shows that monomeric globins bound to Hp .....  | 36   |
| 3.1. Schematic representation of CD163 .....  | 43   |
| 3.2 Molecular models of CD163 Domain 2 and 3.....   | 50   |
| 3.3. Ca <sup>2+</sup> binding to site 1 on domain 2 reduces fluctuations.....   | 54   |
| 3.4 Snapshots of the domain 2 structures during the MD simulations .....  | 55   |
| 3.5. Ca <sup>2+</sup> binding to site 1 in domain 3 reduces fluctuations .....  | 57   |
| 3.6. Experimentally driven molecular models of Hb/Hp in complex with A), holo-domain 2, or B, holo-domain 3.....  | 59   |
| 3.7. Experimentally driven molecular models of Hb/Hp in complex with CD163 both domain 2 and 3.....   | 61   |

|   |    |
|---|----|
| 3.8. Molecular models of Hb/Hp in complex with apo-domain 3.....  | 63 |
| 3.9. Results of the molecular dynamics simulations performed on Hp<br>loop/domain 3.....  | 66 |
| 3.10. Continued results of the molecular dynamics simulations performed on Hp<br>loop/holo-domain 3.....  | 67 |
| 3.11. Snap shots from molecular dynamics simulations performed on Hp<br>loop/holo-domain 3 and apo domain 3.....  | 68 |
| 3.12. Comparisons of Hp/domain 3 interface in the Hb/Hp/CD163 molecular<br>models to the interface of experimentally solved protein-protein structures<br>involved in calcium-dependent, electrostatic receptor-ligand interactions ..... | 71 |

## LIST OF ABBREVIATIONS

Acidic residue cluster- Aspartic acid 27, Aspartic Acid 28, Glutamic Acid 94; Apo-  $\text{Ca}^{2+}$  free or heme free; holo- bound to  $\text{Ca}^{2+}$  or heme.  $\alpha\beta$ , Hemoglobin alpha/beta Dimer; H, Haptoglobin Heavy Chain; Hp, Haptoglobin; Hb/Hp, Hemoglobin-Haptoglobin Complex; Hb, Hemoglobin; Hb $\alpha$ , Hemoglobin alpha Chain; Mb, Myoglobin; Mb<sub>2</sub>- Myoglobin Dimer; Mb( $\alpha$ -site)- Myoglobin bound to the Hb $\alpha$  binding site on Hp; Mb( $\beta$ -site)- Myoglobin bound to the Hb $\beta$  binding site on Hp; Mb/Hp, Myoglobin-Haptoglobin Complex; L, Haptoglobin Light Chain; Hb/Hp/CD163- Hemoglobin-Haptoglobin/CD163 complex;



**CHAPTER 1**  
**INTRODUCTION**

**1.1. Haptoglobin**

**1.1.1. Function**

During intravascular hemolysis, erythrocytes (red blood cells) rupture, releasing hemoglobin (Hb) into the extracellular environment. Circulating Hb is potentially toxic because it can cause severe oxidative tissue damage and renal failure. Hb toxicity arises from its tetrameric structure dissociating into dimers (Hb $\alpha_1\beta_1$ ) in the extracellular environment, exposing residues that are prone to oxidative modification<sup>1</sup>. In addition, iron, which is present on the heme prosthetic group on Hb can react with hydrogen peroxide to generate reactive oxygen species (ROS) through Fenton and Haber-Weiss iron catalyzed reactions<sup>2</sup> (Figure 1.1.).

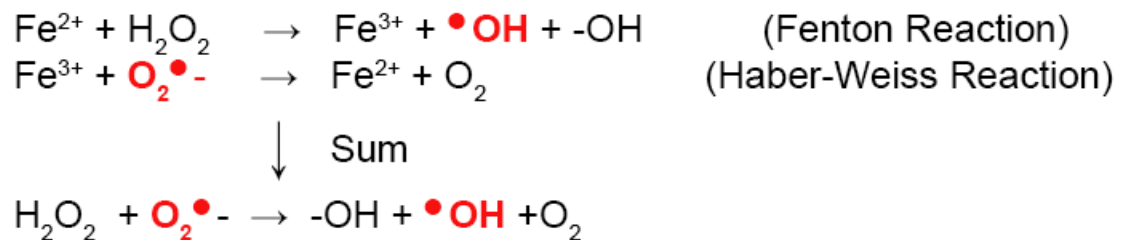


**Figure 1.1.** Reactions with Fe<sup>2+</sup> associated with the generation of reactive oxygen species.

Moreover, both globin proteins and heme constituents of free Hb can cause excessive oxidative damage to the body by reacting with small molecules in circulation such as hydrogen peroxide. Extracellular Hb, can also react irreversibly with nitric oxide (NO), a critical regulator of smooth muscle tone and platelet activation<sup>3</sup>. The consumption of NO by Hb leads to limited bioavailability of NO and the production of nitrate and methemoglobin<sup>3</sup>. To counteract the negative physiological consequences of intravascular hemolysis, haptoglobin (Hp), an acute phase glycoprotein, binds Hb<sup>2, 4</sup> in

one of strongest non-covalent events known in nature ( $K_d \sim 1 \times 10^{-15} \text{ mol/L}$ )<sup>5-7</sup>. Upon Hb/Hp complex formation, a neo-epitope is exposed, which interacts with CD163, resulting in signaling events and endocytosis of the receptor/ligand complex (see Figure 1.2). During this process Hb/Hp complexes are released from CD163 in the early endosome, and the receptor recycles to the cell surface, while the Hb/Hp complexes continue through the endocytic pathway and become degraded in the lysosome<sup>4</sup>. Free heme is converted into ferrous iron, CO, biliverdin and by the endoplasmic reticulum enzyme heme-oxygenase 1 in the cytosol. Biliverdin is reduced to bilirubin by biliverdin reductase, binds to albumin, and transported to the liver<sup>8</sup>.

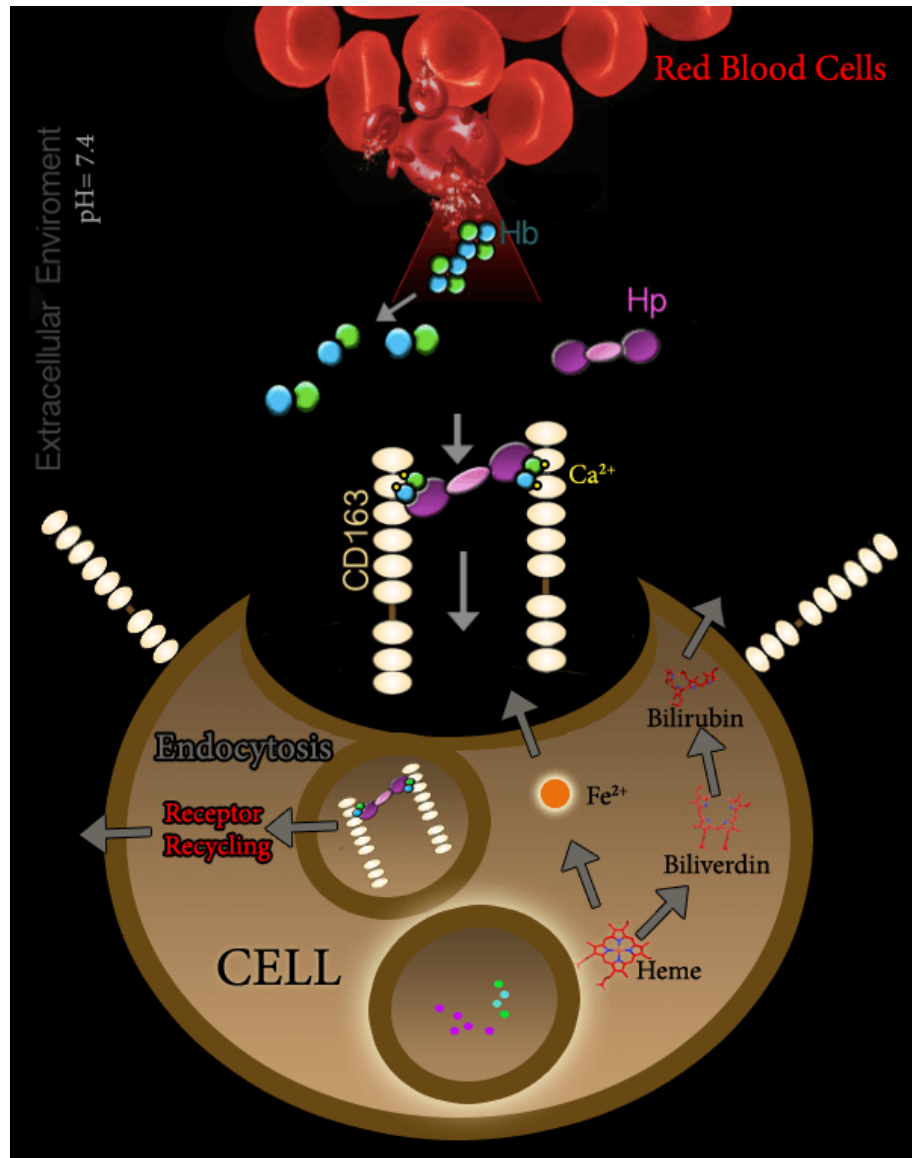


**Figure 1.2. Schematic representation of Hb/Hp complex uptake by macrophages via CD163-mediated endocytosis.** Upon Hb/Hp complex formation, a neo-epitope is exposed. This epitope interacts with CD163 resulting in signaling events and endocytosis of the receptor/ligand complex. The Hb/Hp complexes are released from CD163 in the early endosome, and the receptor recycles to the cell surface, while the Hb/Hp complexes continue through the endocytic pathway and become degraded in the lysosome.

Recent X-ray crystal structures of the porcine Hb/Hp complex<sup>9</sup> and of human Hb/Hp in complex with a trypanosome receptor<sup>10, 11</sup>, have revealed important molecular details of the interactions between Hp heterotetramers and Hb dimers. Although there is no crystal structure of Hb/Hp in complex with CD163, a few insights can be gained from previous experiments. Mutagenesis experiments have suggested that negatively charged residues on CD163 domains 2 and 3 and positively charged residues on Hp<sup>12</sup> are critical for CD163 associations with Hb/Hp complexes. Specifically, site-directed mutagenesis of Hp residues R252 and K262 and acidic residues E27, E28 and D94 (acidic residue cluster) conserved in CD163 domain 2 abrogated Hb/Hp high affinity complex formations<sup>12</sup>. In addition, small angle X-ray scattering (SAXS) data suggests that CD163 binds Hb/Hp complexes on the longitudinal axis<sup>9</sup>.

### **1.1.2. Other functions of haptoglobin**

- **Antibacterial Activity**

When Hb binds to Hp, Hb and iron are no longer available to *Escherichia coli* and other bacteria that require iron<sup>13</sup>. Thus, when Hp was administered intravenously to rats that have been also injected with *E. coli* and Hb, Hp was able to prevent fatal effects and survive. Whereas, 85% of the rats only injected with *E. coli* and Hb died within a 72 hours observation period<sup>14</sup>.

- **Antioxidant Activity**

Hp has a significant role as an antioxidant<sup>15</sup>. Free hemoglobin also increases the peroxidation of purified arachidonic acid and other polyunsaturated fatty acids within neuronal cell membranes<sup>16</sup>. Iron released from heme proteins can catalyze oxidative injury to neuronal cell membranes and might have a role in posttraumatic central nervous system (CNS) damage<sup>16</sup>. Hp binds to Hb removing it from the circulation and preventing iron-stimulated formation of oxygen radicals<sup>17</sup>.

- **Prevention of Renal Damage**

Another consequence of free Hb is oxidative damage in renal tissues following intravascular hemolysis<sup>13</sup>. Yet when Hp binds to Hb, the complex is too large to pass through the glomeruli of the kidney and will be removed via the reticuloendothelial system<sup>13</sup>. Therefore Hb induced injury to the parenchyma is prevented by Hp.

### **1.1.3. Structural features**

Human Hp exists in 2 genotypes, Hp1 and Hp2. Hp in its simplest form, the so-called isoform 1-1, is a 92 kDa heterotetramer composed of two light (L) chains (8.9 kDa) and two heavy (H) chains (40 kDa), connected by disulfide bridges in the H-L-L-H configuration<sup>18</sup> as shown in Figure 1.3. The Hp2 genotypes can form many polymorphs of Hp consisting of larger molecular weights with Hp 2-1 and Hp 2-2 being 90-300 kDa and 170-900 kDa respectively<sup>19</sup>. The light chains in Hp are linked by the disulfide bond formed between C33 on one L-chain and C33 on the other L-chain, while a disulfide bond between L-chain C72 and H-chain C105 link the light and heavy chains<sup>20</sup>. In addition, there are 4 N-linked glycosylation sites found on each monomer in Hp1-1<sup>21</sup>.

The Hp light chain shares 25% homology with complement control proteins<sup>18</sup> while the heavy chain is 29-33% homologous to serine proteases<sup>18, 22</sup>. The serine proteases catalytic triad required for activity typically consists of H57, D189 and S195. In Hp, the His and Ser are replaced by lysine and alanine, respectively while the aspartic acid is retained<sup>15</sup>.

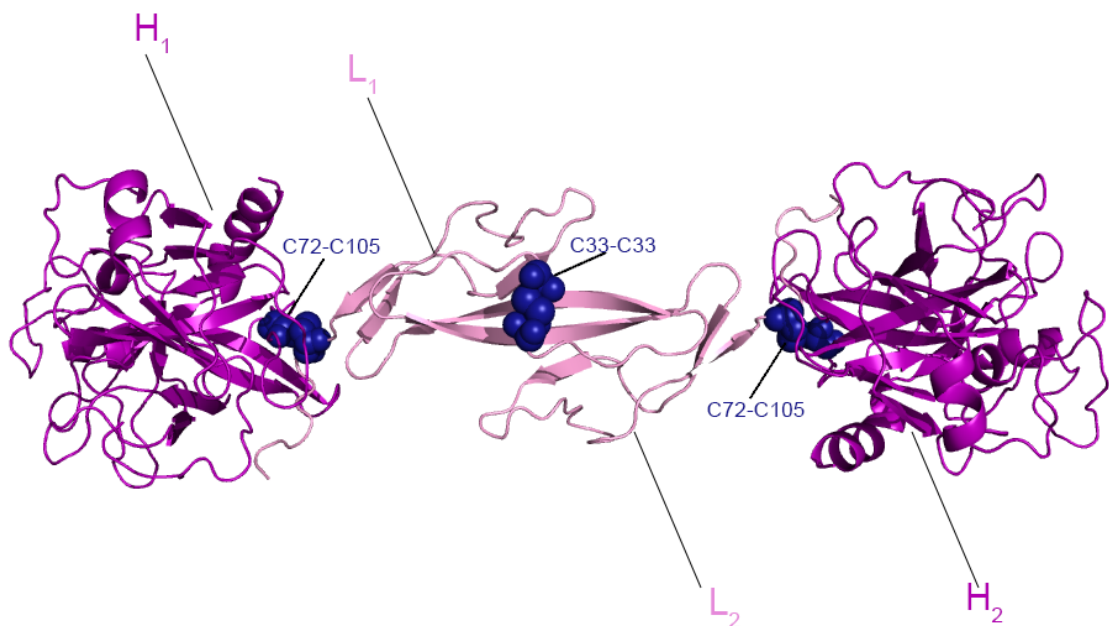


**Figure 1.3** Structure of human haptoglobin removed from the hemoglobin-haptoglobin bound to a trypanosomal receptor (PDBID: 4WJG)<sup>11</sup>.

#### 1.1.4. Haptoglobin and its potential as a drug carrier and therapeutic

- **Haptoglobin potential as a drug carrier**

Since macrophages (and their progenitors monocytes) play a prominent role in the establishment of certain types of viral infections (including HIV), virus dissemination, and development of viral reservoirs<sup>23</sup>, an ability to deliver antiviral therapeutics directly to macrophages by conjugating them to Hp should result in a dramatic improvement in drug efficacy. Another high value target for such a strategy might be hepatitis C virus (HCV), since there is evidence that resident liver macrophages are infected by and support replication of HCV<sup>24</sup>. In addition to viral infections, a similar strategy can be envisioned as a way to design novel therapies against certain types of cancers (most notably acute myeloid leukemia, AML), as the monocyte/macrophage lineage specificity of CD163 expression is preserved beyond malignant transformation<sup>25, 26</sup>. The specificity

of targeted cytotoxin delivery in this case would be particularly beneficial, as Hp-mediated drug delivery specifically to the CD163- expressing cells will be limited to monocytes and macrophages and spare normal stem cells in the bone marrow<sup>25</sup>. Clinical success of therapies based on Hp as a delivery vehicle (e.g., Hp- cytotoxin or Hp- antiviral conjugates) requires detailed understanding of conformational dynamics and interactions in the Hb/Hp/CD163 protein/receptor system both in the extracellular and the endosomal environments, as well as the effects exerted by the conjugated drug.

- **Haptoglobin potential therapeutic**

Circulating Hb wreaking oxidative havoc in the extracellular environment is one of the main unfavorable consequences of hemolysis. Hemolysis affects hematologic diseases such as sickle cell anemia and non-hematologic diseases such as acute myeloid leukemia. Currently, there is no established treatment that targets circulating extracellular globins<sup>27</sup>. However, Hp-administered therapy has recently showed promises in the clinical community as a natural therapy for the sequestration of free Hb<sup>28</sup>. In past studies, the treatment of such patients suffering from hemoglobinuria with Hp administration has led to a noticeable improvement in their conditions<sup>29</sup>. In other very recent research efforts, Hp-administered therapy is being investigated for the treatment of Hb toxicity implicated in sickle cell anemia patients<sup>30</sup>.

## **1.2. In silico methods to characterize protein structure, interaction and/or dynamics**

### **1.2.1. Homology modeling**

A myriad of biological events are dependent on molecular machines composed of a variety of components. These essential molecular processes are often dependent on protein-protein interactions that keep these machines interacting at the exact right time. The standard means for elucidating protein-protein interactions is X-ray crystallography. However, since residues critical for binding are likely to be evolutionarily

conserved, protein-protein interactions could be predicted through computational biology approaches<sup>31</sup>. There are two ways of predicting a protein's 3D-structure: ab-initio and homology modeling. The latter is used to predict the unknown structure of a protein by inference based on a known structure. The homology modeling technique assumes that the target protein and the template protein share a common ancestry.

The success of homology modeling relies on various factors including identifying a homologous experimental template, the efficiency of homologue detection through BLAST searches or other methods for sequence alignments, and the quality of the model building process once the homologue is detected<sup>32</sup>. A template used to model a protein should have high sequence similarity with the unknown protein and a sequence identity of 30% or greater<sup>32</sup>. One of the ultimate goals in computational structural biology is to generate models of protein structures as accurate as those determined by high-resolution experimental studies. This would require more advancement in computational strategies and more experimental templates.

- **Assessment of Predicted Models**

The assessment of a homology model's accuracy is direct when the experimental structure is known. The root-mean-square deviation (RMSD) between the model and a known structure is the most common method of comparing two homologous protein structures to a generated model. RMSDs measure the mean distance between the corresponding atoms in the two structures after they have been superimposed. There are various software used to make these RMSDs measurements including VMD<sup>33</sup> and PYMOL<sup>34</sup>. PROCHECK<sup>35</sup> is another commonly used homology modeling assessment program that provides sensitive and consistent methods for evaluating the accuracy of a model<sup>35</sup>. PROCHECK examines various structural properties, such as the bond length, bond angles, and atom clashes, detecting atoms that have abnormal stereo-chemical



values. PROCHECK can also distinguish between homology models of higher and lower accuracy<sup>35</sup>.

The PROCHECK outputs are Ramachandran plot quality, peptide bond planarity, bad non-bonded interactions, main chain hydrogen bond energy, C-alpha chirality and overall g-factor. Generally, highly quality models are models with a g-factor above -0.5 and a Ramachandran score of 90% in the most favored regions<sup>36</sup>. The latter is an indication of the stereochemical quality of the model. The 90% is calculated based on an analysis of 118 structures of resolution of at least 2.0 Å and R-factors no greater than 20%<sup>37</sup>. R-factors are used in crystallography to measure the agreement between the crystallographic model and the original X-ray diffraction data<sup>38</sup>. For structural models, the G-factor mimics the R-factor used to assess crystal structures. The G-factor is also known as an 'uncertainty factor' because a high value implies high uncertainty, or low confidence about a specific part of a model.

WhatIf<sup>39</sup> is another program used to assess a protein. WhatIf is based on the amount of structural information that supports each part of the model. The program requires the user to input a target sequence with predicted secondary structure and a template to do the calculations. Whatif then outputs "Z-scores or z-values" which are used to indicate the normality of a score. The Z-score is the number of standard deviations that the score deviates from the expected value.

A property of Z-scores is the root-mean-square of a group of Z-scores (the RMS Z-value) is expected to be around 0<sup>40</sup>. A protein is certain to be incorrect if the Z-score is below -3.0<sup>39</sup>.

### **1.2.2. Macromolecular docking**

Determining the tertiary structure of a protein complex experimentally is usually more challenging than determining the structure of an individual protein. Macromolecular docking is an inexpensive, valuable tool for the computational prediction of quaternary

structures of two or more interacting biological macromolecules. A wide range of successful blind docking experiments have been showcased in the Critical Assessment of Prediction of Interactions (CAPRI)<sup>41</sup>.

The two main methods for protein docking are rigid-body docking or flexible docking<sup>42</sup>. In rigid-body docking bond angles, bond lengths and torsion angles of the components are not modified at any stage during complex generation. Sometimes conformational changes occur upon protein-protein complex formations. In this case, molecules should be docked using flexible docking, which accounts for changes in internal geometry upon protein-protein complex formation. Flexible docking requires a lot more computing power than rigid-body docking because the sampling of all possible conformational changes can be computationally expensive.

Assessments of docked protein-protein models outputs require the same tools used to evaluate homology models including Ramachandran plots and Z-scores. Additionally, models are assessed by using scoring functions that are based on weighted sums of the free energy estimations (e.g., from the CHARMM or GROMOS force fields), phylogenetic desirability of the interacting regions, clustering coefficients, and other scores based on residue contacts<sup>42</sup>.

The success of molecular docking many times relies heavily on experimental information gathered from X-ray crystallography, NMR, mutagenesis, and other biophysical experiments. For example, in a commonly used molecular docking software, Haddock<sup>43</sup>, biophysical information derived from previous experiments, such as NMR shifts and limited proteolysis experiments, can be incorporated as constraints used in predicting protein-protein interactions.

### **1.2.3. Molecular dynamics (MD) simulations**

While the structural information of a protein target is almost always essential for most of the goals in targeted drug delivery, ultimately conformational dynamics play a

tremendous role in the success. Unfortunately, the dynamics of proteins and especially protein complexes are much more difficult to probe experimentally. Molecular dynamics has been emerging as a useful tool for elucidating structural, dynamic, and thermodynamic information of protein and protein complexes. In molecular dynamics simulations, the numerical motions (dynamics) of proteins and protein complexes are investigated under the influence of internal and external forces. Simulations can provide non-trivial details about the motions of individual particles as a function of time.

One practical consideration in molecular dynamics simulations is choosing the appropriate molecular mechanic force field which is a energy function for describing the intramolecular and intermolecular interactions<sup>44</sup>. The parameters of the force fields are derived from both computational and experimental studies of small molecules. The underlying idea is small molecules will behave the same as larger biomacromolecules. The most broadly used force fields in biomacromolecules simulations are OPLS<sup>45</sup>, GROMOS<sup>46</sup>, AMBER<sup>47</sup>, and CHARMM<sup>48</sup>. Why all force fields have been shown to provide valuable insights in the field of structural biology, they all have similar setbacks that due to their parameters being over simplified.

In addition, like nuclear magnetic resonance (NMR), MD simulations also have size limitations. The larger the system, the longer the computations take and the more computing power required. As technology is evolving worldwide, advancements are always made to improve computing power and accuracy of the computation. For a more detailed description of MD simulations see references<sup>49, 50</sup>.

### **1.3. Experimental methods to characterize protein structure, interaction and/or dynamics**

#### **1.3.1. Conventional methods: X-ray crystallography and (NMR)**

Traditionally, X-ray crystallography and NMR are the golden means of elucidating the tertiary structure of proteins and protein complexes. NMR has the ability to analyze

protein in solutions, which is very valuable for studying protein complex formation, dynamics, and kinetics. In addition, NMR is also useful for observing hydrogen because it has NMR active nuclei. However, X-ray crystallography has the advantage of ability to obtain atomic resolution data of proteins and protein complexes in the mega dalton range unlike NMR.

Both NMR and X-ray crystallography require very pure protein samples at high concentrations. In addition, to conduct these experiments highly specialized equipment is preferable: for NMR a very powerful electromagnet (600-900 MHz), and for X-ray crystallography data collection at a synchrotron has become more common, for its more powerful and highly stable beam. As mentioned before, disadvantages of NMR include a size limit on proteins that can be used for NMR (detecting limitations). Typically the proteins must around 60 kDa or less. Recent advancements in NMR have been made for solving macromolecular structures of larger proteins such as isotopic labeling, TROSY, and CRINEPT experiments. Yet even with these advancements, one of the largest determined NMR structures is malate synthase G, with molecular mass of 82kDa protein. The disadvantages of X-ray crystallography are not trivial either, there are limitations in the ability to see the flexible regions of proteins, crystal formation can be unpredictable, and the resulting structure is from a solid-state conformation, which lacks information about protein dynamics. An additional consideration when selecting a method for solving macromolecular structures is the length of the experiment, which can range from days to months.

Although X-ray crystallography and NMR are the standard means for gathering and assessing structural information of proteins, limitations in both methods have influenced some scientists to explore computational approaches in predicting the tertiary structure of proteins. Therefore, it is important to understand that computational

predictions rely heavily on the accuracy of experiments. The models can only be as good as the templates derived from experimental structures.

### **1.3.2. Mass spectrometry**

Mass spectrometry (MS) is a very powerful technique that can be applied to characterizing protein-protein interactions and architecture. While mass spectrometry cannot be used to determine the 3D structure of a protein, depending on the technique, MS can be applied to confirming protein interactions, stoichiometry, and dynamics. Fundamentally, mass spectrometry provides spectra of a sample based on the analyte's mass to charge ratio. The basic components of a mass spectrometer are an ion source, a mass analyzer, and a detector. In tandem mass spectrometry (MS/MS) there is often at least one additional mass analyzer, although quadrupole ion traps and many fourier transform ion cyclotron resonance (FTICRs) do not require an additional mass analyzer for MS/MS experiments. MS/MS experiments allow more selective detection of a target compound, better structure elucidation, and greatly reduce interferences from other sample components. One clear advantage of mass spectrometry over conventional techniques is the ability to handle large masses and allow users to analyze several species in one spectrum, simultaneously.

- **Native Mass Spectrometry: Electrospray Ionization Mass Spectrometry (ESI MS)**

ESI is typically the MS method of choice in studying intact biomolecular structures of proteins in the gas phase. This is due ESI being a soft ionization technique and allowing preservation of the quaternary structure of non-covalent protein interactions. In the technique, the sample is first prepared in a volatile buffer, and then a high voltage is applied to the sample to create an aerosol. This allows the sample to be transferred from a solution phase to the gas phase, where it is then passed through an analyzer and the ions are separated according to their mass-to-charge ratio, and subsequently detected.

Native ESI MS has a few advantages in structural biology over conventional methods. The technique has the ability to preserve native-like conditions, is faster, and is very sensitive in providing information on spatial arrangement of the subunits in the complex, stability, and stoichiometry<sup>51, 52</sup>. Native ESI MS requires the use of volatile aqueous buffers prepared at neutral pH such as ammonium acetate and ammonium bicarbonate. For highly quality measurements, high sample quality and the removal of salts and of non-volatile solvents into the spraying solution, is necessary.

A practical consideration in native mass spectrometry is observing large proteins, protein complexes, and proteins with post-translational modification (such as Hp) are often non-trivial. Advancements such as charge reductions strategies have been used to improve accuracy in charge assignment. An incomplete charge reduction technique has been previously been developed in our lab and applied for the accurate charge assignment of Hp<sup>53</sup>. In addition to developing methods, our lab has been successful in designing novel experimental strategies based on electrospray ionization mass spectrometry (ESI MS)<sup>54</sup>, which has allowed us to study protein conformations and interactions with their receptors in great detail<sup>55</sup>.

One of the latest trends in the field of structural biology is moving towards combining computational biology approaches to guide or integrate mass spectrometry experiments<sup>52</sup>. Researchers in this field have usually focused on using experimental information to improve computational modeling design. Politis and coworkers have generated a method that incorporates data collected from various MS experiments in order to generate constraints used for the prediction of protein complexes<sup>56</sup>. Computational experiments could be used to guide and improve MS experiments as well. A well-constructed framework for predicting novel or unknown interactions using both computational approaches and native ESI-MS experiments will be very useful for the development in this field.

#### 1.4. Objectives

This work aims to provide new insights into physiologically important Hp protein-protein interactions. Simultaneously, we aim to design new frameworks for investigating protein interactions by combining computational modeling with native ESI MS to predict and confirm physiologically relevant protein complexes.

This study will make use of enhanced computational and experimental technologies in order to understand the molecular mechanisms of the interaction between Hp and monomeric globin species. In addition, we will utilize advanced computational techniques to provide a detailed dynamic picture of the role  $\text{Ca}^{2+}$  plays in the Hp/CD163 associations. This knowledge will be invaluable in guiding the design of novel therapies against a variety of pathologies, including AIDS and AML.

Specific objectives of this work include: (i) separation of hemoglobin  $\alpha$  and  $\beta$  chains through LC to characterize monomeric Hb/Hp interactions through native ESI MS and (ii) combine computational modeling with native mass spectrometry to study complexes between monomeric globins and haptoglobin, *Chapter 2*. (iii) Generate new template-based molecular models of CD163 using molecular modeling, investigate the role of  $\text{Ca}^{2+}$  in CD163 using molecular dynamics, and (iv) for the first time, generate experimentally driven molecular models of the Hb/Hp/CD163 system that provides atomic detail and characterizes the role of  $\text{Ca}^{2+}$  in receptor-ligand associations using molecular dynamics, *Chapter 3*.

## CHAPTER 2

# HAPTOGLOBIN INTERACTIONS WITH MONOMERIC GLOBIN SPECIES: INSIGHTS FROM MOLECULAR MODELING AND NATIVE ELECTROSPRAY IONIZATION MASS SPECTROMETRY

This work was accomplished in collaboration with Dr. Rinat R. Abzalimov.

### 2.1 Introduction

Haptoglobin (Hp) is an abundant plasma glycoprotein that binds free hemoglobin (Hb) dimers ( $\alpha\beta$ ) following their escape from red blood cells, preventing oxidative damage to kidneys and other organs. Hp/Hb binding is one of the strongest non-covalent associations known in biology.<sup>57</sup> Recent X-ray crystal structures of the porcine Hb/Hp complex<sup>9</sup> and of human Hb/Hp in complex with a trypanosome receptor<sup>10, 11</sup> have revealed important molecular details for the interactions between Hp heterotetramers and Hb dimers. Above and beyond the fundamental biophysical interest, Hp has long attracted attention in the clinical community not only due to its obviously important role in detoxifying free Hb following hemolytic events that occur in a range of pathologies<sup>27, 29, 58</sup> and modulating the action of Hb-based blood substitutes,<sup>59</sup> but also due its potential as a carrier for targeted drug delivery to macrophages.<sup>60</sup> Further understanding of Hp physiological interactions beyond its interactions with Hb dimers will likely be useful for future clinical applications of Hp.

Human Hp in its simplest form, the so-called isoform 1-1, is a 92 kDa heterotetramer composed of two light (L) and two heavy (H) chains connected by disulfide bridges in the H-L-L-H configuration.<sup>18</sup> The Hb binding site is localized on the H-chains of Hp, and Hb binding exposes a neo-epitope on Hp which is recognized by the Hb/Hp scavenger receptor (cluster differentiation 163, CD163) on the macrophage surface, followed by internalization of the entire complex and its routing to the lysosome,



where the Hb/Hp complex is catabolized.<sup>1, 61</sup> Although the Hb/Hp binding stoichiometry in a fully saturated complex is 1:1, i.e. one Hp heterotetramer per Hb tetramer, each H-chain can only bind a single Hb  $\alpha\beta$  dimer, giving rise to both unsaturated complexes, H-L-L-H( $\alpha\beta$ ), and saturated complexes, ( $\alpha\beta$ )-H-L-L-H( $\alpha\beta$ ), when the Hp concentration exceeds that of Hb.<sup>53</sup> Hb dissociation to dimers exposes the binding epitopes normally buried in the dimer-dimer interface of the Hb tetramer and is thus essential for Hp binding.

While the Hb tetramer-to-dimer dissociation occurs immediately upon release from red blood cells (RBCs) due to the dramatic decrease in concentration, further dissociation, to monomeric globin chains, is also possible<sup>62, 63</sup> especially when oxidative damage alters the polypeptide structure by inducing non-enzymatic post-translational modifications or the protein environment is acidified.<sup>64</sup> However, it is unclear if Hp can bind monomeric globin chains. In addition to the  $\alpha$ - and  $\beta$ -globin chains produced upon Hb dissociation, human blood may contain another monomeric globin, the 17.5 kDa protein myoglobin (Mb), which is normally confined to muscle tissue, but can be released into circulation in relatively large quantities during myocardial related injuries such as rhabdomyolysis, reaching concentrations as high as 1 mg/mL<sup>65</sup>. Free Mb in circulation presents the same dangers, such as renal toxicity<sup>67</sup>, as its close cousins, the Hb  $\alpha$ - and  $\beta$ -subunits, with which it shares a very high degree of sequence homology and an iron-containing prosthetic heme group. Despite the similarities between Mb and the globins comprising Hb, the mechanism of Mb detoxification remains an area of on-going debate, and whether Mb can associate with Hp is a matter of controversy<sup>68, 69</sup>.

In this work we use a combination of computational and experimental tools to address whether and how Hp can interact with monomeric globins (both Mb molecules and  $\alpha$ -globins derived from Hb). While molecular modeling shows that some key local

interactions are absent in the putative Hp/Mb complex relative to Hb/Hp, it is unclear whether the absence of these key residues renders Mb binding-incompetent or simply reduces the binding affinity, an issue that can be resolved only by using experimental tools.

Modern experimental biophysics offers a very impressive armamentarium of techniques that can be used to study protein interactions; however, the large size of the Hb/Hp and putative Hp/Mb complexes (well over 100 kDa) and significant structural heterogeneity make their characterization a challenging task. Native electrospray ionization mass spectrometry (ESI MS) has been used extensively to probe the structure of protein complexes,<sup>51, 70-72</sup> and the reach of this technique can be further expanded by combining it with non-denaturing separation techniques, such as size exclusion chromatography<sup>73</sup> or methods of ion chemistry in the gas phase.<sup>53, 74</sup> In this work we used native ESI MS to determine whether Hp can associate with monomeric globins. The experimental data provide clear evidence that both  $\alpha$ -globin (derived from Hb) and Mb can associate with Hp under non-denaturing conditions, a finding which is in excellent agreement with the results of the molecular modeling work. The results of these experiments reveal that Hp can bind monomeric globins and demonstrate how computational tools can aid in planning MS experiments and interpreting their results.

## 2.2 Materials and methods

### 2.2.1 Homology modeling and molecular docking

The porcine Hb/Hp complex structure (PDB ID: 4F4O) was used as a template for homology models of the human Mb/Hp complexes. Sequences of human Mb and porcine Hp were obtained from Uniprot (accessions P02144 and Q8SPS7, respectively). The Hb/Hp and the Mb/Hp sequences were aligned using ClustalW<sup>75</sup> and the BLOSUM<sup>76</sup> multiple alignment scoring matrix, with a gap start penalty value of 10 and a gap extension penalty value of 1. This alignment was then used in Modeller<sup>77</sup> to construct ten structural models of Mb/Hp complexes. The top model was selected based on the discrete optimized protein energy score (DOPE score)<sup>77</sup>. This model was then minimized using GROMACS 4.5<sup>78</sup>, the Gromos96 force field<sup>79</sup> and 5,000 steepest descent logarithm steps. The quality of the refined and minimized model was assessed through PROCHECK.<sup>35</sup> PYMOL<sup>34</sup> and VMD<sup>33</sup> were used to analyze and visualize the resulting structure. Residues that interact with Hp were identified through CocoMaps.<sup>80</sup>

To further validate predicted interactions between monomeric globins and Hp, the Haddock molecular docking server<sup>43</sup> was used to dock Hb $\alpha$ , Hb $\beta$  or Mb to Hp. Haddock generates molecular models of protein-protein complexes based on residues the user defines as active (interface residues) or passive (surrounding interface residues). The resulting complexes are given a “Haddock Score” based on energy calculations associated with complex formation including electrostatic energies and van der Waals energies.<sup>32</sup> Hb $\alpha$  was docked to Hp defining the Hb $\alpha$ /Hp interface residues in the human Hb/Hp model (82% sequence identity to porcine Hb/Hp complex<sup>9</sup>) as active residues in Haddock. Hb $\beta$  docking to Hp was performed in a similar manner. Mb was docked to Hp by setting the same Hb $\alpha$ /Hp interface residues as active in Hp and the corresponding Mb residues as active in Mb.

### **2.2.2. Structural comparisons of Mb/Hp models with the Hb $\alpha$ and Hb $\beta$ binding sites on Hp**

The 3-D models of Hb $\alpha$ /Hp and Hb $\beta$ /Hp complexes were generated by removing the complementary Hb chain from the porcine Hb/Hp crystal structure in the Hb/Hp X-ray crystal structure using Pymol<sup>34</sup>. The Mb-Hp homology model was structurally aligned with these Hb $\alpha$ /Hp and Hb $\beta$ /Hp structures, using the VMD<sup>33</sup> tool MultiSeq and the degree of conservation was determined from the BOLSUM62 scoring matrix<sup>76</sup>. Per residue root mean square deviations (RMSDs) were calculated from the structural alignment in VMD.<sup>33</sup>

### **2.2.3. Identification of critical Hb interface residues**

Mutations to critical interface residues are likely to perturb protein-protein interactions. To identify residues important for Hb/Hp association, computational alanine scanning was performed on the Hb/Hp and Mb/Hp complexes using the DrugScore-PPI Server<sup>81</sup>. DrugScore-PPI uses a knowledge-based scoring function based on pair potentials from known protein-protein interactions and results from alanine scanning experiments to predict protein-protein interaction hotspots and outputs the effects of alanine mutations on the binding energy,  $\Delta\Delta G$ , in kcal/mol.

### **2.2.4. Materials and HPLC separation of Hb chains**

Lyophilized horse heart Mb, human Hb, and hemin chloride were purchased from Sigma-Aldrich Chemical Co. (St. Louis, MO). Human Hp1-1 was purchased from Athens Research and Technology (Athens, GA). All other chemicals, buffers, and solvents were of analytical grade or higher. Apo-Hb (heme-free) was prepared using a modified acetone precipitation method<sup>14</sup> where the cold acetone was at -40 °C rather than -20 °C. The resulting apo-Hb precipitate was suspended in 50 mM ammonium acetate, pH 7.5 and lyophilized. Hb  $\alpha$ - and  $\beta$ -chains were separated with reverse phase HPLC (HP1100, Agilent Technologies, USA) using a 4.6 mm  $\times$  150 mm C8 analytical column with 5  $\mu$ m

pore size (Separation Methods Technologies, Newark, DE). Multiple fractions corresponding to the  $\alpha$ -chain peaks were collected, pooled and lyophilized and the protein identity confirmed by ESI MS. Holo-Hb $\alpha$  was prepared by reconstituting the apo-form of isolated  $\alpha$ -globin with a heme group as described previously<sup>14</sup> the integrity of the heme/globin complex was confirmed by ESI-MS

### **2.2.5. Mass spectrometry.**

All ESI MS measurements were carried out with a QSTAR-XL (ABI Sciex, Toronto, Canada) hybrid quadrupole-time-of-flight mass spectrometer equipped with a nanospray source. Aqueous protein solutions were buffer exchanged into 100 mM ammonium acetate and the pH was adjusted to 7.6 with diluted ammonium hydroxide. Repeated concentration and dilutions were done using Centricon (Millipore) centrifugal filters with a 5-kDa, 15-kDa and 30-kDa cut-off for Mb, Hb, and Hp, respectively (fixed angle rotor operated at 4 °C and 4000g). Concentrations of all heme-containing proteins were determined by measuring the Soret band, using the extinction coefficient of 191.5  $\text{mM}^{-1}\text{cm}^{-1}$ .<sup>82</sup> Hp concentrations were determined by measuring absorption at 280 nm, and using the extinction coefficient 57340  $\text{M}^{-1}\text{cm}^{-1}$  determined by the EXPASY server ProtParam tool<sup>83</sup>. Concentrations of all stock solutions were adjusted to 1 mg/mL (corresponding to 15.5  $\mu\text{M}$  Hb tetramer, 63.5  $\mu\text{M}$  Hb  $\alpha$ -chain 56.8  $\mu\text{M}$  Mb, and 11  $\mu\text{M}$  Hp) unless noted otherwise.

## 2.3 Results and discussion

### 2.3.1. Construction and evaluation of the Mb/Hp model

The Hb/Hp complex contains two Hb  $\alpha\beta$  heterodimers, one bound to each H-chain of Hp.<sup>18</sup> Although the Hb  $\alpha$  and  $\beta$  chains are highly homologous (41% identical and 64% similar), each has a distinct Hp binding site on the Hp surface. Mb is similar to both Hb chains with 27% and 28% identity, and 48% and 50% similarity to Hb $\alpha$  and Hb $\beta$ , respectively (Figure 2.1A), including 7/14 ( $\alpha$ ) and 8/11 ( $\beta$ ) of the residues involved in Hp/Hb binding. This suggests that Mb may be capable of binding to Hp at either Hb subunit binding site. To investigate the likelihood of Mb binding to Hp, as well as its preference for either the Hb $\alpha$  or Hb $\beta$  sites, Mb/Hp models were constructed using Modeller for homology modeling (Figure 2.2A) and Haddock for molecular docking (models not shown). The stereo chemical quality of the models was assessed and compared to X-ray crystal structures of human Mb (PDB: 3RGK 1.65 Å resolution) (Figure 2.5) and porcine Hb/Hp complex (PDB: 2.4 Å resolution) using PROCHECK<sup>29</sup>, QMEANClust<sup>84</sup>, and PYMOL<sup>46</sup>. High-resolution X-ray structures have Z-scores of around 0, from a range of -5 to 5, and a Ramachandran score of 90% in the most favored regions.<sup>29</sup> The Mb/Hp stereochemical assessment of models fell within the range of a good quality model according to results output from QMEANClust and which calculated a Z-score of -1.4 and PROCHECK calculated Ramachandran plots of 89.1% of the residues to be in the most-favored regions, 9% in the allowed regions, and 1% in the generously allowed regions (Figure 2.3). This comparison is also favorable relative to the Hb/Hp structure, which has a Z-score of -0.7 and 90.8%, 8.9% and 0.3% of the residues in the favored, allowed and in generous regions of the Ramachandran plot, respectively. The Mb model superimposed on the Mb crystal structure indicated a positional RMSD of 1.3 Å (Figure 2.5).



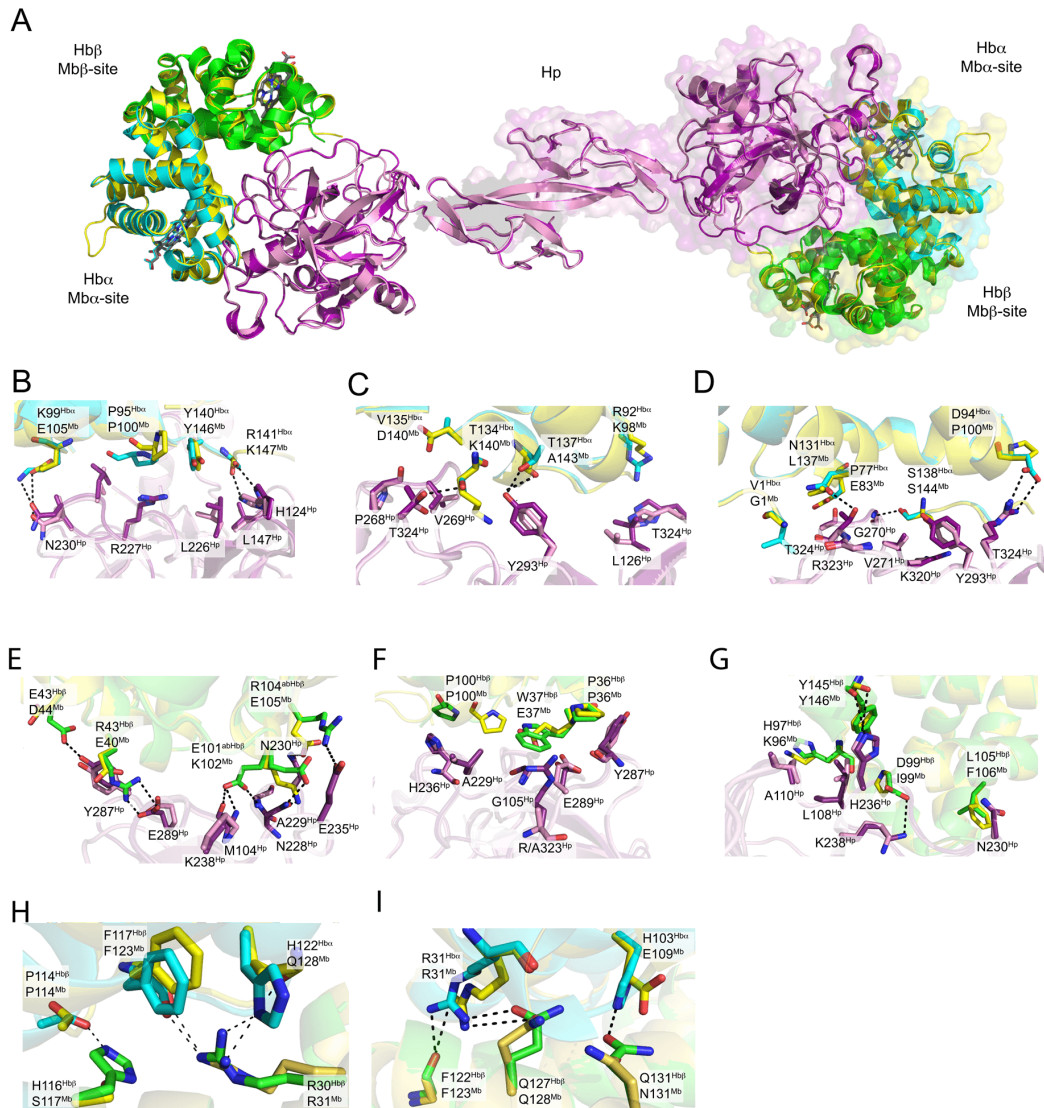


**Figure 2.2 Structure of porcine Hb/Hp complex superimposed on the human Mb/Hp model structures:** Hbα cyan, Hbβ green, Hp purple and models: Mb yellow, Hp pink, heme as sticks. Stick representation of protein-protein interactions in (B-D), Hbα/Hp structures superimposed on Mbα-site/Hp models and (E-G), Hbβ/Hp structures superimposed on Mbβ-site/Hp models, and (H,I) Hb α/β dimers structure superimposed on Mb<sub>2</sub> models to show the globin-globin interactions.



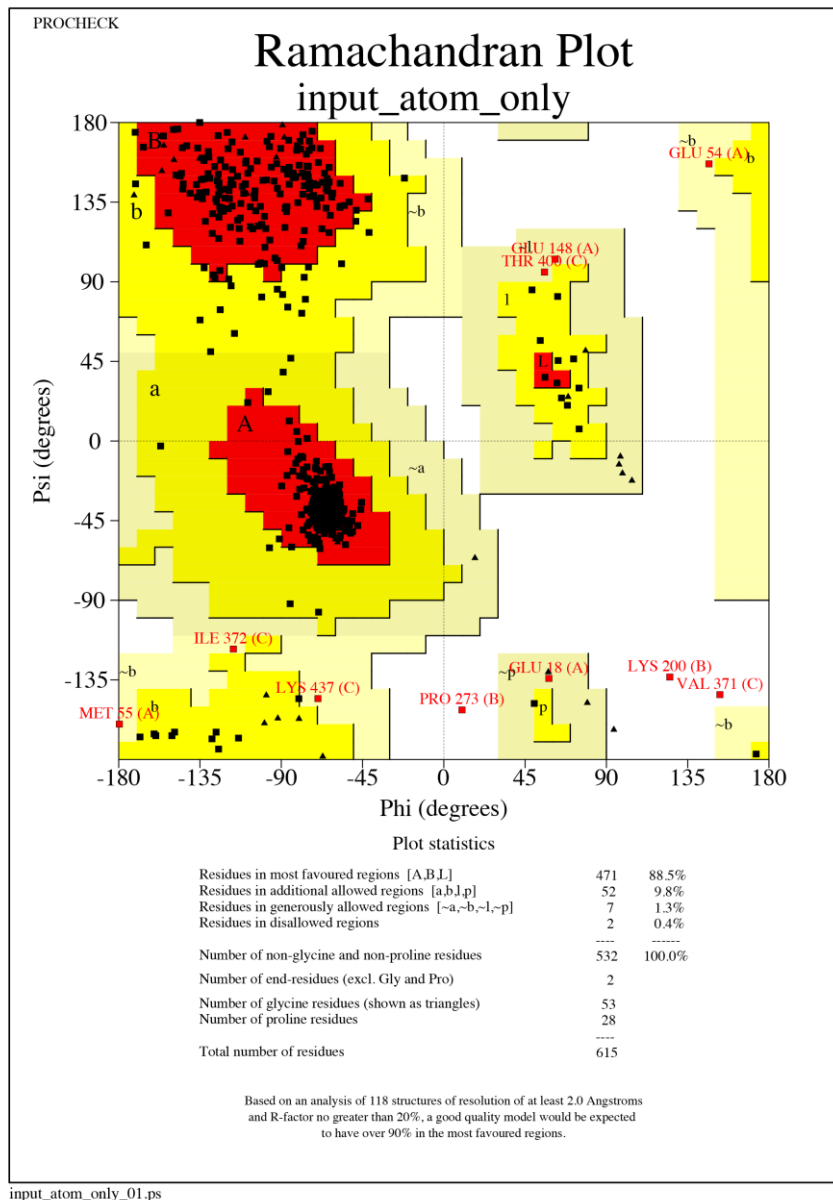


**Figure 2.3. Ramachandran plot prepared by “Procheck” for the Mb2/Hp homology model shown in Figure 2A.** Glycine and proline residues are represented by triangles and squares are used for all other residues. The most favorable combinations of the phi psi values are shown in red (89.1%) areas. Additionally allowed regions (9.4%) are shown in dark yellow areas, generously allowed (1.0%) regions are light yellow areas, and disallowed regions (.6%) are in the white areas.

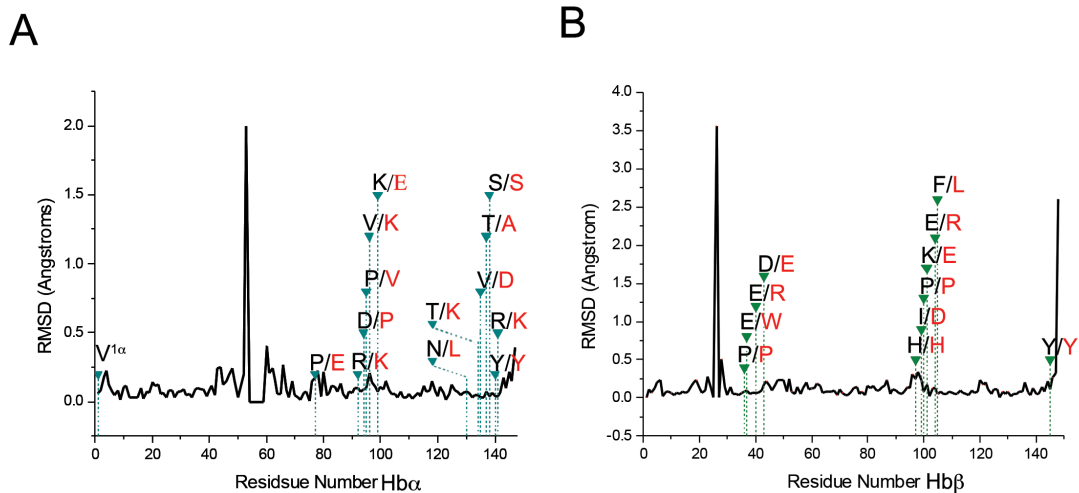


**Figure 2.4.** RMSD per residue in angstroms for structural alignments of Hb/Hp structures and Mb/Hp models as calculated by VMD. (A) Hb $\alpha$ /Mb( $\alpha$ -site) RMSD. (B) Hb $\beta$  to Mb( $\beta$ -site) RMSD. Hb residues, black and corresponding Mb residues, red.

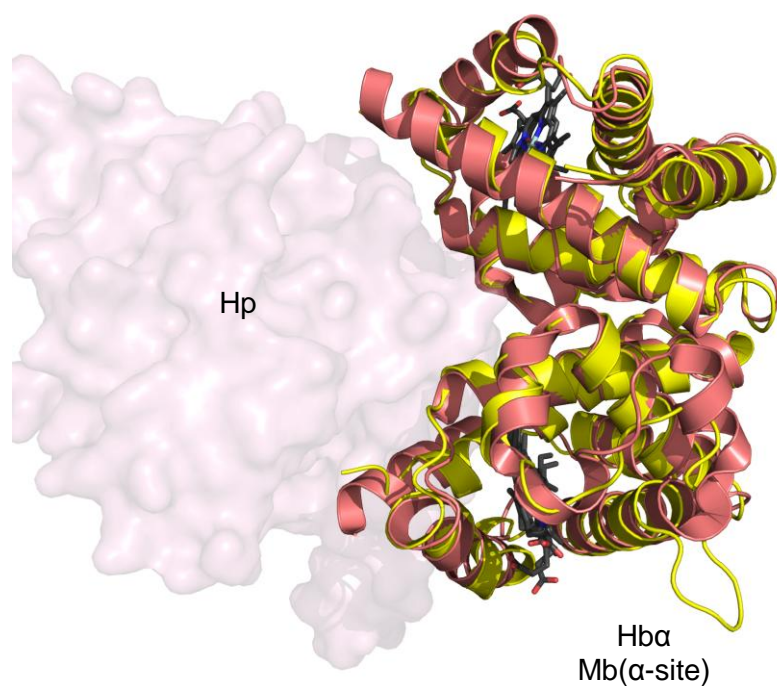


**Figure 2.5. Structural alignment of free Mb and Mb bound to the Hp  $\alpha$ -site and  $\beta$ -site.** The 1.65 Å structure of free human Mb (PDB ID: 3RGK, red) superimposed on Mb from the homology model (yellow). The heme prosthetic group is shown as sticks and the total RMSD is 1.2 Å at both sites.

### 2.3.2. Analysis of the Mb/Hp model interface

The inter-chain contacts at the globin/Hp binding interface were identified in both the Hb/Hp X-ray crystal structure and the top-scoring Mb/Hp homology model using CocoMaps. This analysis reveals that 73% of the Hb $\alpha$ /Hp interactions are shared with Mb bound to the  $\alpha$  site, which will be referred to as Mb $\alpha$ -site/Hp (Figure 2.6A, Table 1). In comparison, Mb bound to the  $\beta$  site of Hp (Mb $\beta$ -site/Hp) shared 50% of the Hb $\beta$ /Hp interactions (Figure 2.6B, Table 2.1). Many of the non-conserved residues are charged residues involved in electrostatic interactions and salt bridges. Specifically, Hb $\beta$  residues R40, E101 and R104 are charge swapped in Mb (residues E40, K102 and E105, respectively, as highlighted in Figure 2.2E), which may indicate unfavorable interactions

between Mb and Hp at the Hb $\beta$  binding site.

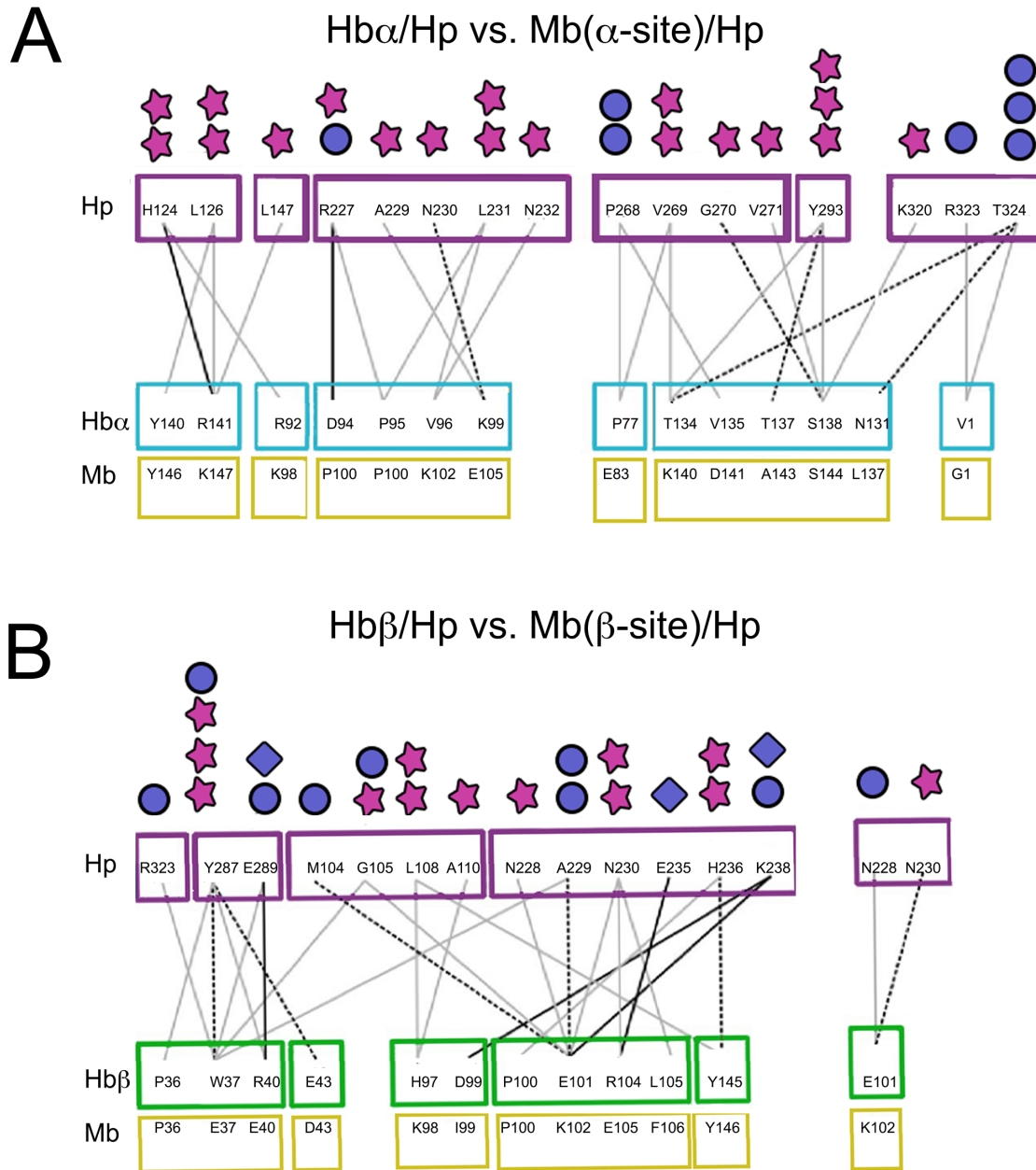


**Figure 2.6. Schematic overview of porcine Hp/Hb interactions and the corresponding interactions in the human Mb/Hp homology models.** (A) Comparison of Hb $\alpha$  and predicted Mb $\alpha$ -site interactions with Hp shows that 76% of the interactions are conserved. (B) Similar comparisons between Hb $\beta$  bound to Hp and Mb $\beta$ -site show 52% conservation. Grey lines represent van der Waals contacts, dashed black lines represent hydrogen bonds and black lines represent salt bridges. Stars denote conserved interactions, blue circles denote non-conserved interactions, and blue diamonds denote unfavorable interactions in the order of the the lines drawn. For example, H124<sup>Hp</sup> has 2 stars because its salt bridge with R141 and van der Waals with

interaction with R92 is conserved in the Mb/Hp models. H124<sup>Hp</sup> interacts with K147<sup>Mb</sup> and K98<sup>Mb</sup> respectively.

It is possible that some of these residues in Mb may still interact with other nearby residues in Hp. For instance, the salt bridge formed between R104<sup>B</sup> and E235<sup>Hp</sup> is not conserved at the Mb/Hp interface because the basic R104<sup>B</sup> (Figure 2.2E) residue is replaced with the negatively charged E105<sup>Mb</sup>. However, E105<sup>Mb</sup> may form a hydrogen bond with the nearby Hp residue N228.

Hb and Hp have extensive interactions that contribute to the extremely low dissociation constant of  $1 \times 10^{-15}$  M.<sup>7</sup> As shown in Table 2.1 and Figure 2.5 many of these interactions are conserved in the Mb/Hp model structure. The Hb/Hp crystal structure reveals that 16 Hp residues interact with 14 Hb $\alpha$  residues through 26 interactions and 13 Hp residues interact with 12 Hb $\beta$  residues through 25 different interactions. In the Mb/Hp models, 23 Hp residues interact with 9 residues for Mb  $\alpha$ -site binding in 19 conserved interactions and 8 residues for Mb  $\beta$ -site binding in 13 conserved interactions. This comparison alone suggests that Mb is likely to bind to Hp albeit with lower affinity than does Hb.

**Table 2.1.** Comparisons of Hb/Hp and Mb/Hp molecular interactions.

|                       | van der Waals | Salt Bridges | H-Bonds    |
|-----------------------|---------------|--------------|------------|
| Hp/Hb $\alpha$        | 19            | 2            | 5          |
| Hp/Mb                 | 15            | 1            | 3          |
| <b>% Conservation</b> | <b>78%</b>    | <b>50%</b>   | <b>60%</b> |
| Hp/Hb $\beta$         | 15            | 4            | 5          |
| Hp/Mb                 | 10            | 0            | 2          |
| <b>% Conservation</b> | <b>67%</b>    | <b>0%</b>    | <b>40%</b> |

Although the modeling results suggest that Mb binding to Hp is more likely to occur at the Hb $\alpha$ /Hp interface, many contacts appear to be preserved at the Hb $\beta$ /Hp interface as well, prompting us to explore the possibility that an Mb dimer could bind to a single Hp H-chain (Figure 2.2). Although Mb is usually a monomeric protein, at high concentrations in solution Mb is commonly known to dimerize as revealed by ESI MS and size exclusion chromatography.<sup>85</sup> The Hb $\alpha\beta$  heterodimer was used as the template to create a molecular model of an Mb dimer (Mb<sub>2</sub>). The Hb/Hp complex model was structurally aligned to the Mb<sub>2</sub> homo-dimer (Figure 2.2A) and the interface of the Hb  $\alpha/\beta$  heterodimer in the Hb/Hp structure was compared to the Mb/Mb homodimer interface in the Mb/Hp models (Table 2.2).

**Table 2.2** Comparison of globin-globin hydrogen bond interactions in human Hb $\alpha/\beta$  or Mb<sub>2</sub> dimers in complex with Hp.

| Interaction | Hb $\alpha/\beta$ heterodimer |            | Mb/Mb homodimer     |                    |
|-------------|-------------------------------|------------|---------------------|--------------------|
|             | Hb $\alpha$                   | Hb $\beta$ | Mb( $\alpha$ -site) | Mb( $\beta$ -site) |
| 1           | R31                           | F122       | R31                 | F123               |
| 2           | R31                           | Q127       | R31                 | Q128               |
| 3*          | H103                          | Q131       | E109                | N131               |
| 4*          | P114                          | H116       | P114                | S117               |
| 5           | F117                          | R30        | F123                | R31                |
| 6           | H122                          | R30        | Q128                | R31                |

\*non-conserved interactions.

Analysis of the contacts across the binding interface reveal that 67% of the interactions in the  $\alpha/\beta$  heterodimer are conserved in the Mb/Mb interface (Table 2.2, Figure 2.2H,I). Although this analysis suggests a high percentage of conservation, the non-conserved interactions may be particularly important for  $\alpha/\beta$  interface stability. In particular, two non-conserved residues, Hb H116 $^{\beta}$  corresponding to S117<sup>Mb</sup> and A111 $^{\alpha}$ , were previously shown to be important for Hb  $\alpha/\beta$  heterodimer association and stabilization.<sup>86</sup> This lack of two important residues and the high concentrations required

for Mb<sub>2</sub> formation suggest that an Mb/Mb homodimer interface is unlikely even when bound to Hp.

- **Docked models**

The Haddock molecular docking server was also used to generate molecular models of Mb docked to the Hb $\alpha$  and Hb $\beta$  sites on Hp. To test the accuracy of the docking Hb $\alpha$  and Hb $\beta$  were individually docked to Hp by specifying the interface residues found in the Hb/Hp crystal structure in the Haddock program. Haddock accurately mimicked Hb $\alpha$ /Hp and Hb $\beta$ /Hp interactions in Hb/Hp with overall structural RMSDs of 0.4 Å compared to the experimentally determined porcine structure<sup>9</sup>. Following this validation, Mb was docked to Hp. The docked structure contained Mb in the Hb $\alpha$  binding site in a similar orientation to that observed in the Mb $\beta$ -site/Hp homology model with RMSDs of 0.3 and 0.5 Å compared to the Mb $\alpha$ -site/Hp homology model and the Hb $\alpha$ /Hp porcine crystal structure, respectively. However, attempts to dock Mb in the Hb $\beta$  binding site failed. This is consistent with the results from homology modeling indicating that Mb binding to the Hb $\alpha$  site is more favorable. The energies for complex formations, as calculated by the Haddock server are -287  $\pm$ 52 kJ/mol and -253  $\pm$ 44 kJ/mol for Hb $\alpha$ -Hp complexes and Mb-Hp complexes respectively. While we do not want to over-interpret these theoretical energy values, they do indicate that Mb binding to Hp may be slightly less favorable than Hb $\alpha$  binding, again agreeing with the results from homology modeling.

### **2.3.3. Further identification of residues important for binding**

Predictions of the effects of alanine substitutions on the binding energies of Hb/Hp and Hb $\alpha$ / $\beta$  heterodimers was determined using the DrugScorePPI webserver (Figure 2.6). In protein-protein interactions there are often key contacts in binding interfaces, referred as “hot spot” residues that make the largest contributions to the protein-protein interactions. Mutation of these hot spot residues to alanine is likely to

perturb the protein-protein interactions resulting in  $\Delta\Delta G$  values for binding of 1.5 kcal/mol or higher.<sup>87</sup> The less critical warm spot residues have  $\Delta\Delta G$  0.5 - 1.5 Kcal/mole) and unimportant residues are designated as having  $\Delta\Delta G > 0.5$  Kcal/mol.<sup>87, 88</sup>



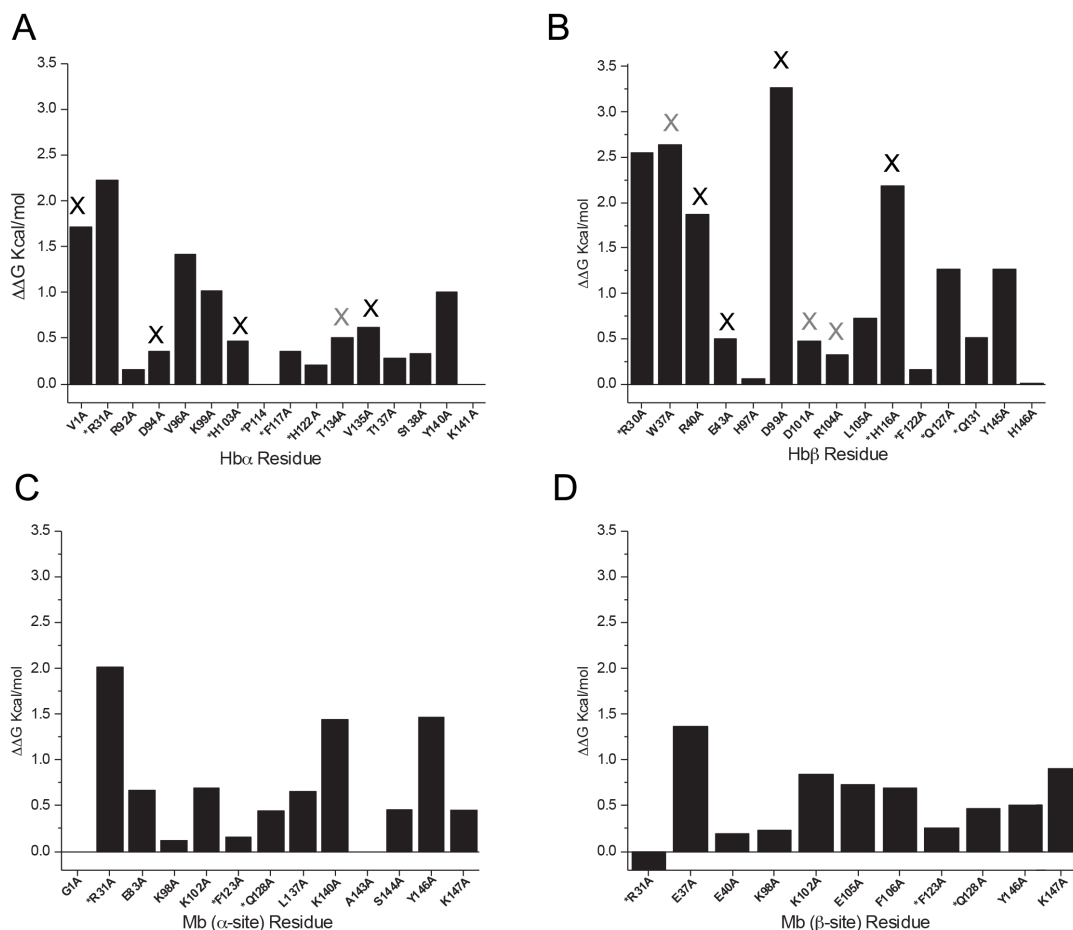


**Figure 2.7. Predicted effects of alanine substitutions on the binding energy of the Hb/Hp structures and Mb/Hp models calculated by the DrugScorePPI Web server in kcal/mole. A black “X” denotes a non-conserved residue in Mb and a gray “X” denotes a partially conserved residue. The results were categorized into three sets: hot spots ( $\Delta\Delta G \geq 1.5$  kcal/mol), warm residues (0.5 - 1.5 kcal/mol), and unimportant residues ( $< 0.5$  kcal/mol).<sup>87, 88</sup>**

In the Hb/Hp and Mb/Hp interface, DrugScorePPI identified Hb residues K99 $^{\alpha}$ , Y140 $^{\alpha}$ , V135 $^{\alpha}$ , R40 $^{\beta}$ , Y145 $^{\beta}$ , K140 $^{Mb}$ , Y146 $^{Mb}$  as warm spot residues and V1 $^{\alpha}$ , D99 $^{\beta}$ , W37 $^{\beta}$  as hot spot or warm spot residues (Figure 2.7). The interactions involved in the predicted warm and hot spot residues in Hb/Hp were then compared to the corresponding Mb/Hp interactions. The V1 $^{\alpha}$  (G1 $^{\alpha}$ )/R323, T324 $^{Hp}$  interactions are not conserved in Mb $\alpha$ -site/Hp (Figure 2.2D) models while the K99 $^{\alpha}$  (E105 $^{Mb}$ )/N230, A229 $^{Hp}$

and Y140<sup>α</sup> (Y146<sup>mb</sup>)/L126<sup>Hp</sup> (where the corresponding Mb residues are in parentheses) are conserved (Figure 2.2B). This analysis suggests that Mb binds to the Hb<sup>α</sup> site on Hp but with lower affinity. In contrast, the predicted Hb<sup>β</sup> hot spot residues were mostly non-conserved in Mb<sup>β</sup>-site/Hp. In particular alanine mutations on D99<sup>β</sup>, (Figure 2.2G) non-conserved in Mb, had the highest predicted  $\Delta\Delta G$  affect of 3.2 kcal/mol. Again, Mb binding to the Hb<sup>α</sup> site on Hp appears to be more favorable.

Still, if Mb were capable of binding both the Hb<sup>α</sup> and Hb<sup>β</sup> sites on Hp, this may require a favorable Mb/Mb homodimer interface. Determining critical residues in the Hb<sup>α</sup>/β heterodimer interfaces would likely provide more inference on the likelihood of Mb/Mb associations. The Hb<sup>α</sup>/β heterodimer interfaces were also analyzed by DrugScorePPI (Figure 2.7) to determine if alanine mutations at any of the Hb<sup>α</sup>/β heterodimer interface residues (denoted with an asterisk in Figure 2.7) would be likely to affect binding. Alanine mutations on Hb indicated the conserved R31<sup>α</sup>, R30<sup>β</sup>, R31<sup>Mb(α-site)</sup> (Figure 2.2H and 2I) and non-conserved R116<sup>β</sup> (in porcine, H116<sup>β</sup> in human, see Figure 2.2H) residues as hot spot residues ( $\Delta\Delta G > 1.5$  kcal/mol). Porcine residue R116<sup>β</sup> (or human H116<sup>β</sup>) forms a hydrogen bond with P114<sup>α</sup> and is not conserved in Mb (Figure 2.2H). As mentioned before R116<sup>β</sup> was previously shown to be important for Hb  $\alpha/\beta$  associations.<sup>86</sup> These results further support the hypothesis that only one monomer of Mb will interact with Hp because the Mb<sup>β</sup>-site is missing key residues in both the Mb/Mb and Mb<sup>β</sup>site/Hp interfaces that are predicted to affect binding.

#### **2.3.4. Native ESI MS of Hb/Hp and Hb<sup>α</sup>/Hp Complexes.**

Previous native ESI MS experiments<sup>53, 63</sup> provide clear indications that interactions between Hb and Hp occur in a step-wise fashion, with one  $\alpha/\beta$  heterodimer binding to a single H-chain of Hp, so that the fully saturated complex has 1:1 stoichiometry (one tetrameric Hb ( $\alpha\beta$ )<sub>2</sub> per one covalent dimer of Hp H-L-L-H). Therefore, depending on the Hb/Hp concentration ratio in solution, both H-L-L-H·( $\alpha\beta$ ) or ( $\alpha\beta$ )·H-L-L-

H-( $\alpha\beta$ ) complexes were observed by MS. Figure 2.8B shows a mass spectrum of the Hb/Hp mixture where the former is present in slight molar excess (6.1  $\mu$ M tetramer Hb  $\alpha\beta$  dimer: 3  $\mu$ M Hp tetramer). Even though the ionic signal in the low  $m/z$  region (inset in Figure 2.8B) reveals the presence of some residual Hb in solution, its binding partner is completely consumed, as no ionic signal corresponding to the free Hp or the partially saturated complex is observed in the mass spectrum (see Figure 2.8A for the reference spectrum of free Hp in the absence of Hb).

While it has long been known that Hp binds Hb  $\alpha\beta$  heterodimers, there is still no consensus vis-à-vis the ability of individual globins to associate with Hp. However, the computational modeling does suggest that Hb monomers can bind to Hp. In order to address this question,  $\alpha$ -globin was prepared by isolation from Hb tetramers followed by reconstitution with heme. The resulting  $\alpha$ -globin was mixed with Hp at a 5:1 molar ratio and the protein solution was immediately analyzed by native ESI MS. Only the ionic signal of  $\alpha_2$ Hp species could be observed in the high  $m/z$  region of the resulting mass spectrum (Figure 2.8C), while ionic species corresponding to either free Hp or the partially saturated complex  $\alpha$ -Hp were absent. This result not only shows that Hp is capable of binding monomeric globins, it also suggests that Hp has high affinity (at least in the sub- $\mu$ M range) for  $\alpha$ -globin.

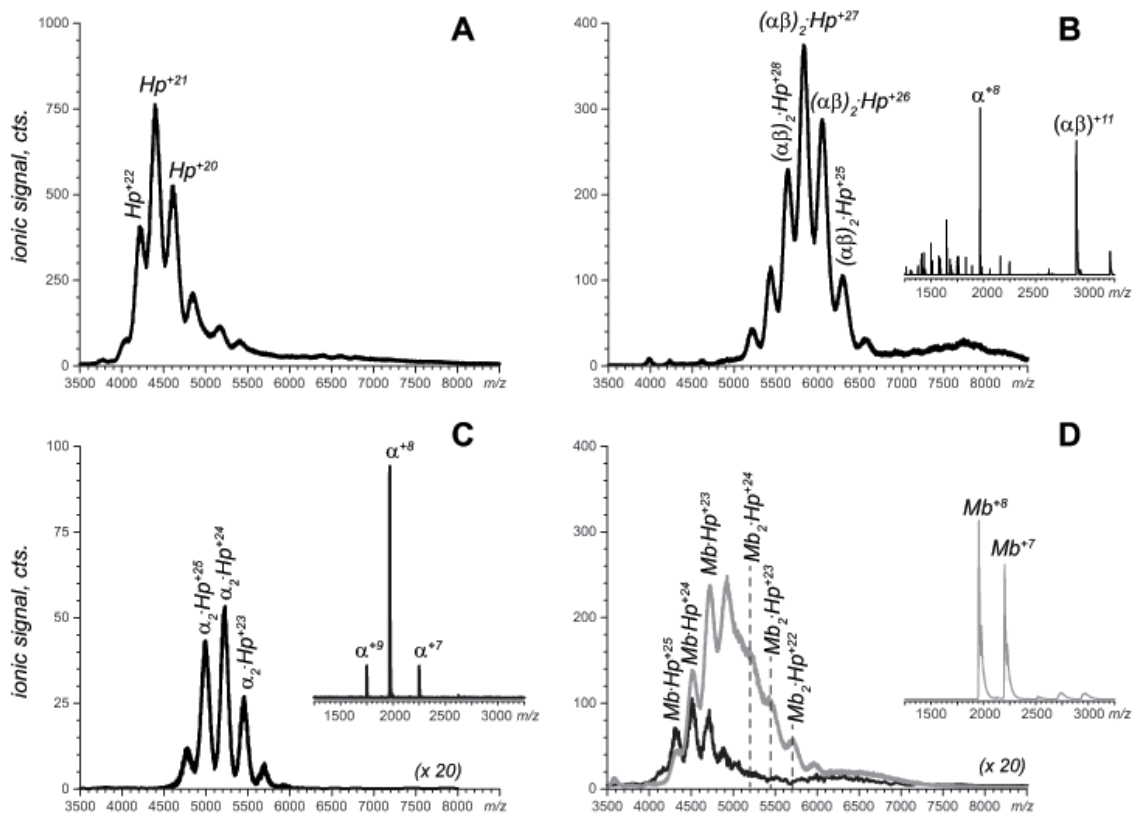


**Figure 2.8. ESI-MS shows that monomeric globins can bind to Hp.** (A) Native ESI mass spectra of free Hp in the absence of binding partners. Native ESI mass spectra of Hp in the presence of (B) a slight molar excess of Hb, (C) 5-fold molar excess of heme-reconstituted  $\alpha$ -globin and (D) 5-fold molar excess of Mb. The gray trace in panel D shows a mass spectrum of Hp in the presence of 2-fold molar excess of Mb. Insets in all panels show low- $m/z$  regions of the respective mass spectra.

The modeling also predicts that Mb will bind to Hp. This hypothesis was evaluated by mixing the two proteins at a 2:1 Mb:Hp molar ratio, followed by immediate acquisition of native ESI mass spectra. Interestingly, the spectra were devoid of ionic signal corresponding to free Hp, while displaying prominent signals for the partially saturated Mb/Hp complex (with 1:1 stoichiometry). Increasing the Mb:Hp molar ratio to 5:1 led to the appearance of the Mb<sub>2</sub>/Hp complexes, although Mb/Hp complexes were still the predominant species (Figure 2.8D). The presence of abundant ionic species corresponding to both partially unsaturated Mb/Hp complexes and free monomeric Mb

(see the inset in Figure 2.8D) indicates that Mb affinity for Hp is lower than that of  $\alpha$ -globin. Another noteworthy feature of the mass spectra presented in Figure 2.8D is the absence of Mb/Hp complexes with stoichiometry higher than 2:1, indicating that only a single Mb monomer can associate with an Hp heavy chain, giving rise to Mb-H-L-L-H and Mb-H-L-L-H-Mb species. This result agrees with the modeling, where Mb binding was more favorable in the  $\alpha$  site.

- **Computational and native-ESI results suggest Hb $\alpha$  and Mb are similar.**

Molecular modeling results suggest that Mb, Hb $\alpha$  and Hb $\beta$  are structurally quite similar. But, deeper investigation of the binding interface suggests that the Hb $\alpha$  binding site on Hp is more favorable for Mb binding (76% conserved interactions Hb $\alpha$ /Hp vs 50% in Hb $\beta$ /Hp). Additionally while the non-conserved Mb/Hp interactions at the Hb $\alpha$  binding site were electrostatically favorable, various modeled contacts for Mb at the Hb $\beta$  binding site were predicted to be unfavorable. In particular, *in silico* mutagenesis results suggest that partially conserved W37 $^{\beta}$  (Figure 2.2F) and non-conserved residues D99 $^{\beta}$  (Figure 2.2G) and R40 $^{\beta}$  (Figure 2.2E), which participate in salt bridges with Hp, are important for Hb $\beta$ /Hp binding. In comparison, most of the interactions predicted to be important for Hb $\alpha$  binding, e.g. K99 $^{\alpha}$  (Figure 2.2B) and Y140 $^{\alpha}$  (Figure 2.2B), are conserved in Mb. These computational results imply that Mb is likely to bind to Hp in the Hb $\alpha$  binding site but with lower affinity than does Hb $\alpha$ . An Mb/Mb homodimer interface where two Mb monomers bind to the  $\alpha$  and  $\beta$  sites on the same Hp heavy chain also seems unlikely since Mb/Mb homodimers are missing key contacts shown to be critical for  $\alpha/\beta$  heterodimer interface stability.<sup>86</sup>

Native-ESI analysis of Hb $\alpha$  or Mb alone and Hb $\alpha$ /Hp or Mb/Hp complexes are consistent with predictions from the computational studies. Isolated Hb $\alpha$  and Mb solutions are detected as monomers, with a minor dimer component for Mb. Hb $\alpha$ /Hp and

Mb/Hp complexes are detected and even when monomeric globins are in slight excess relative to Hp, they only bind one Hp heavy chain. The lower 2:1 Mb:Hp complexes (Figure 2.8D) present in the native ESI-MS spectra than Hb $\alpha$ /Hp complexes (Figure 2.8C) under the same conditions suggest Mb binds Hp at lower affinity as predicted by the computations.

- **Could Hp complexes with monomeric globins be recognized by CD163 for internalization?**

The ability of Mb to associate with Hp is important, since it is present in blood serum in significant levels during certain cardio-pathological events, such as rhabdomyolysis, a type of myocardial injury.<sup>89</sup> The exact mechanism of Mb clearance from circulation, where it certainly poses a danger of severe oxidative damage, remains largely unknown. The results of this work indicate that Hp may play a critical role in Mb sequestration and catabolism.<sup>89</sup> Just as Hb/Hp structures illustrate the Hp protective role by shielding some of the residues to prone to oxidative modification<sup>9</sup>, the Mb/Hp models suggest that the redox active<sup>90</sup> and conserved Y146<sup>Mb</sup> (equivalent to Y140 <sup>$\alpha$</sup>  and Y145 <sup>$\beta$</sup> ) is deeply buried within the Mb/Hp interface. The apparent ability of Hp to act as a scavenger of free Mb following its release to circulation in the same way it scavenges free Hb raises a few interesting questions. What happens after Mb binds Hp, i.e. is the association event only the first step in the catabolic chain? Are Mb/Hp complexes recognized by CD163, the Hb/Hp scavenger receptor, which binds Hb/Hp complex at the surface of the macrophages and mediates its transport to the lysosomal compartments? If Hp is indeed capable of neutralizing free Mb in circulation, a very intriguing question would be whether or not it could be used as a therapy in patients with myocardial injuries to control oxidative damage by removing free Mb from circulation.

Andersen and coworkers have characterized Hb/Hp<sup>9</sup> and Hb/Hp/CD163 receptor

complexes<sup>12</sup>. According to these studies, Hb/Hp complex formation induces a conformational change on Hp that exposes a loop recognized by the Hb/Hp receptor CD163 allowing complexes to be internalized into cells and degraded<sup>12</sup>. Hp alone has been shown to have very low to no binding affinity for CD163<sup>91-93</sup>, further indicating that Hb/Hp complex formation is critical for CD163 recognition. Since the Mb/Hp complexes were modeled after the Hb/Hp structures, this recognition loop is exposed in the Mb/Hp models. The use of Hp as a possible therapeutic for mediating clearance of monomeric globins will require knowledge on whether Hp interactions with CD163 are preserved when only a single globin is bound per heavy chain.

That CD163 might recognize Mb/Hp complexes is suggested by recently documented uses of Hp as an emergency therapeutic in hemolysis patients. In fact, rhabdomyolysis is a well-known complication leading to Mb release to circulation in patients with severe burns; and the recently reported treatment of such patients with Hp had led to noticeable improvement in their conditions.<sup>29</sup> Even though the success was ascribed to the free Hb sequestration, our results suggest that it is possible that elimination of free Mb was also a contributing factor. However, it remains to be seen if Hp administration may limit some of the damage following other cardiac pathologies, such as myocardial infarction, where the levels of Mb released from muscle tissue to circulation are similar to those associated with rhabdomyolysis.

## 2.4. Conclusions

We have used computational tools to explore the possibility that Hp binds monomeric globins, including the  $\alpha$ -chain of Hb and intrinsically monomeric Mb. The computational results suggest that Mb can interact with Hp, and that the  $\alpha$ -globin chain binding site on the Hp surface is the preferred site for Mb binding. These conclusions were verified by native ESI MS, which showed that both monomeric  $\alpha$ -globin (derived from human Hb) and Mb can associate with Hp in solution, although the Mb/Hp complex is somewhat less stable compared to the Hb $\alpha$ /Hp complex. Even when monomeric globins were present in significant molar excess (5-fold), only a single monomeric globin per each heavy chain of Hp was observed (despite the fact that Mb undergoes limited dimerization in solution at this high concentration), further supporting the conclusion of the molecular modeling work that Mb only binds to the  $\alpha$ -globin chain binding site on Hp.



**CHAPTER 3**  
**MOLECULAR MODELS OF THE HEMOGLOBIN-HAPTOGLOBIN COMPLEX**  
**DOCKED TO CD163 AND CALCIUM-INDUCED DYNAMICS REVEALED BY**  
**MOLECULAR DYNAMICS**

This work was accomplished in collaboration of the Scott Auerbach Group at the University of Massachusetts Amherst, chemistry department.

### **3.1 Introduction**

During intravascular hemolysis, Hb is released from erythrocytes and it can potentially become physiologically very toxic in the extracellular environment. The haptoglobin-CD163-mediated-heme pathway is an efficient route for the removal of free Hb from the extracellular environment. In this pathway, Hp first binds to circulating Hb dimers, shielding redox active residues. Once Hb/Hp complexes are formed, they proceed to bind CD163, a cell surface receptor on expressed exclusively on cells of the monocyte/macrophage lineage, leading to complex internalization and catabolism. The Hb/Hp complexes are released from CD163 in the early endosome, and the receptor recycles to the cell surface<sup>4</sup>. There are currently no experimentally determined structures of full-length CD163 or of the Hb/Hp/CD163 complex.

Elucidating the structural basis of the Hb/Hp/CD13 pathway has gained high interest in the clinical community. Recent better understandings of the Hp-CD163-mediated-heme pathway for Hb clearance have provided strong indications that this

pathway may be used for targeted drug delivery<sup>94</sup>. Since macrophages (and their progenitors monocytes) play a prominent role in the establishment of certain types of viral infections (including HIV), virus dissemination, and development of viral reservoirs<sup>23</sup>, an ability to deliver anti-viral therapeutics directly to macrophages (e.g., by conjugating them to Hp) should result in a dramatic improvement of the drug efficacy. Another high value target for such strategy might be hepatitis C virus (HCV), since there is evidence that resident liver macrophages are infected by and support replication of HCV<sup>24</sup>. In addition, to viral infections, a similar strategy can be envisioned as a way to design novel therapies against certain types of cancers (most notably acute myeloid leukemia, AML), as the monocyte/ macrophage lineage specificity of CD163 expression is preserved beyond malignant transformation<sup>25, 26</sup>.

While there is no crystal structure of CD163 alone or in Hb/Hp in complex with CD163, a number of experiments have shed some light on structural information about CD163 and in complex with Hb/Hp<sup>12, 92, 95</sup>. SPR studies have indicated Hb alone has lower affinity for CD163 compared to Hb/Hp complexes and Hp alone has little to no affinity to CD163. Another critical biophysical detail in the Hb/Hp/CD163 interaction is surface plasmon resonance (SPR) experiments revealed  $\text{Ca}^{2+}$  containing conditions is critical for CD163 associations with Hb/Hp complexes. The same researchers also concluded  $\text{Ca}^{2+}$  free conditions renders CD163 unstable and induces autolysis (self-cleavage) of CD163<sup>95</sup>.

Structurally, CD163 contains 9 scavenger receptor cysteine rich (SRCR) domains belonging to the ancient and highly conserved SRCRs superfamily. Although the specific functions of SRCR domains have not been defined with certainty, SRCRs are thought to mediate ligand binding. Along with the 9 SRCR domains, CD163 also consists of a transmembrane segment, and a cytoplasmic tail as illustrated in Figure 3.1. Site-directed mutagenesis experiments performed by Nielson et al, and coworkers

revealed alanine mutations on the acidic residues D27, D28 and E94 (acidic residues cluster) found in CD163 domains 2 and 3<sup>12</sup> severely reduced the binding affinity of CD163 to Hb/Hp/CD163 complexes. On the other hand, mutations on Hp basic residues R252T and K262 (located in a protruding loop in Hp and called the Hp-CD163 recognition loop), drastically reduced binding and or completely abrogated binding of Hb/Hp complexes to CD163, respectively. These results suggest the Hp/CD163 interfaces are driven by electrostatic interactions between the basic Hp and acidic CD163 domain 2 and 3 residues. Additionally, these results are consistent with experimental structures of endocytic receptor-ligand complexes involved in calcium-dependent interactions such as cubilin in complex with intrinsic factor<sup>12</sup>.

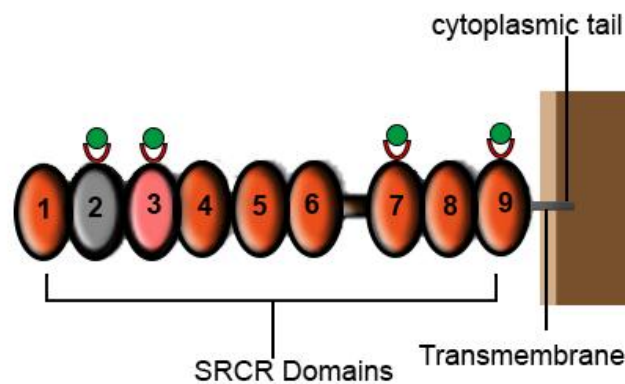


**Figure 3.1. Schematic representation of CD163.** Orange eclipses represent the SRCR domains. Gray and salmon colors are used to highlight CD163 domain 2 and 3, the domains known to be involved in Hb/Hp binding. Green spheres represent Ca<sup>2+</sup> ions.

While researchers were unable to locate a CD163 binding site on Hb after numerous attempts mutagenesis attempts<sup>12</sup>, the Hp-CD163 recognition loop has been extensively studied. In an earlier Hb/Hp/Cd163 binding study, a synthetic 26 amino-acid peptide containing residues found in the Hp-CD163 recognition loop (which includes Hp residues R252 and K262) was synthesized<sup>92</sup> and experimentally shown to compete with

Hb/Hp binding to CD163<sup>92</sup>. Whereas, a synthetic loop containing residues in the same region of a protein called haptoglobin related protein (Hpr), a protein that share 91% identity with Hp1 but does not bind CD163, did not compete. Results of these experiments further implicate the importance of the specific basic Hp residues in the Hp/CD163 associations and also suggest that a peptide containing the essential basic Hp residues is sufficient to monitor Hp/CD163 interactions.

Since the CD163 SRCR domains are highly homologous to various proteins with experimentally solved structures, high quality molecular models of CD163 can be generated. The current molecular models of CD163 domain 2 and 3 (the suggested interacting domains) deposited in the protein model portal (PMP) are modeled based on the structure of mac-2 binding protein scavenger receptor (PDBID: 1BY2), a protein that is not known to bind  $\text{Ca}^{2+}$ . In light of the goal of generating more accurate molecular models of CD163 domain 2 and 3 we explored the SRCR domain of MARCO, a calcium-binding macrophage receptor, as a probable template. MARCO is a trimeric protein composed of a transmembrane segment, a short intracellular domain, and a large extracellular region. The SRCR domain of MARCO (spanning amino acids 421-522) is located within its extracellular region, and contains the calcium coordinating acidic acid cluster (447D/448D/511E). This calcium coordinating acidic acid cluster is conserved in CD163 domains 2, 3, 7, 9 corresponding to D27/D28/E94 in each domain. These similarities suggest the structure of MARCO may serve as an excellent template for CD163 domains 2 and 3 since mutagenesis and surface plasmon resonance experiments revealed the importance of these specific acidic residues and  $\text{Ca}^{2+}$  respectively.

In order to first elucidate the structural role of  $\text{Ca}^{2+}$ , molecular models of CD163 domain 2 and 3 were generated using the crystal structure of the SRCR domain of MARCO as template. Since  $\text{Ca}^{2+}$  has experimentally been shown to be critical for CD163

stability and Hb/Hp/CD163 formations, molecular dynamics was then used to investigate the dynamic changes of apo ( $\text{Ca}^{2+}$  free) vs  $\text{Ca}^{2+}$  bound forms of CD163 domains 2 and 3. Towards the goal of elucidating the structural determinants of the Hb/Hp/CD163 interaction, we docked the molecular models of  $\text{Ca}^{2+}$  bound CD163 domains 2 and 3 to Hb/Hp complexes defining Hp and CD163 residues that were experimentally shown to be critical for binding as residues along the interface. While experimental data suggests the acidic residue cluster in CD163 domain 2 and 3 and basic residues in Hp are significant, the structural role of calcium is not well understood. In order to better understand the role of  $\text{Ca}^{2+}$  in CD163 structure and function, molecular dynamics simulations were employed to determine the dynamics of apo and  $\text{Ca}^{2+}$  bound CD163 models in complex with the Hp-CD163 recognition loop peptide. Our molecular modeling and molecular dynamics results support the importance of the experimentally identified acidic residue clusters in both CD163 domains 2 and 3, in interactions with Hp. In addition, the results of the molecular dynamics simulations provide additional evidence on why  $\text{Ca}^{2+}$  is important for the association and stabilization of Hb/Hp/CD163 complexes, enhancing our knowledge in the Hb/Hp/CD163 pathway.

## **3.2 Materials and methods**

### **3.2.1. Homology modeling of CD163 domain 2 and 3.**

The X-ray crystal structure of the SRCR domain from mouse MARCO (PDB ID: 2OY3) was used as the template for homology models of human CD163 domains 2 and 3. The sequences of SRCR domain of mouse MARCO and human CD163 were obtained from Uniprot accessions codes Q60754 and Q86VB7, respectively. Clustal Omega<sup>96</sup> program was employed to align the sequences of the SRCR domain of mouse MARCO with the sequences of CD163 domains 2 and 3 FIGURE 3.2A. This alignment was then used to construct ten structural models each of domain 2 and 3 each using Modeller<sup>97</sup>. The top model for each domain was selected based on the discrete optimized protein energy score (DOPE score)<sup>98</sup>. Energy minimization of the structural models was then conducted using GROMACS, the Gromos96 force field<sup>79</sup> and 5,000 steepest decent logarithm steps. The quality of the refined and minimized models were assessed through PROCHECK<sup>35</sup> and QMEAN<sup>99</sup>. PYMOL<sup>34</sup> and Visual Molecular Dynamics (VMD)<sup>33</sup> were used to analyze and visualize the resulting structures.

### **3.2.2. Molecular docking of Hb/Hp/CD163.**

In order to predict the molecular basis of the Hp/CD163 interaction, the generated CD163 domain 2 and 3 with Ca<sup>2+</sup> bound to site 1 models were docked to Hp in the human Hb/Hp structure (PDBID:4WJG chains: 1,2,3) using the Haddock molecular docking software. Haddock allows users to docks proteins based on residues defined as confidently involved in the interface “active”, residues that should not be in the interface “inactive”, and residues that do not have constraints “neutral”. Neutral residues could still participate in the binding interface. The residues identified in mutagenesis experiments as critical for Hb/Hp/CD163 complex formation, R252<sup>Hp</sup> and/or K262<sup>Hp</sup> and D27, D28, E94 in domain 2 and/or domain 3 with Ca<sup>2+</sup> bound to site 1 were set as active residues in Haddock. Since it is unclear whether Hp interacts with one or both CD163 domains, a

total of 4 docking trials were carried out: (i) Hp complex docked to domain 2, (ii) Hp complex docked to domain 3, and (iii) Hp complex docked to domain 2 then domain 3 (iv) Hp complex docked to domain 3 then domain 2. Once the docking runs are complete, Haddock outputs the highest ranked structures and ranks them based on their Haddock score. Table 1 summarizes the different docking trials, parameters, and ranking results. As mentioned before, based on previous mutagenesis experiments, CD163 only binds to Hb/Hp complexes in the presence of  $Ca^{2+}$ <sup>95</sup>. To test whether the presence of  $Ca^{2+}$  will impact these results, apo-domain 3 was also docked to the human Hb/Hp complex. In the Hb/Hp/apo-CD163 docking experiments, R252<sup>Hp</sup>, K262<sup>Hp</sup>, D27<sup>domain 3</sup>, D28<sup>domain 3</sup>, E94<sup>domain 3</sup> were set as active residues that should be in the interface.

**Table 3.1.**

Summary of interaction restraints used in protein-protein docking and score.

| Experiment                            | Hp         | CD163 Domain 2 | CD163 Domain 3 | Haddock Score | Z-score |
|---------------------------------------|------------|----------------|----------------|---------------|---------|
| 1. Hp complex-CD163 domain 2          | R252, K262 | D26, D27, E94  | -----          | -40.1 +/- 3.7 | -1.3    |
| 2. - Hp complex - CD163 domain 3      | R252, K262 | -----          | D26, D27, E94  | -60.7 +/- 8.9 | -1.9    |
| 3. Hp complex-CD163 domain 2-domain 3 | R252       | D26, D27, E94  | -----          | -37.8 +/- 5.1 | -1.8    |
|                                       | K262       | -----          | D26, D27, E94  |               |         |
| 4. Hp complex-CD163 domain3-domain 2  | R252       | -----          | D26, D27, E94  | -27.0 +/- 6.9 | -1.3    |
|                                       | K262       | D26, D27, E94  | -----          |               |         |

### 3.2.3. Molecular dynamics.

Molecular dynamics (MD) simulations were performed using the OPLS-AA/L force field with GROMACS version 4.6.1<sup>78</sup>. The protein was placed at the center of a rhombic dodecahedral box and the distance to the edge of the box was set to 1.5 nm. The box was solvated with single point charge (SPC) water molecules. Periodic boundary conditions were applied to satisfy the minimum image convention and simulate bulk systems. The counter ions sodium or chloride were added to neutralize the system charge and the final NaCl concentration was 0.1 M. An energy minimization of the solvated protein and neutralized structures was performed to correct the inappropriate geometry. The minimization was performed for a maximum of 5,000 steps with the steepest descent algorithm. The convergence criterion of the energy minimization is achieved when the potential energy reached a plateau and the maximum force was less than  $10 \text{ kJ mol}^{-1}\text{nm}^{-1}$ .

The number of particles, volume and temperature (NVT) were kept constant in first equilibration. This was followed by a second equilibration step where the number of particles, pressure and temperature (NPT) were kept constant. In the NVT ensemble, the system was heated to 300 K over 100 ps by randomly assigning initial velocities taken from the Maxwell-Boltzmann distribution. The temperature was scaled by the modified Berendsen thermostat<sup>100</sup>. In an NPT ensemble, the pressure was scaled to 1 bar with a compressibility of  $4.5 \times 10^{-5}$  bar by the Parrinello-Rahman barostat<sup>101</sup>. Time constants for controlling the temperature and pressure were set to with 0.1 ps and 2 ps, respectively.

The van der Waals and electrostatic interactions were applied with cutoff distances of 1.4 nm using the Verlet cutoff scheme<sup>102</sup>. The short-range neighbor list was set to 10.0 nm. The Linear Constraint Solver (LINCS) algorithm was used to constrain bond lengths<sup>103</sup>. The production run was performed for 60 ns at a temperature of 300 K



and pressure of 1 atm, respectively. In all simulations a time step of 2 fs was used and the trajectory was updated every 10 ps. Analysis of MD trajectories was carried out using utilities within the GROMACS package and VMD.

### **3.3 Results and discussion**

#### **3.3.1. Homology models of CD163 domains 2 and 3.**

Ca<sup>2+</sup> has previously been shown to be critical for CD163 domains 2 and 3 stability and Hb/Hp/Cd163 complex formation. To elucidate structural the role of Ca<sup>2+</sup>, new CD163 domain 2 and 3 molecular models were regenerated since the previous models that were modeled based on mac 2-binding protein, a homologous SRCR receptor that does not contain Ca<sup>2+</sup> or the conserved coordinating acidic residue cluster. In this study, the SRCR domain of MARCO protein was a selected as the template to generate models of domain 2 and 3 because the structure of MARCO contains a conserved calcium coordinated acidic amino acid cluster bound to calcium (447D/448D/511E) found in domains 2 (corresponding to 27D/28D/94E) and 3 (27D/28D/94E).

CD163 domains 2 and 3, and the SRCR domain in MARCO belong to the SRCR family of proteins that contain a conserved compact globular fold stabilized by 5 disulfide bridges. Clustal Omega alignments indicated the MARCO protein is 45% and 49% identical to domain 2 and domain 3 respectively (Figure 3.2A). The CD163 domain 2 and 3 models aligned closely to the MARCO template indicating structural RMSDs of 0.2Å and 0.1 Å respectively (Figure 3.2B) and contained the correct disulfide bridge connectivity. Ramachandran plots calculated by PROCHECK for the domain 2 and 3 models showed that 94% and 93%, respectively, of the residues were in the most favorable regions and QMEAN calculated Z-scores of 0.2 and 0.1 respectively. These

score were comparable to MARCO structure, with 95% of the residues in the most favored regions of the Ramachandran plot and a Z-score of 0.3.

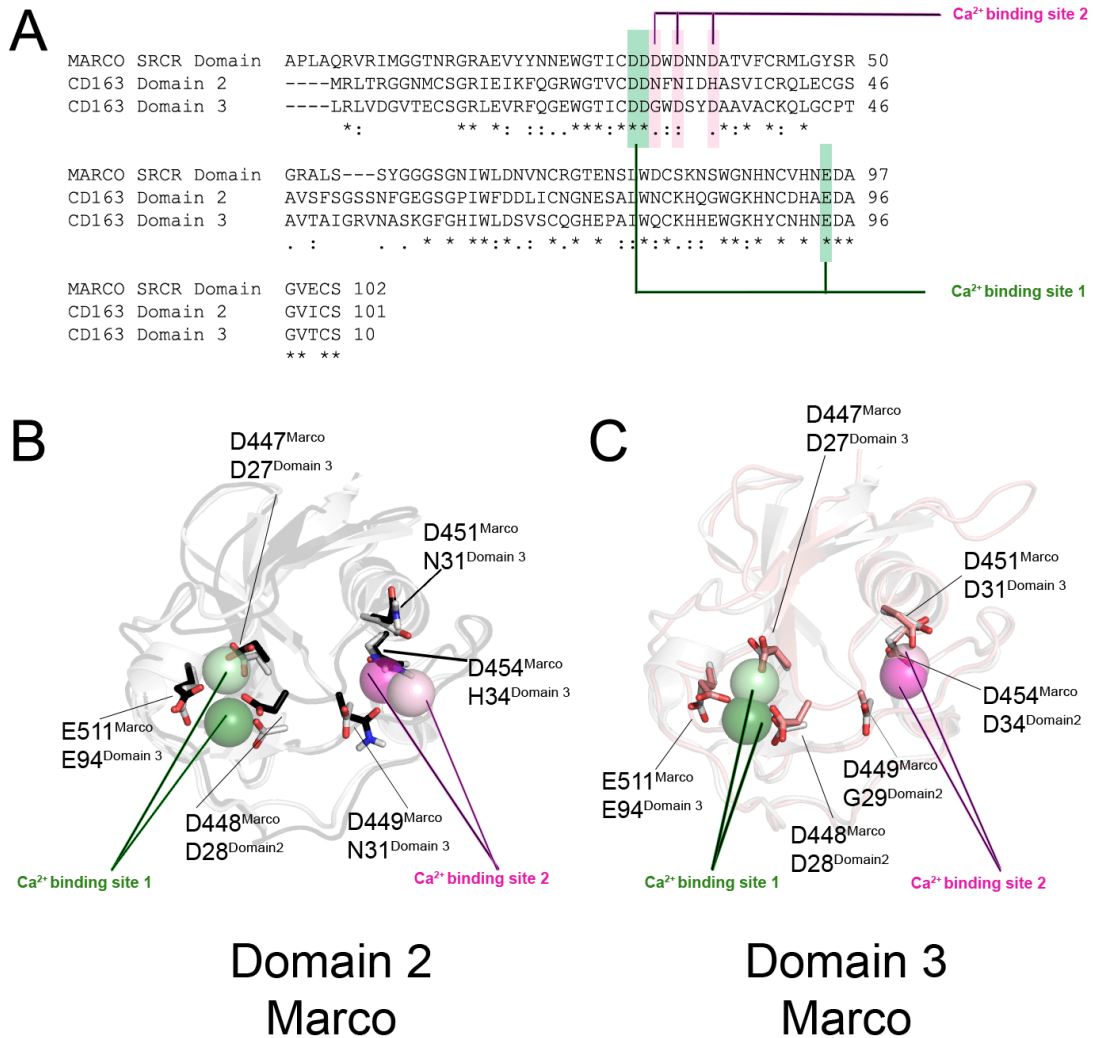


**Figure 3.2. Molecular models of CD163 domains 2 and 3** A) Sequence alignment of the SRCR domain of MARCO to CD163 domains 2 and 3 generated by ClustalOmega. The acid residue cluster coordinated to the  $\text{Ca}^{2+}$  binding site 1 (highlighted in green) is conserved in domains 2 and 3. On the other hand, the acidic residue cluster coordinating  $\text{Ca}^{2+}$  binding site 2 is 66% conserved in domain 3 (highlighted in pink). B). The crystal structure of the SRCR domain of MARCO (shown in white) superimposed on the molecular models of domain 2 (black) and 3 (salmon) generated by Modeller<sup>97</sup>. The  $\text{Ca}^{2+}$  ions are colored in darker green and pink in the MARCO structure and lighter (green and pink) colors are used to show  $\text{Ca}^{2+}$  ions coordinated in the domain 2 and 3 models.

As Figure 3.2 illustrates, one of the  $\text{Ca}^{2+}$  containing acidic residue cluster (27D/28D/94E) is conserved in domain 2 (corresponding to 27D/28D/94E) FIGURE 3.1B and 3 (27D/28D/94E) and will be referred as  $\text{Ca}^{2+}$  site 1. The second  $\text{Ca}^{2+}$  binding site found in MARCO (coordinated with D29, D31, D34) is not conserved in domain 2 (corresponding to N29, N31, and H4) and is only partially conserved in domain 3 (27G/28D/94E) and will be referred to as  $\text{Ca}^{2+}$  site 2. In models generated of domain 2 and 3,  $\text{Ca}^{2+}$  is modeled at both site 1 and 2 to further characterize the specific purpose of  $\text{Ca}^{2+}$  on site 1 in reference to the flexibility and preferred confirmations of the models.

The  $\text{Ca}^{2+}$  sites in calcium-binding proteins have a diverse set of polygonal geometries and adopt a wide range of ligand coordination. Commonly, calcium binding proteins prefer to adopt octahedral, trigonal bipyramidal, and distorted geometries<sup>104</sup> composed of oxygen atoms from side chains, backbone carbonyl groups, and water molecules<sup>105</sup>. An acidic triad cluster called the “DxDxD motif”<sup>106</sup> (as found in the MARCO protein and CD163 domain 2, 3, 7, 8), is frequently conserved in calcium binding proteins. Although many proteins with the DxDxD motifs probably share a common ancestor, some appear to have evolved independently<sup>106</sup>.

The calcium binding sites in domain 2 and 3 models were evaluated by comparing the calcium binding sites to other known receptors involved in calcium dependent protein-protein interactions. Cubilin, LDLR, and reelin are all endocytic receptors in which the acidic clusters in their calcium binding sites interact with basic residues on their respective ligands. This is consistent with Hb/Hp/CD163 experimental results indicating the acidic residue cluster in CD163 domain 2 and 3 and basic residues in Hp are critical for Hb/Hp associations with CD163. Table 3.2 lists these various calcium binding proteins involved in calcium-dependent, receptor-ligand Interactions. The distances between  $\text{Ca}^{2+}$  to coordinating oxygen atom in the acidic residue were measured. The molecular models of domain 2 and distances to the calcium fell within

the 2.2-2.9 Å, which is expected, between oxygen atoms of basic residues and bound  $\text{Ca}^{2+}$  <sup>107</sup>.

**Table 3.2.** Comparisons of the calcium-binding sites in the modeled CD163 domains 2 and 3 molecular models to  $\text{Ca}^{2+}$  binding sites in proteins with known structures

|                   | ASP- $\text{Ca}^{2+}$<br>distance | ASP- $\text{Ca}^{2+}$<br>distance | GLU-<br>$\text{Ca}^{2+}$<br>distance | PBD:ID              |
|-------------------|-----------------------------------|-----------------------------------|--------------------------------------|---------------------|
| Usual             | 2.2-2.6Å                          | 2.2-2.6Å                          | 2.2-2.6Å                             | NA*                 |
| Cubilin (site 1)  | 2.3                               | 2.3                               | 2.3                                  | 3KQ4 <sup>108</sup> |
| Cubilin (site 2)  | 2.3, 2.7                          | 2.3                               | 2.3                                  | 3KQ4 <sup>108</sup> |
| LDLR              | 2.4                               | ---                               | 2.5                                  | 2W2O <sup>109</sup> |
| Reelin            | 2.3                               | 2.3                               | 2.3                                  | 3A7Q <sup>110</sup> |
| CD163<br>Domain 2 | 2.2                               | 2.2                               | 2.2                                  | NA                  |
| CD163<br>Domain 3 | 2.2                               | 2.3, 2.2                          | 2.3                                  | NA                  |

\*NA, not applicable

The results of CD163 molecular models suggest  $\text{Ca}^{2+}$  stabilizes the acidic residue clusters, but no significant structural changes are observed in the overall models of  $\text{Ca}^{2+}$  bound CD163. The  $\text{Ca}^{2+}$  binding sites are also consistent with geometries found within other  $\text{Ca}^{2+}$  binding proteins. The dynamic effect of  $\text{Ca}^{2+}$  will further be studied through MD simulations.

### 3.3.2. Molecular dynamics CD163 domain 2 and 3.

Since there was no significant structural changes  $\text{Ca}^{2+}$  has previously been shown to be critical for CD163 domains 2 and 3 stability and Hb/Hp/CD163 complex formation. As mentioned above, CD163 domains 2 and 3 contain a conserved acidic residue motif, coordinated with a calcium atom at site 1 Figure 3.1A and 3.1B. However it remains unclear whether another calcium binding site as shown in Figure 3.1A and 3.1B is conserved in domain 3. In order to investigate the role of  $\text{Ca}^{2+}$  in domain 2 and 3

MD simulations were used to determine how  $\text{Ca}^{2+}$  binding might affect the overall structural fluctuations the modeled CD163 domains.

- **Domain 2 MD simulations**

The root mean square deviations (RMSDs) calculated over the course of 60 ns of domain 2 is shown in Figure 3.2A. The 60 ns MD simulations results suggest that domain 2 with  $\text{Ca}^{2+}$  at site 1 is more rigid than other forms resulting in RMSDs of 0.17 nm relative to the starting structure. Conversely, apo domain 2 and especially domain 2 with  $\text{Ca}^{2+}$  placed at site 2 appear to be more flexible with overall RMSDs of 0.21 nm and 2.5 nm, respectively. This result is expected because the  $\text{Ca}^{2+}$  binding site 2 is not conserved in domain 2 and further demonstrates the importance of  $\text{Ca}^{2+}$  being modeled in an energetically favorable site. At 41 ns, the RMSDs values show an increase for domain 2 bound to  $\text{Ca}^{2+}$  binding site 2. This may be because the  $\text{Ca}^{2+}$  is placed at an unfavorable site where there are no negativity charged residues. When  $\text{Ca}^{2+}$  is placed at both binding sites 1 and 2, RMSDs results in Figure 3.3A suggests the protein is more rigid (RMSD 0.20 nm) likely due to the calcium binding at site 1. In these simulations, the  $\text{Ca}^{2+}$  ion at site 2 dissociates from the protein at 30 ns (shown in Figure 3.3B and in more detail in Figure 3.4). These results further support the importance of  $\text{Ca}^{2+}$  at binding site 1 for the protein's conformational integrity. Figure 3.2C shows the calculated  $C_{\alpha}$  root mean square fluctuations (RMSF) per residue in domain 2. According to  $C_{\alpha}$  RMSFs per residue values, apo-domain 2 loops are especially more flexible from starting structures compared of CD163 domain 2 with  $\text{Ca}^{2+}$  at binding site 1.

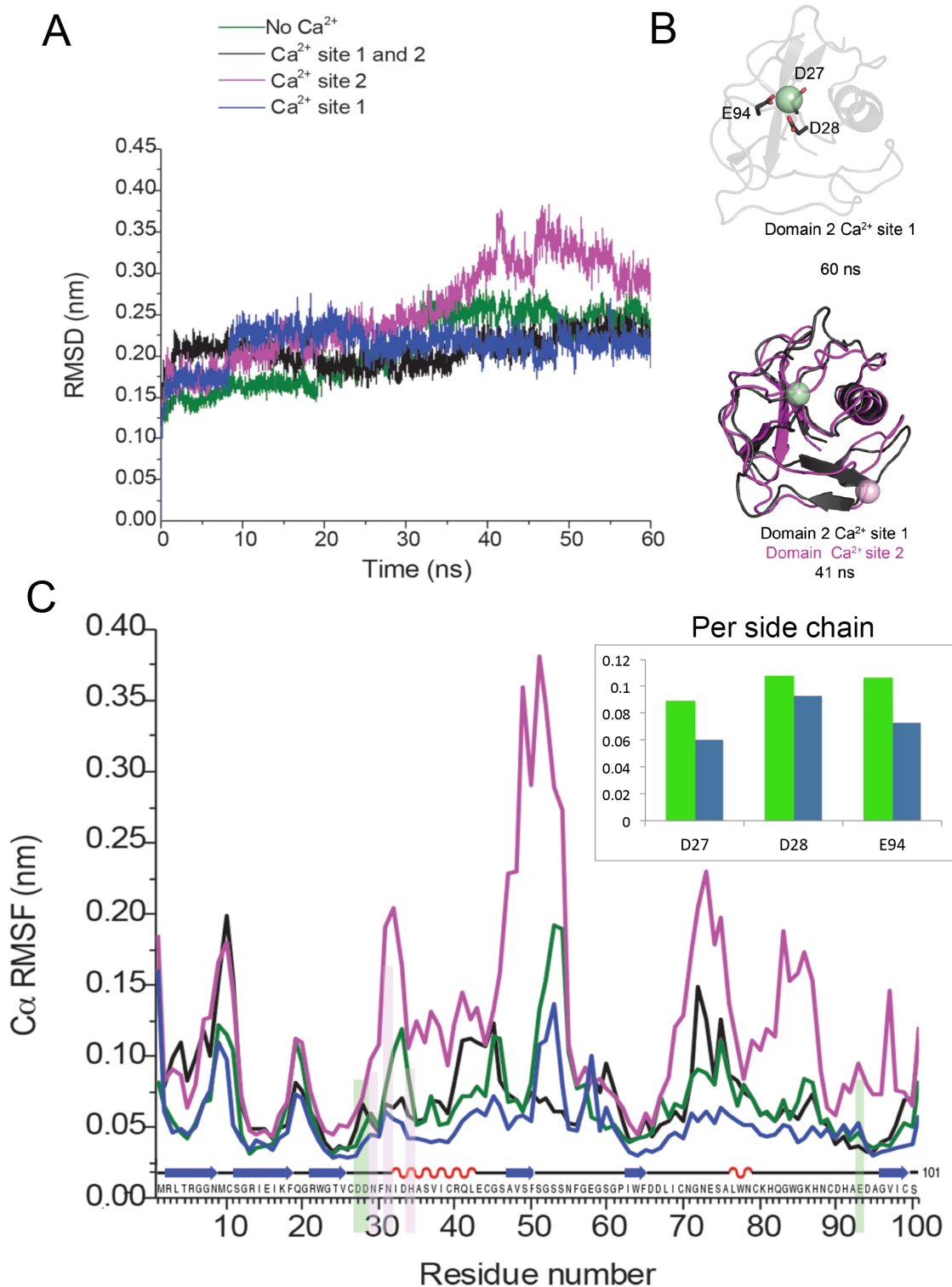


**Figure 3.3. Ca<sup>2+</sup> binding to site 1 in domain 2 reduces fluctuations.** A), C<sub>α</sub> RMSDs calculated over the course of 60 ns. B), Domain 2 with Ca<sup>2+</sup> bound to site 1 is the least flexible model. At 41 ns, the RMSDs values increase in domain 2 with Ca<sup>2+</sup> bound to site 2. This is likely due to the placement of Ca<sup>2+</sup> in an unfavorable site where

there are no negatively charged residues. C), Calculated  $C_{\alpha}$  root mean square fluctuations (RMSFs) per residue in domain 2. In the inset, the side-chain RMSFs per residue for the  $\text{Ca}^{2+}$  binding residues in site 1 are shown in blue with the apo RMSFs in green.

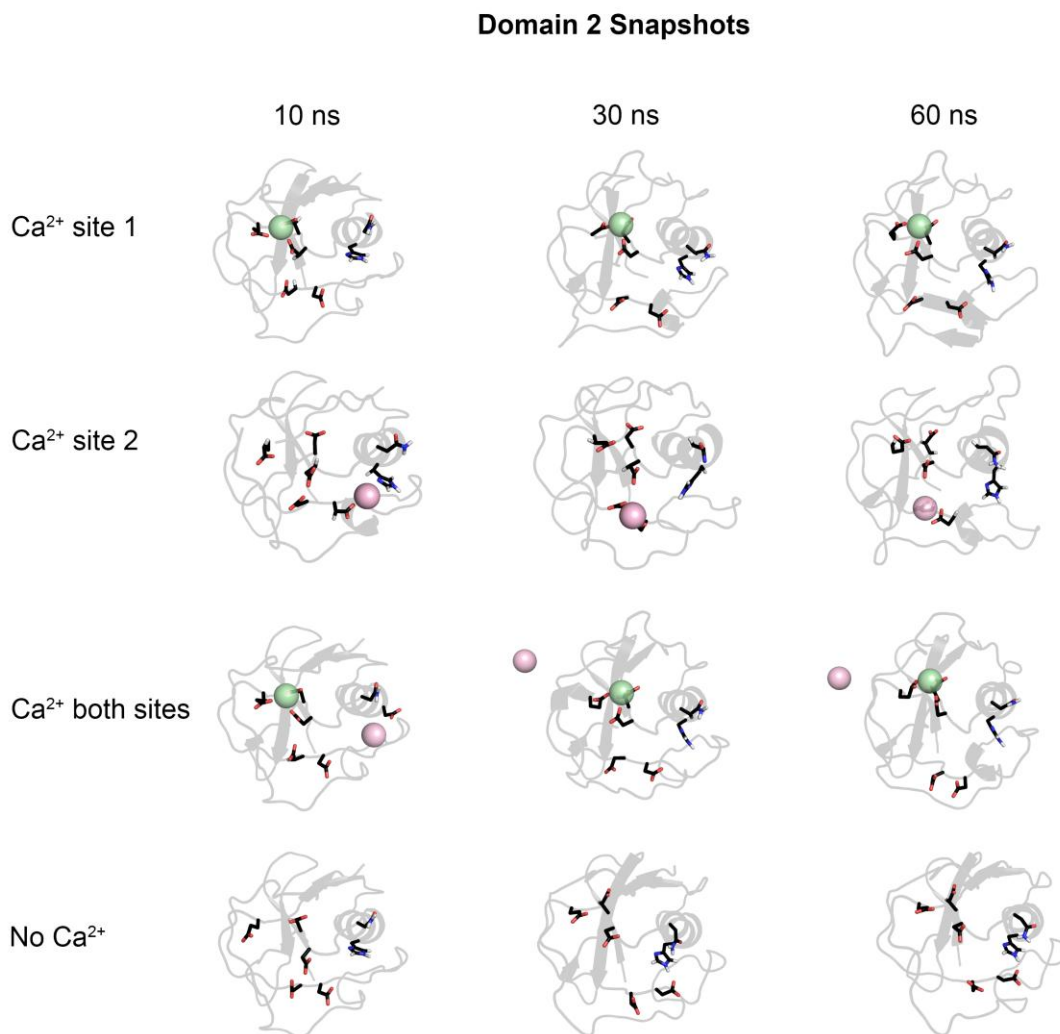


**Figure 3.4. Snapshots of the domain 2 structures during the MD simulations.** Note the loss of  $\text{Ca}^{2+}$  from site 2 as might be expected from the unfavorable sequence of this putative binding site.

- **Domain 3 MD simulations**

Similar to CD163 domain 2, the overall RMSD of CD163 domain 3 with  $\text{Ca}^{2+}$  at site 1 (0.19 nm) was observed to be less than domain 3 with  $\text{Ca}^{2+}$  at site 2 (0.22 nm), domain 3 with  $\text{Ca}^{2+}$  at site 1 and 2 (0.20 nm), apo-CD163 (0.23 nm) (Figure 3.5A). Unlike domain 2, the  $\text{Ca}^{2+}$  ion at binding site 2 stayed bound to domain 3 during the entire 60ns simulation, but rendered domain 3 more flexible as shown in Figure 3.5C. This may be due the  $\text{Ca}^{2+}$  binding site 2 being energetically more favorable than domain 2 yet still not in the proper coordination for  $\text{Ca}^{2+}$  ions. It is probable; a second  $\text{Ca}^{2+}$  ion is not preferred on site 2 in domain 3 as well. Since CD163 domain 2 and 3 models with  $\text{Ca}^{2+}$  bound to site 1 produced the most rigid conformations, their energy-minimized models were used for the molecular docking of Hb/Hp complexes to CD163 models.



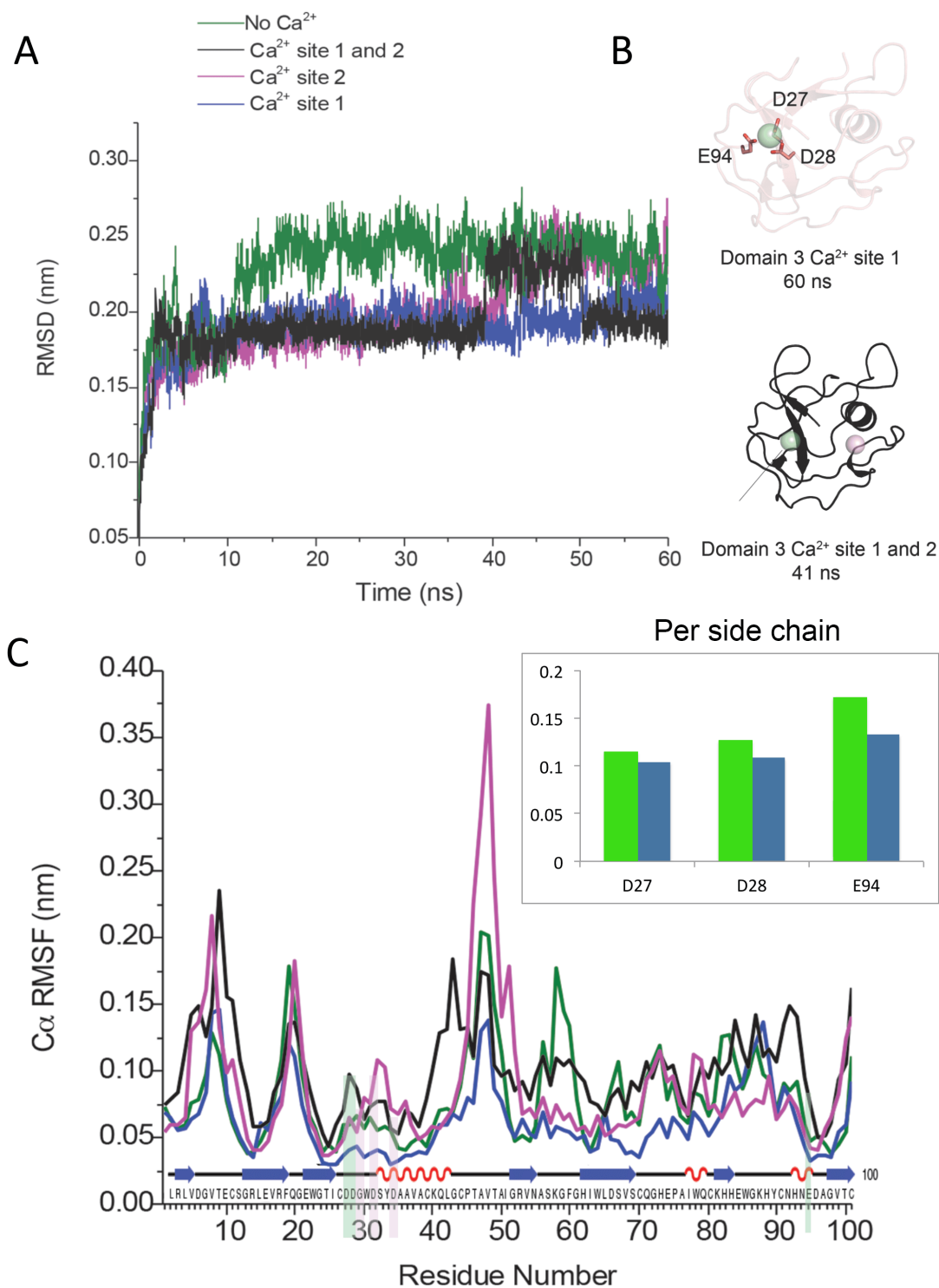


**Figure 3.5 Ca<sup>2+</sup> binding to site 1 in domain 3 reduces fluctuations..** Similar to the results for domain 2, Ca<sup>2+</sup> binding at site 1 appears to be important for constraining the protein structure. A), C<sub>α</sub> RMSDs over the course of 60ns for domain 3. B), C<sub>α</sub> RSMFs per residue calculated from the MD simulations. Domain 2 shows the lowest RMSFs when Ca<sup>2+</sup> is bound to site 1, as also observed for domain 2. C), Results of the domain 3

models with  $\text{Ca}^{2+}$  at site 1 (black) at the end of the simulation and domain 3 model with  $\text{Ca}^{2+}$  on both site 1 and 2 at 41 ns. Inset: The side-chain RMSFs per residue for the  $\text{Ca}^{2+}$  binding residues in site 1 shown in blue and apo domain 3 shown in green.

### 3.3.3. Molecular docking of Hb/Hp complex to CD163 domains.

Previous biophysical experimental<sup>12, 92, 95</sup> data enabled us to develop 4 different hypotheses for the Hb/Hp/CD163 interactions and incorporate distinct interaction restraints<sup>12,92</sup> in Haddock (inputs and results shown in Table 3.1). The basic Hp loop in Hb/Hp complexes could be interacting with the negative acidic residue cluster coordinating with  $\text{Ca}^{2+}$  site 1 in a) just domain 2, b) just domain 3, c) domain 2 at R252<sup>Hp</sup> and domain 3 at K262<sup>Hp</sup> or d) domain 2 at R252<sup>Hp</sup> and domain 3 at K262<sup>Hp</sup>. Since previous experiments and our MD simulations suggest that  $\text{Ca}^{2+}$ <sup>95</sup> is important for rigidity, models of domain 2 and 3 with  $\text{Ca}^{2+}$  bound to site 1 was used in the docking simulations. The best ranked molecular models (on the basis of the lowest Haddock score) in each hypothesis that was generated by Haddock<sup>43</sup> are depicted in Figure 3.5 and 3.6. All models agree with previous experimental mutagenesis<sup>12</sup>. Where in all cases, residues that were experimentally determined to be critical for binding are located in the binding interface. The oxygen atoms in the acidic residues cluster in the CD163 models are still coordinating with the bound  $\text{Ca}^{2+}$  ions with the appropriate 2.2-2.6 Å distance lengths.

- **Hp/Domain 2 vs Hp/Domain 3 models.**

Figure 3.4 displays experimentally driven<sup>12,92</sup> molecular models of Hb/Hp docked to just domain 2 (Figure 3.6A), or just domain 3 (Figure 3.6B). In the Hb/Hp/domain 2 interaction, residues D28<sup>domain 2</sup> and E94<sup>domain 2</sup> form hydrogen bonds with K262<sup>Hp</sup> and R252<sup>Hp</sup> respectively (Figure 3.6A). Hb/Hp/domain 3 molecular models, Figure 3.6B), show a similar arrangement of residues and interactions. The main difference is R262<sup>Hp</sup> additionally forms a hydrogen bond with an oxygen atom in D27<sup>domain 3</sup> (Figure 3.6B). Haddock scores for Hb/Hp/domain 3 complexes, -40.1 +/- 3.7, is slightly higher than that

for Hb/Hp/domain 2,  $-60.7 \pm 8.9$ . The additional hydrogen bond in the Hp/domain 3 models may have contributed to the score since electrostatic energies (which includes hydrogen bonds) are weighted into the Haddock score.

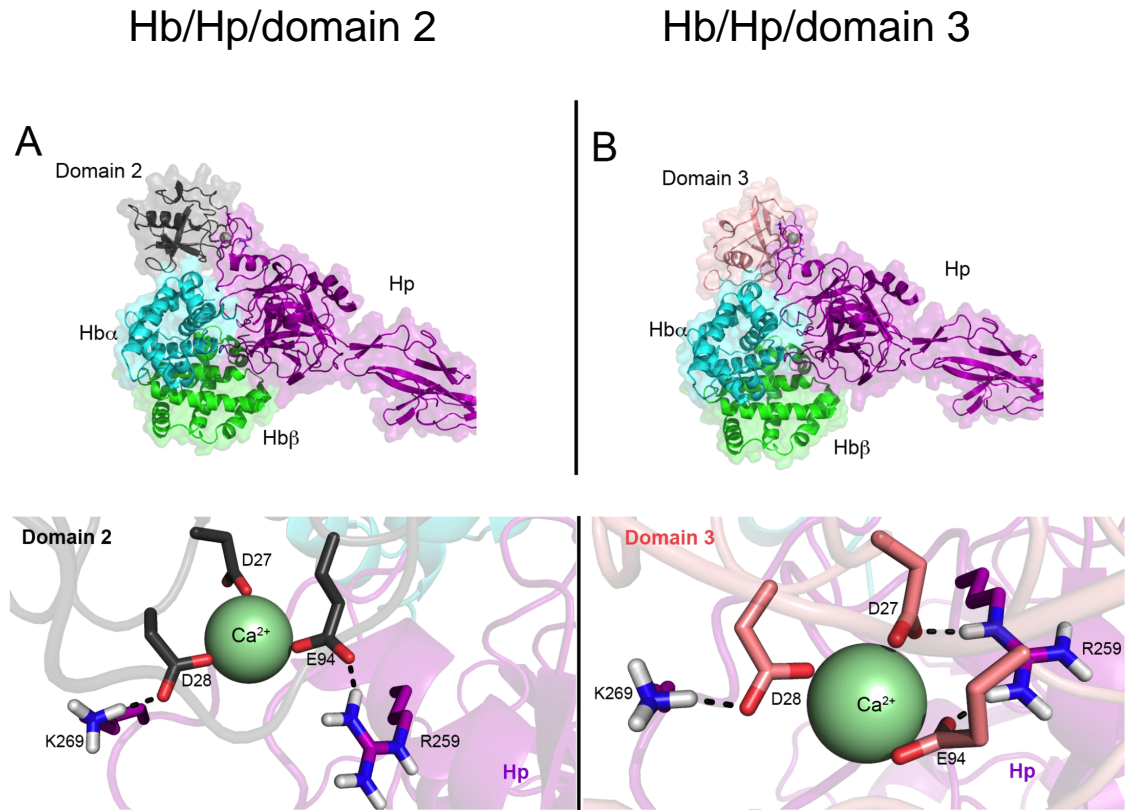


**Figure 3.6. Experimentally driven molecular models of Hb/Hp in complex with A), CD163 domain 2 with  $\text{Ca}^{2+}$  bound to site 1, or B) CD163 domain 3 with  $\text{Ca}^{2+}$  bound to site 1.** When Hb/Hp complexes are docked to domain 2, residues  $\text{D28}^{\text{domain2}}$  and  $\text{E94}^{\text{domain2}}$  interact with  $\text{K269}^{\text{Hp}}$  and  $\text{R259}^{\text{Hp}}$  respectively (shown in A), while in Hb/Hp/domain 3 molecular models, an additional residue,  $\text{D27}^{\text{domain2}}$ , interacts with  $\text{R269}^{\text{Hp}}$ .

- **Hp/domain 2-domain 3 vs Hp/domain 3-domain 2 models.**

In various calcium-dependent receptor-ligand interactions, a single basic residue interacts with the acidic residues coordinating calcium-binding<sup>108-110</sup> (Table 3.2). This led us to speculate that each of the basic residues on Hp could be independently interacting with an acidic residue in domain 2 and 3. In addition, various unsuccessful attempts to locate a CD163 binding site on Hb<sup>12</sup> also drove our thought process to generate models of domains 2 and 3 interacting on the basic residues in Hp loop. Molecular models of the Hb/Hp/CD163 complex were constructed based on two alternative hypotheses: (i) R262<sup>Hp</sup> and K252<sup>Hp</sup> interact with acidic residues in domains 2 and domain 3 respectively (Figure 3.6A) or (ii) R262<sup>Hp</sup> and K252<sup>Hp</sup> interact with Hp domains 3 and domain 2 (Figure 3.6B). Table 3.1. summarizes the interactions and restraints used in protein-protein docking and the Haddock score.

In order to create Hb/Hp/CD163 molecular models specific to R262<sup>Hp</sup> and K252<sup>Hp</sup> interacting with domains 2 and domain 3 respectively, the acidic residue cluster in CD163 domain 2 with Ca<sup>2+</sup> bound to site 1 and R252<sup>Hp</sup> were set as active in Haddock. The highest ranked Hb/Hp/domain 2 model was selected and docked to domain 3. In a separate run, the acidic residue cluster in domain 3 and K262<sup>Hp</sup> was set as active. The results of this output are shown in Figure 3.6A. The binding interface of the generated molecular model was analyzed and indicated K262<sup>Hp</sup> formed salt bridges with D27<sup>Domain 3</sup>, and R252<sup>Hp</sup> formed salt bridges with D28<sup>domain 2</sup> and E94<sup>domain 3</sup>. Interestingly, oxygen atoms in T270<sup>Hp</sup> backbone oxygen atom and E267<sup>Hp</sup> side-chain oxygen atom coordinate Ca<sup>2+</sup> binding sites in domain 3 and domain 2 respectively, both having distances of 2.2Å. These results suggest that Ca<sup>2+</sup> helps to stabilize both the CD163 acidic clusters and the Hb/Hp/CD163 interface. The interactions between CD163 domains 2 and 3 were also analyzed. This interface appears to be stabilized by hydrogen bonds between Q19<sup>domain 2</sup>

and the backbones of V52<sup>domain 3</sup>, K87<sup>domain 2</sup> and Q71<sup>domain 3</sup>, and the backbone of I63<sup>domain 2</sup> and Y33<sup>domain 3</sup>.

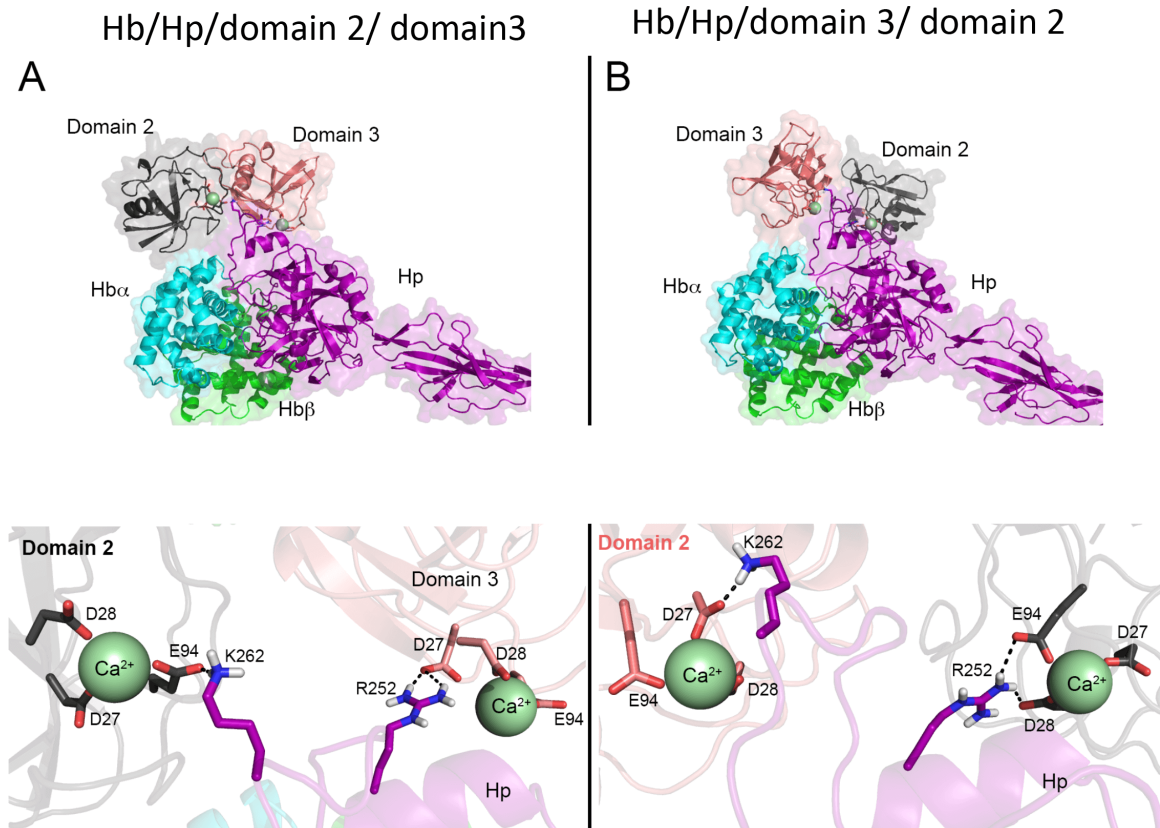


**Figure 3.7. Experimentally driven molecular models of Hb/Hp in complex with domains 2 and 3.** 2A), CD163 domain 3 with Ca<sup>2+</sup> bound to site 1 interacting with R252<sup>Hp</sup> and CD163 domain 2 with Ca<sup>2+</sup> bound to site 1 interacting with K262<sup>Hp</sup> (Haddock score: -27.0 +/- 6.9, or 2B), CD163 domain 2 with Ca<sup>2+</sup> bound to site 1 interacting with R252<sup>Hp</sup> and CD163 domain 3 with Ca<sup>2+</sup> bound to site 1 interacting with K262<sup>Hp</sup> (Haddock score: -37.8 +/- 5.1). Molecular models suggest there in the Hp loop, can simultaneously bind to two receptors. The binding interface between domain 2/domain 3 is also stabilized by hydrogen bonds (see results section).

To generate the Hb/Hp/CD1613 molecular models where R262<sup>Hp</sup> and K252<sup>Hp</sup> are interacting with CD163 domains 3 and domain 2 respectively, molecular models of the the acidic residue cluster in CD163 domain 2 with Ca<sup>2+</sup> bound to site 1 interacting with and K262<sup>Hp</sup> were first generated. The highest ranked Hb/Hp/domain 2 model was

selected to be docked to domain 3. In the next run, the acidic residue cluster in domain 3 and residue R252<sup>Hp</sup> were set as active and the binding interface of the highest ranked generated model was analyzed. The Hp/CD163 binding interfaces in these models were relatively similar to the previous models (Figure 3.5B). The major difference is T270<sup>Hp</sup> was no longer coordinated to the Ca<sup>2+</sup> ion in domain 2. The molecular models suggest R252<sup>Hp</sup> formed a salt bridge with D27<sup>Domain 3</sup> and K252<sup>Hp</sup> formed a salt bridge E94<sup>domain 2</sup>. Additionally, the interface between domains 2 and 3 showed fewer interactions than observed in the models discussed above, but Q71<sup>domain 3</sup> and Y33<sup>domain 3</sup> were still interface residues with hydrogen bonds between H87<sup>Domain 2</sup> and Q71<sup>domain 3</sup> as well as between D91<sup>domain 2</sup> and Y33<sup>domain 3</sup>.

These molecular models also agree with previous experimental mutagenesis results, and present 2 more possibilities for Hp/CD163 interactions in the Hb/Hp complex, and are consistent with previous acidic basic calcium dependent receptor interactions (Figure 3.9).

- **Hb/Hp/Apo domain 3**

According to previous experiments<sup>95</sup>, CD163 does not bind Hb/Hp complexes in Ca<sup>2+</sup> free conditions. We created molecular models of Hb/Hp/ apo-domain 3 complexes using the same parameters used to generate the Hb/Hp/domain 3 with Ca<sup>2+</sup> bound site 1 complexes. The results suggests, Hp/domain 3 interactions are still energetically favorable since the absence of Ca<sup>2+</sup> enabled the CD163 basics residues to form more salt bridges with the acidic residue cluster in Hp as shown in Figure 3.7. These results suggest the need for dynamics to monitor this interaction to better understand the importance of Ca<sup>2+</sup> in Hb/Hp/CD163 associations.

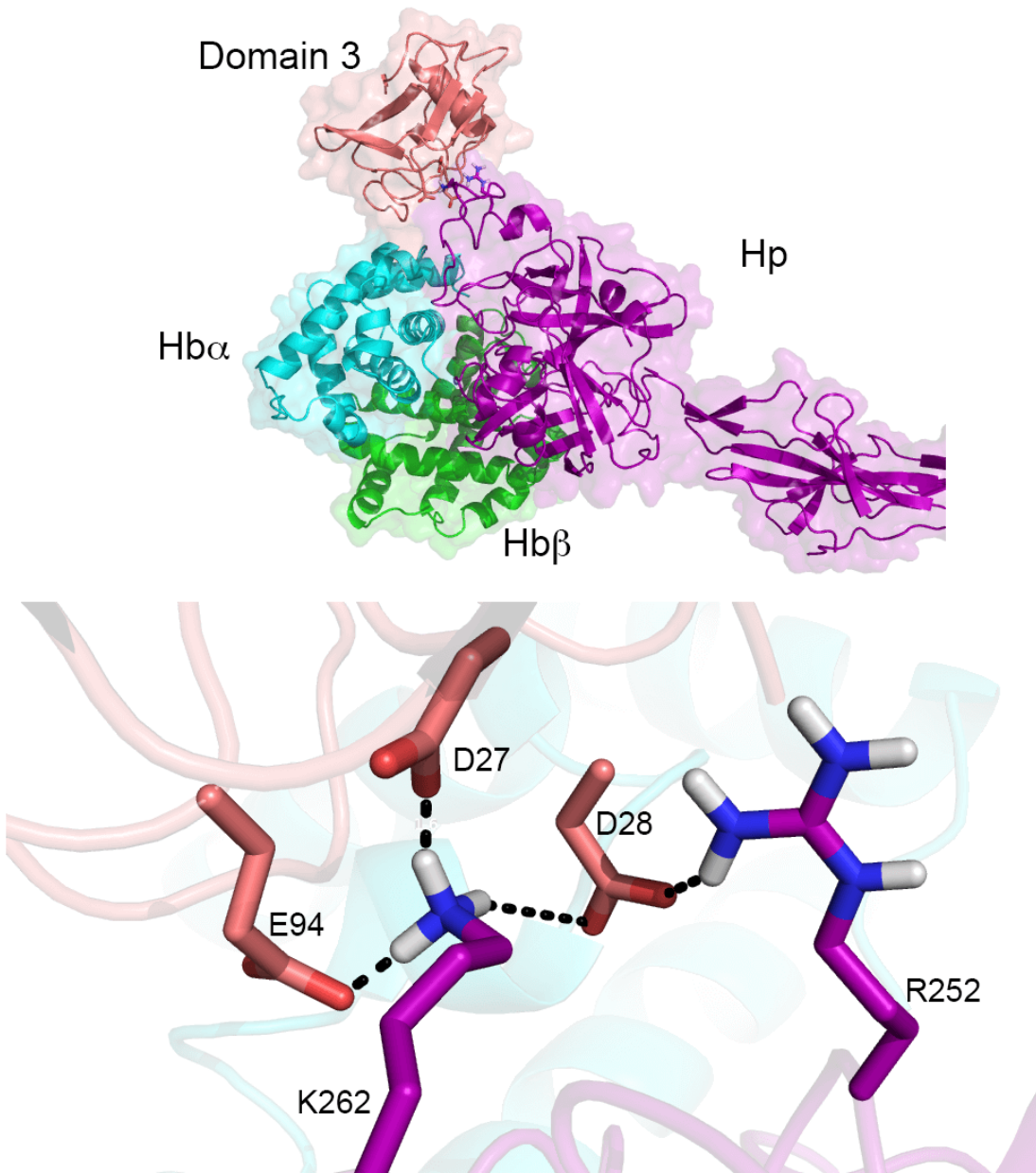


**Figure 3.8. Molecular models of Hb/Hp in complex with apo-domain 3.** According to previous experiments<sup>95</sup>, CD163 does not bind Hb/Hp complexes in  $\text{Ca}^{2+}$  free conditions. Our molecular models results show apo-domain 3 ( $\text{Ca}^{2+}$  free domain 3) still docks to Hp with all previously identified interface residues at the interface.

### 3.3.4. Molecular dynamics of Hp loop/domain 3

MD simulations were performed on  $\text{Ca}^{2+}$  bound and  $\text{Ca}^{2+}$  free Hp/CD163 domain3 complexes to further investigate the structural role  $\text{Ca}^{2+}$  in Hp/CD163

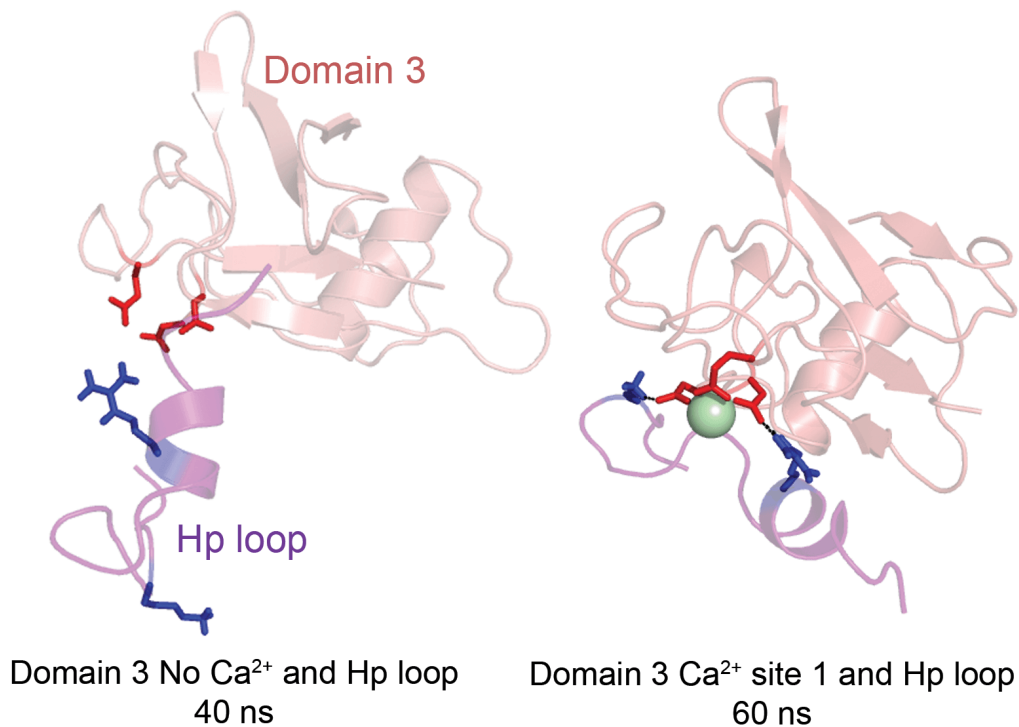
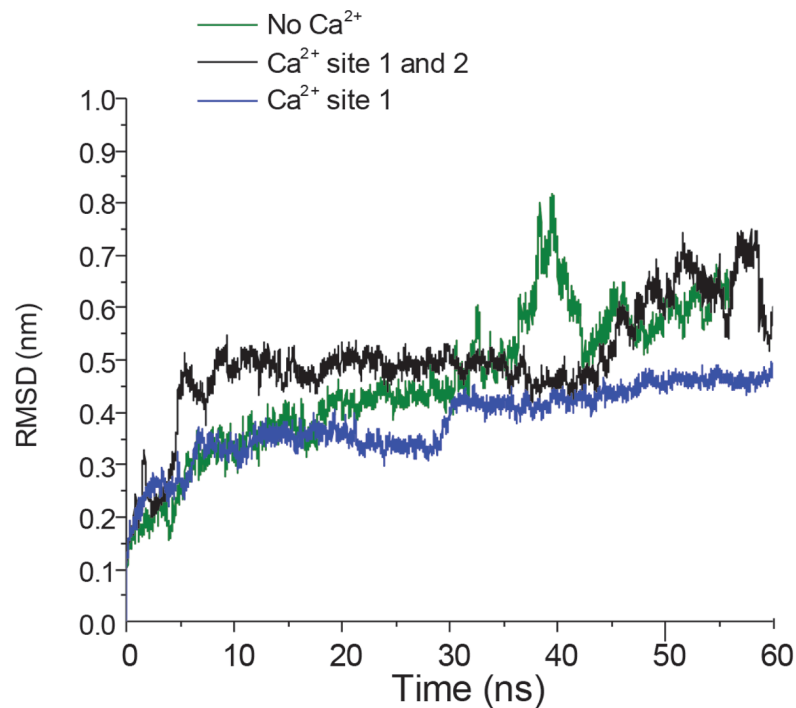
associations. Hp shares 91% sequence identity<sup>111</sup> with another protein called haptoglobin related protein (Hpr). Hpr binds Hb at high affinity, but does not bind CD163 because residues R252<sup>Hp</sup>, E261<sup>Hp</sup>, K262<sup>Hp</sup> and T264<sup>Hp</sup> in the CD163 recognition loop are replaced with T253<sup>Hpr</sup>, K262<sup>Hpr</sup>, W263<sup>Hpr</sup>, and A265<sup>Hpr</sup>. Previously, a 26 amino-acid peptide containing the R252<sup>Hp</sup> – T264<sup>Hp</sup> loop region was synthesized<sup>92</sup> and experimentally shown to compete with Hb/Hp binding to CD163 whereas the peptide from the same region in Hpr did not disrupt Hb/Hp/CD163 complex formation<sup>92</sup>. These results suggest that a peptide containing the essential basic Hp residues is sufficient to monitor Hp/CD163 interactions. The Hb/Hp/domain 3 molecular models (Figure 3.5B) were truncated to just the Hp loop (residues 244-261) in complex with domain 3 and the Ca<sup>2+</sup> bound and apo states of Hp loop/domain 3 complexes were studied dynamically using molecular dynamics simulations. These simulations were conducted to understand whether Ca<sup>2+</sup> is essential for these interactions to occur.

The molecular dynamics results suggest a wonderful explanation as to why Ca<sup>2+</sup> is important for Hp/CD163 associations (Figure 3.9, 3.10, and 3.11). The Hp loop/CD163 domain 3 with Ca<sup>2+</sup> bound to site 1 remains bound during the entire 60 ns simulation with overall RMSDs of 0.30 nm but the interaction does change slightly. During this simulation, K252<sup>Hp</sup> maintains its interaction with D28<sup>domain 3</sup> while, R252<sup>Hp</sup> shifts from interacting with both D27<sup>domain 3</sup> and E94<sup>domain 3</sup> (Figure 3.5B) to just E94<sup>domain 3</sup> by the end of the simulation (as shown in Figure 3.9 and 3.10). This result is pretty interesting because the Hp loop/CD163 domain 3 with Ca<sup>2+</sup> bound to site 1 models become more similar to interactions between Hp loop/CD163 domain 2 with Ca<sup>2+</sup> bound to site 1 where R252<sup>Hp</sup> is only interacting with E94<sup>domain 2</sup> as shown in Figure 3.5A. Additionally, this result probably suggests R252<sup>Hp</sup> not interacting with D27<sup>domain 3</sup> is energetically more favorable, since this allows the oxygen atom in D27<sup>domain 3</sup> to stay coordinated to Ca<sup>2+</sup>. On the other hand, the Hp loop/apo-domain 3 complexes dissociate completely after 20

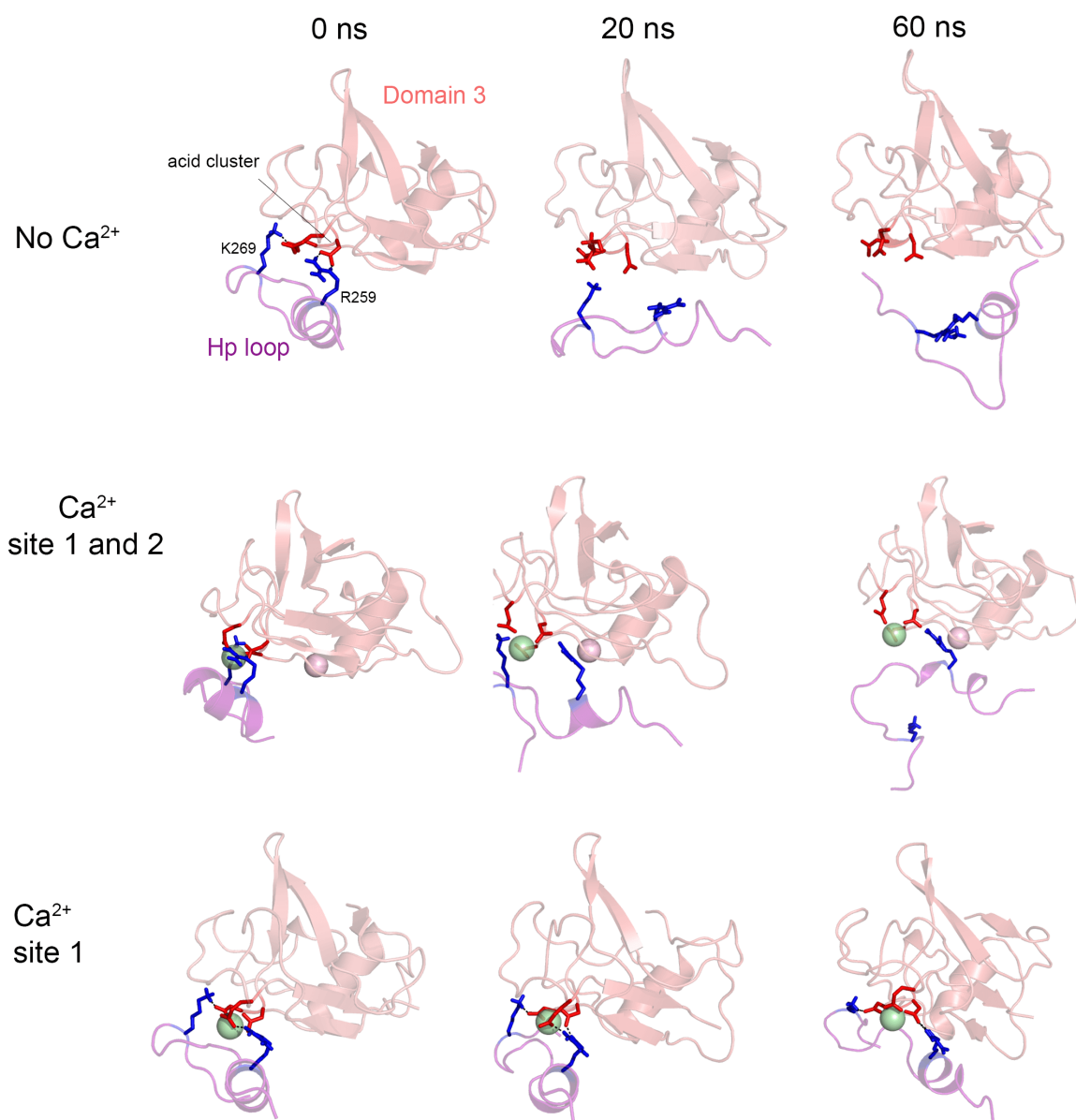


ns and the RMSD were larger with an overall RMSD of 0.50 nm. This suggests that  $\text{Ca}^{2+}$  facilitates domain 3 associations with Hp, agreeing excellently with experiments. In the simulations performed on Hp loop/CD163 domain 3 bound to site 1 and 2, the Hp loop stays bound to domain 3 but eventually  $\text{K262}^{\text{Hp}}$  dissociates from the and stay dissociated (Figure 3.9 and 3.10). The overall RMSDs calculated in the Hp loop/domain 3 with  $\text{Ca}^{2+}$  bound to site 1 and 2 models are also higher than Hp loop/domain 3 with  $\text{Ca}^{2+}$  bound to site 1 models (0.50nm). The results of this experiment further show the significance and specificity of  $\text{Ca}^{2+}$  at site 1.

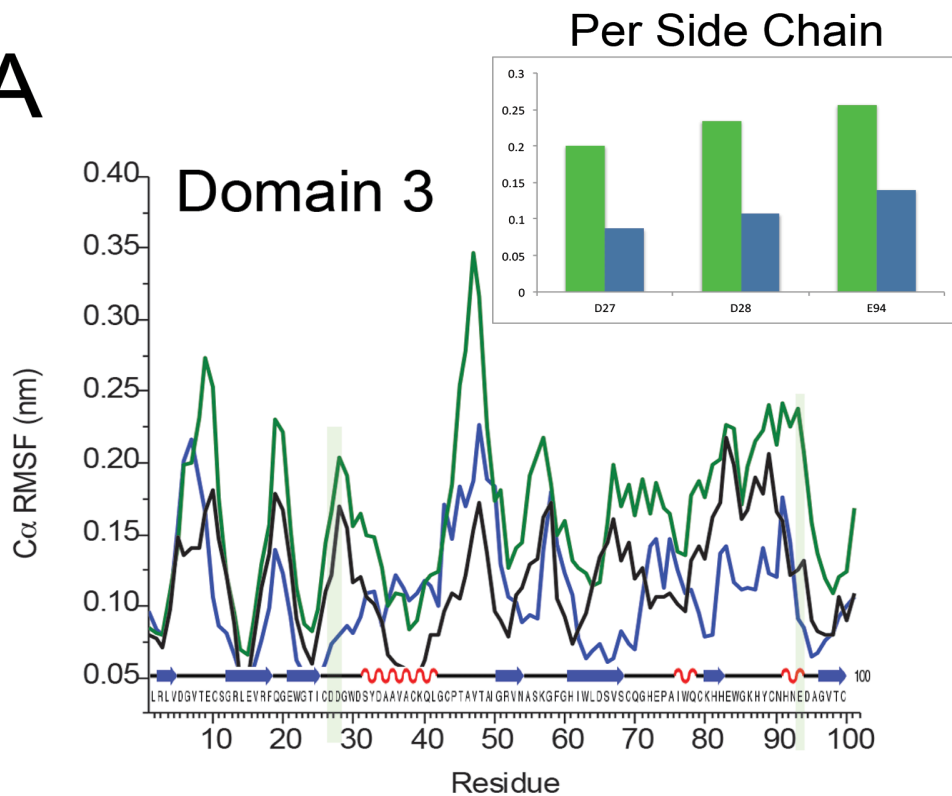
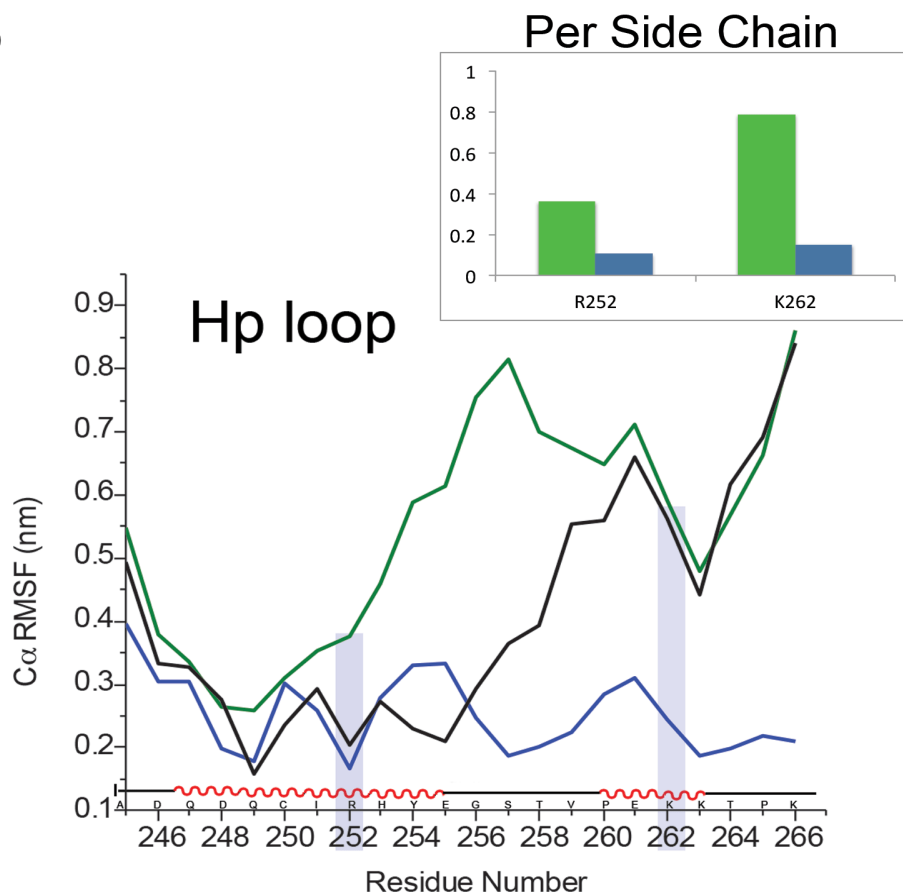
These results suggest new helpful insights in understanding the Hb/Hp/CD163 pathway more explicitly.  $\text{Ca}^{2+}$  bound CD163 adopts a rigid confirmation, stabilizing the coordinating D27/D28/E94 acidic residue cluster. This rigid confirmation is favorable for the basic Hp residues R252 and K262 to form salt bridges with the acidic residue cluster. After endocytosis occurs, the pH drops releasing  $\text{Ca}^{2+}$ , rendering CD163 more flexible. The flexibility of apo-CD163 induces the dissociation of Hb-Hp complexes. Then continuing the understood Hb/Hp/CD163 pathway, apo-CD163 receptor is now able to recycle to the cell well and Hb/Hp proceed to be degraded in the lysosome.



**Figure 3.9. Molecular models of Hp loop/CD163 domain 3 with Ca<sup>2+</sup> bound to site 1 stays in complex and Hp loop/apo-CD163 domain 3 dissociate during MD simulation.** Hp loop/ CD163 domain 3 with Ca<sup>2+</sup> bound to site 1 remains in complex with Hp over the entire 60 ns simulation with overall RMSD of 0.3 nm (represented in blue). On the other hand, the Hp loop/apo- domain 3 complex dissociates completely after 20 ns and the RMSD was larger with an overall RMSD of 0.5 nm (represented in green).



**Figure 3.10. Hp loop/CD163 domain 3 with  $\text{Ca}^{2+}$  bound to site 1 stays in complex and Hp loop/apo-CD163 domain 3 dissociate during MD simulation.** Snapshots from MD simulations performed on Hp loop/apo-domain 3, Hp loop/CD163 domain 3 with  $\text{Ca}^{2+}$  bound to site 1 and 2, and Hp loop/CD163 domain 3 with  $\text{Ca}^{2+}$  bound to site 1.

**A****B**

**Figure 3.11. Fluctuations of the Hp loop/CD163 domain 3 model.** Calculated  $C_{\alpha}$  RMSFs per residue during the 60 ns in A) CD163 domain 3 the Hp loop (apo- green,  $Ca^{2+}$  bound to site 1- blue, and  $Ca^{2+}$  site 1 and 2 - black). B), The side-chain RMSFs per residue of the interacting residues in the apo (green) and with  $Ca^{2+}$  bound to site 1 models (blue) are displayed by bar graphs. The calculated side-chain RMSFs per residue show a dramatic difference in the interface residues of the Hp loop/domain 3 complex. These MD simulations results suggest the importance of  $Ca^{2+}$  in maintaining and stabilizing the association of the complexes.

### 3.4. Conclusions

We have successfully generated molecular models of CD163 domain 2, domain 3, and Hb/Hp/CD163 complexes that correlate with the existing mutagenesis and SPR experimental data on Hb/Hp/CD163 complexes. The molecular models are consistent with the interface of experimentally solved protein-protein structures with calcium-dependent receptor-ligand interactions as shown in Figure 3.12, Table 3.1. The Molecular dynamics simulation results suggest that the apo models of domain 2 and 3 are more flexible than the  $\text{Ca}^{2+}$  bound models. However, since the both apo and  $\text{Ca}^{2+}$  bound models formed a favorable interface in Hb/Hp/CD163 models, molecular dynamic simulations was employed to clarify the importance of  $\text{Ca}^{2+}$ . The molecular dynamics simulation results show that the Hp CD163 recognition loop stays bound to CD163 when  $\text{Ca}^{2+}$  is present but when  $\text{Ca}^{2+}$  is absent, the complex dissociates. These results give explanation as to why calcium is important of Hp/CD163 associations.

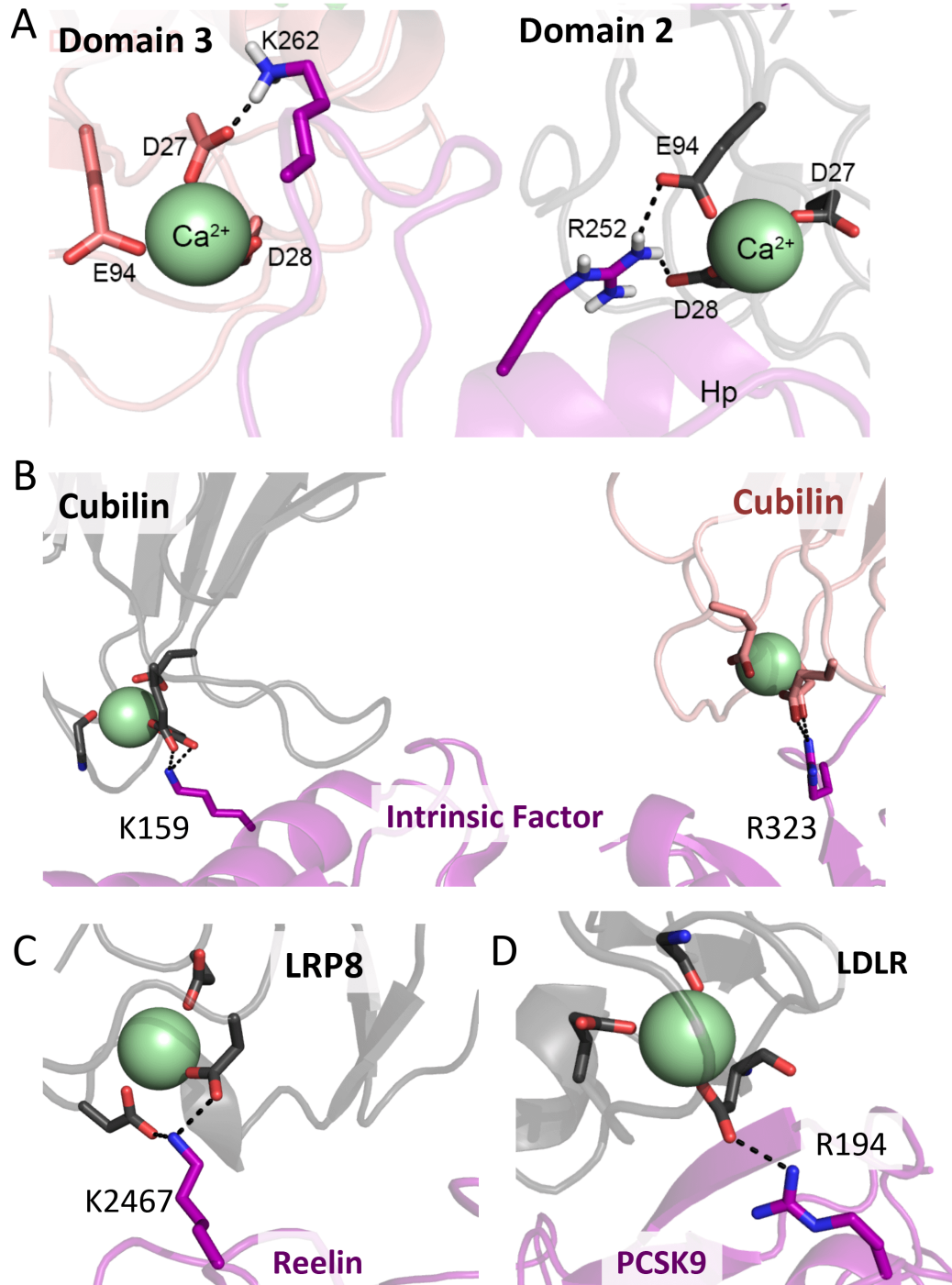


**Figure 3.12. Comparisons of Hp/domain 3 interface in the Hb/Hp/CD163 molecular models to the interface of experimentally solved protein-protein structures with calcium-dependent receptor-ligand interactions. A), Hb/Hp/CD163, B), intrinsic factor/cubilin (PDBID:3KQ4<sup>108</sup>), C), Reelin/LRP8 (PDBID:3A7Q<sup>110</sup>), D), PCSK9/LDLR (PDBID:2W2O<sup>109</sup>).**

**Table 3.3.** Comparison of the distances between acidic and basic residues in calcium-dependent, electrostatic receptor-ligand interactions. In this case, Hb/Hp/CD163 distance measurements exclude hydrogen since hydrogen is not present in the X-ray structures as well.

| Protein- Protein Complex  | X-R(-X)<br>distance | X-K(-X)<br>distance |
|---------------------------|---------------------|---------------------|
| Cubilin*/Intrinsic Factor | 2.9 Å, 3.24 Å       | 2.9 Å, 2.7Å         |
| PCSK9/LDLR                | ----                | 2.7 Å               |
| LRP8/ Reelin              |                     | 2.7, 2.7 Å          |
| Hb/Hp/Domain 2            | 2.8 Å               | 2.7                 |
| Hb/Hp/ Domain 3           | 2.7Å, 2.7 Å         | 2.8 Å               |
| Hb/Hp/ Domain 2/domain 3  | 2.7 Å, 2.9 Å        | 2.7 Å               |
| Hb/Hp/ Domain 3/domain 2  | 2.7 Å, 3.4 Å        | 2.6 Å               |



## CHAPTER 4

### SUMMARY AND FUTURE OUTLOOKS

Elucidating the structural details and dynamics in Hp physiological interactions are important for the development of Hp-based therapeutics. Myoglobin (Mb) is highly homologous to Hb and shares high structural and sequence similarity with both  $\alpha$ - and  $\beta$ -chains of Hb, with residues critical for Hb binding to Hp conserved yet its ability to bind to Hp has been debated. *In Chapter 2*, we employed computational biology techniques to predict binding preferences of Mb to Hp, followed by experimental verification of the predictions using native electrospray ionization mass spectrometry (ESI MS). Using the Hb/Hp crystal structure as a template, homology modeling was carried out to evaluate Hp/Mb interaction *in silico*, yielding structural models of two Mb molecules bound to a single Hp monomer ( $Mb_2Hp$ ). Molecular modeling suggested that the Hp/Hb binding interface remains conserved in Mb/Hp complex at the  $\alpha$ -chain binding site. Contrary to that, we found several charged residues of the  $\beta$ -chain involved in electrostatic interactions with Hp correspond to ionic residues with opposite polarity in Mb, suggesting unfavorable electrostatic Hp/Mb interactions at the  $\beta$ -chain binding site. Monomeric Hb  $\alpha$  subunits were isolated and shown for first time by native ESI MS to be capable of binding to Hp in the absence of Hb  $\beta$ -chains forming  $\alpha_2Hp$  complexes. Native ESI MS was also used to monitor Hp/Mb interaction, providing evidence also for the first time the existence of both Mb/Hp and  $Mb_2Hp$  species in solution at physiological pH and ionic strength, although Hp affinity appears to be diminished in Mb compared to Hb  $\alpha$ -chains. This change is rationalized based on the structural model of Mb/Hp complexes. These results present a well-constructed framework for predicting novel or unknown interactions using both computational approaches and native electrospray ionization mass spectrometry (ESI-MS) experiments which is very useful for the development in this field.

The ESI MS results demonstrate the success of our computational approaches, motivating us to model Hb/Hp/CD163 complexes. Both CD163 bound  $\text{Ca}^{2+}$  and specific CD163 acidic residues are known to be essential for binding specific Hp basic residues resulting in Hb/Hp/CD163 complex formation, but the structural details of Hb/Hp/CD163 interactions are unknown. *In Chapter 3*, we therefore constructed experimentally driven molecular models of Hb/Hp/CD163 complexes using molecular docking. Then, to understand the significant role of  $\text{Ca}^{2+}$  in Hp/CD163 interactions and dynamics, all-atom molecular dynamics (MD) simulations were conducted for CD163 models in the presence and absence of  $\text{Ca}^{2+}$ . The molecular models of Hb/Hp/CD163 suggest that Hp basic residues R259 and K269 each interact with a conserved acidic residue cluster (E27, E28, D94) in CD163 domains 2 and 3. A calcium ion is postulated to stabilize this CD163 acidic residue cluster, facilitating Hp recognition. Consistent with this, MD simulations on isolated CD163 domains suggest that a specific  $\text{Ca}^{2+}$  binding site preserves the arrangement of the acidic triad and protein structural stability. Our studies show that by combining molecular modeling, native mass spectrometry, and molecular dynamics we can provide a detailed picture of the structural and dynamic basis of interactions between Hp, globins and/or CD163. These molecular models may also be useful for designing therapeutics that utilizes the Hb/Hp/CD263 endocytosis pathway.

- **Future outlook of Chapter 2.**

Since Hp is a natural occurring molecule, the development of Hp as a therapeutic for patients suffering from Mb toxicity due to myocardial injury would be promising, however, there are various necessary tests or investigations that first need to take place to make this realistic. There is no proof showing that Mb actually interacts with Hp in vivo. A future experiment could be to screen the blood of myocardial patients to investigate whether Mb/Hp complexes exist in the blood. Additionally, binding affinity experiments

between Mb/Hp complexes will also be necessary which could be conducted through isothermal titration calorimetry experiments, which could calculate the binding constants.

- **Future outlook of Chapter 3.**

The goal of chapter to 2 was to use computational data generated of Mb/Hp complexes to provide a testable hypothesis for MS experiments. In Chapter 3, the 4 molecular models generated suggest atomic level pictures of Hb/Hp/CD163 complexes that could be validated through H/D exchange and limited proteolysis experiments. These experiments could test whether protected regions shown in the models are consistent with experimental results and help narrow down the computational results.

## BIBLIOGRAPHY

- (1) Buehler, P. W., Abraham, B., Vallelian, F., Linnemayr, C., Pereira, C. P., Cipollo, J. F., Jia, Y., Mikolajczyk, M., Boretti, F. S., Schoedon, G., Alayash, A. I., and Schaer, D. J. (2009) Haptoglobin preserves the CD163 hemoglobin scavenger pathway by shielding hemoglobin from peroxidative modification, *Blood* 113, 2578-2586.
- (2) Quaye, I. K. (2008) Haptoglobin, inflammation and disease, *Trans R Soc Trop Med Hyg* 102, 735-742.
- (3) Rother, R. P., Bell, L., Hillmen, P., and Gladwin, M. T. (2005) The clinical sequelae of intravascular hemolysis and extracellular plasma hemoglobin: a novel mechanism of human disease, *JAMA* 293, 1653-1662.
- (4) Van Gorp, H., Delputte, P. L., and Nauwynck, H. J. (2010) Scavenger receptor CD163, a Jack-of-all-trades and potential target for cell-directed therapy, *Mol Immunol* 47, 1650-1660.
- (5) Okazaki, T., Yanagisawa, Y., and Nagai, T. (1997) Analysis of the affinity of each haptoglobin polymer for hemoglobin by two-dimensional affinity electrophoresis, *Clin Chim Acta* 258, 137-144.
- (6) Carter, K., and Worwood, M. (2007) Haptoglobin: a review of the major allele frequencies worldwide and their association with diseases, *Int J Lab Hematol* 29, 92-110.
- (7) Bowman, B. H., and Kurosky, A. (1982) Haptoglobin: the evolutionary product of duplication, unequal crossing over, and point mutation, *Adv Hum Genet* 12, 189-261, 453-184.
- (8) Deborah Chiabrando, F. V., Veronica Fiorito and Emanuela Tolosano (2011) Haptoglobin and Hemopexin in Heme Detoxification and Iron Recycling, Acute Phase Proteins - Regulation and Functions of Acute Phase Proteins,, In *Acute Phase Proteins - Regulation and Functions of Acute Phase Proteins* (Veas, F., Ed.), Intech.
- (9) Andersen, C. B., Torvund-Jensen, M., Nielsen, M. J., de Oliveira, C. L., Hersleth, H. P., Andersen, N. H., Pedersen, J. S., Andersen, G. R., and Moestrup, S. K. (2012) Structure of the haptoglobin-haemoglobin complex, *Nature* 489, 456-459.
- (10) Lane-Serff, H., MacGregor, P., Lowe, E. D., Carrington, M., and Higgins, M. K. (2014) Structural basis for ligand and innate immunity factor uptake by the trypanosome haptoglobin-haemoglobin receptor, *Elife* 3, e05553.

- (11) Stodkilde, K., Torvund-Jensen, M., Moestrup, S. K., and Andersen, C. B. (2014) Structural basis for trypanosomal haem acquisition and susceptibility to the host innate immune system, *Nat Commun* 5, 5487.
- (12) Nielsen, M. J., Andersen, C. B., and Moestrup, S. K. (2013) CD163 binding to haptoglobin-hemoglobin complexes involves a dual-point electrostatic receptor-ligand pairing, *J Biol Chem* 288, 18834-18841.
- (13) Sadrzadeh, S. M., and Bozorgmehr, J. (2004) Haptoglobin phenotypes in health and disorders, *Am J Clin Pathol* 121 Suppl, S97-104.
- (14) Eaton, J. W., Brandt, P., Mahoney, J. R., and Lee, J. T., Jr. (1982) Haptoglobin: a natural bacteriostat, *Science* 215, 691-693.
- (15) Lange, V. (1992) [Haptoglobin polymorphism--not only a genetic marker], *Anthropol Anz* 50, 281-302.
- (16) Sadrzadeh, S. M., Graf, E., Panter, S. S., Hallaway, P. E., and Eaton, J. W. (1984) Hemoglobin. A biologic fenton reagent, *J Biol Chem* 259, 14354-14356.
- (17) Vercellotti, G. M., Balla, G., Balla, J., Nath, K., Eaton, J. W., and Jacob, H. S. (1994) Heme and the vasculature: an oxidative hazard that induces antioxidant defenses in the endothelium, *Artif Cells Blood Substit Immobil Biotechnol* 22, 207-213.
- (18) Kurosky, A., Barnett, D. R., Lee, T. H., Touchstone, B., Hay, R. E., Arnott, M. S., Bowman, B. H., and Fitch, W. M. (1980) Covalent structure of human haptoglobin: a serine protease homolog, *Proc Natl Acad Sci U S A* 77, 3388-3392.
- (19) Malchy, B., and Dixon, G. H. (1973) Correction to the amino acid sequence of the chain of human haptoglobin, *Can J Biochem* 51, 321-322.
- (20) Smithies, O., Connell, G. E., and Dixon, G. H. (1962) Chromosomal rearrangements and the evolution of haptoglobin genes, *Nature* 196, 232-236.
- (21) Zhang, S., Shu, H., Luo, K., Kang, X., Zhang, Y., Lu, H., and Liu, Y. (2011) N-linked glycan changes of serum haptoglobin beta chain in liver disease patients, *Mol Biosyst* 7, 1621-1628.
- (22) Polticelli, F., Bocedi, A., Minervini, G., and Ascenzi, P. (2008) Human haptoglobin structure and function--a molecular modelling study, *FEBS J* 275, 5648-5656.

- (23) Fischer-Smith, T., Tedaldi, E. M., and Rappaport, J. (2008) CD163/CD16 coexpression by circulating monocytes/macrophages in HIV: potential biomarkers for HIV infection and AIDS progression, *AIDS Res Hum Retroviruses* 24, 417-421.
- (24) Heydtmann, M. (2009) Macrophages in hepatitis B and hepatitis C virus infections, *J Virol* 83, 2796-2802.
- (25) Bachli, E. B., Schaer, D. J., Walter, R. B., Fehr, J., and Schoedon, G. (2006) Functional expression of the CD163 scavenger receptor on acute myeloid leukemia cells of monocytic lineage, *J Leukoc Biol* 79, 312-318.
- (26) Nguyen, T. T., Schwartz, E. J., West, R. B., Warnke, R. A., Arber, D. A., and Natkunam, Y. (2005) Expression of CD163 (hemoglobin scavenger receptor) in normal tissues, lymphomas, carcinomas, and sarcomas is largely restricted to the monocyte/macrophage lineage, *Am J Surg Pathol* 29, 617-624.
- (27) Schaer, D. J., Buehler, P. W., Alayash, A. I., Belcher, J. D., and Vercellotti, G. M. (2013) Hemolysis and free hemoglobin revisited: exploring hemoglobin and hemin scavengers as a novel class of therapeutic proteins, *Blood* 121, 1276-1284.
- (28) Boretti, F. S., Baek, J. H., Palmer, A. F., Schaer, D. J., and Buehler, P. W. (2014) Modeling hemoglobin and hemoglobin:haptoglobin complex clearance in a non-rodent species-pharmacokinetic and therapeutic implications, *Front Physiol* 5, 385.
- (29) Imaizumi, H., Tsunoda, K., Ichimiya, N., Okamoto, T., and Namiki, A. (1994) Repeated large-dose haptoglobin therapy in an extensively burned patient: case report, *J Emerg Med* 12, 33-37.
- (30) Quimby, K. R., Hambleton, I. R., and Landis, R. C. (2015) Intravenous infusion of haptoglobin for the prevention of adverse clinical outcome in Sickle Cell Disease, *Med Hypotheses*.
- (31) Agrawal, N. J., Helk, B., and Trout, B. L. (2014) A computational tool to predict the evolutionarily conserved protein-protein interaction hot-spot residues from the structure of the unbound protein, *FEBS Lett* 588, 326-333.
- (32) di Luccio, E., and Koehl, P. (2011) A quality metric for homology modeling: the H-factor, *BMC Bioinformatics* 12, 48.
- (33) Humphrey, W., Dalke, A., and Schulten, K. (1996) VMD: visual molecular dynamics, *J Mol Graph* 14, 33-38, 27-38.
- (34) WL, D. (2002) PyMOL molecular graphics system.

- (35) Laskowski, R. A., Rullmann, J. A., MacArthur, M. W., Kaptein, R., and Thornton, J. M. (1996) AQUA and PROCHECK-NMR: programs for checking the quality of protein structures solved by NMR, *J Biomol NMR* 8, 477-486.
- (36) Rai, D. K., and Rieder, E. (2012) Homology modeling and analysis of structure predictions of the bovine rhinitis B virus RNA dependent RNA polymerase (RdRp), *Int J Mol Sci* 13, 8998-9013.
- (37) Cui, X., Li, S. C., Bu, D., Alipanahi, B., and Li, M. (2013) Protein Structure Idealization: How accurately is it possible to model protein structures with dihedral angles?, *Algorithms Mol Biol* 8, 5.
- (38) Wlodawer, A., Minor, W., Dauter, Z., and Jaskolski, M. (2008) Protein crystallography for non-crystallographers, or how to get the best (but not more) from published macromolecular structures, *FEBS J* 275, 1-21.
- (39) Vriend, G. (1990) WHAT IF: a molecular modeling and drug design program, *J Mol Graph* 8, 52-56, 29.
- (40) Ullah, M., Hira, J., Ghosh, T., Ishaque, N., and Absar, N. (2012) A Bioinformatics Approach for Homology Modeling and Binding Site Identification of Triosephosphate Isomerase from Plasmodium falciparum 3D7, *J Young Pharm* 4, 261-266.
- (41) Lensink, M. F., and Wodak, S. J. (2010) Blind predictions of protein interfaces by docking calculations in CAPRI, *Proteins* 78, 3085-3095.
- (42) Halperin, I., Ma, B., Wolfson, H., and Nussinov, R. (2002) Principles of docking: An overview of search algorithms and a guide to scoring functions, *Proteins* 47, 409-443.
- (43) de Vries, S. J., van Dijk, M., and Bonvin, A. M. (2010) The HADDOCK web server for data-driven biomolecular docking, *Nat Protoc* 5, 883-897.
- (44) Adcock, S. A., and McCammon, J. A. (2006) Molecular dynamics: survey of methods for simulating the activity of proteins, *Chem Rev* 106, 1589-1615.
- (45) Jorgensen, W. L., Maxwell, D.S., Tirado-Rives, J. (1996) Development and testing of the OPLS all-atom force field on conformational energetics and properties of organic liquids, *J Am Chem Soc* 118, 11225-11236.
- (46) Scott, W. R. P., Hünenberger, P.H., Tironi, I.G., Mark, A.E., Billeter, S.R., Fennen, J., Torda, A.E., Huber, T., Krüger, P., Van Gunsteren, W.F. (1999) The GROMOS biomolecular simulation program package, *Journal of Physical Chemistry A* 103, 3596-3607.

- (47) Wendy D. Cornell, P. C., Christopher I. Bayly, Ian R. Gould, Kenneth M. Merz, David M. Ferguson, David C. Spellmeyer, Thomas Fox, James W. Caldwell, Peter A. Kollman. (1995) A Second Generation Force Field for the Simulation of Proteins, Nucleic Acids, and Organic Molecules, *J Am Chem Soc* 117, 5179-5197.
- (48) MacKerell Jr., A. D. a., Bashford, D.a, Bellott, M.a, Dunbrack Jr., R.L.a, Evanseck, J.D.a, Field, M.J.a, Fischer, S.a, Gao, J.a, Guo, H.a, Ha, S.a, Joseph-McCarthy, D.a, Kuchnir, L.a, Kuczera, K.a, Lau, F.T.K.a, Mattos, C.a, Michnick, S.a, Ngo, T.a, Nguyen, D.T.a, Prodhom, B.a, Reiher III, W.E.a, Roux, B.a, Schlenkrich, M.a, Smith, J.C.a, Stote, R.a, Straub, J.a, Watanabe, M.a, Wiórkiewicz-Kuczera, J.a, Yin, D.b, Karplus, M.ac (1998) All-atom empirical potential for molecular modeling and dynamics studies of proteins, *Journal of Physical Chemistry B* 102, 3586-3616.
- (49) Karplus, M., and Petsko, G. A. (1990) Molecular dynamics simulations in biology, *Nature* 347, 631-639.
- (50) Karplus, M., and McCammon, J. A. (2002) Molecular dynamics simulations of biomolecules, *Nat Struct Biol* 9, 646-652.
- (51) Heck, A. J. (2008) Native mass spectrometry: a bridge between interactomics and structural biology, *Nat Methods* 5, 927-933.
- (52) Pi, J., and Sael, L. (2013) Mass spectrometry coupled experiments and protein structure modeling methods, *Int J Mol Sci* 14, 20635-20657.
- (53) Abzalimov, R. R., and Kaltashov, I. A. (2010) Electrospray ionization mass spectrometry of highly heterogeneous protein systems: protein ion charge state assignment via incomplete charge reduction, *Anal Chem* 82, 7523-7526.
- (54) Kaltashov, I. A., and Abzalimov, R. R. (2008) Do ionic charges in ESI MS provide useful information on macromolecular structure?, *J Am Soc Mass Spectrom* 19, 1239-1246.
- (55) Leverage, R., Mason, A. B., and Kaltashov, I. A. (2010) Noncanonical interactions between serum transferrin and transferrin receptor evaluated with electrospray ionization mass spectrometry, *Proc Natl Acad Sci U S A* 107, 8123-8128.
- (56) Politis, A., Stengel, F., Hall, Z., Hernandez, H., Leitner, A., Walzthoeni, T., Robinson, C. V., and Aebersold, R. (2014) A mass spectrometry-based hybrid method for structural modeling of protein complexes, *Nat Methods* 11, 403-406.



- (57) Hwang, P. K., and Greer, J. (1980) Interaction between hemoglobin subunits in the hemoglobin . haptoglobin complex, *J Biol Chem* 255, 3038-3041.
- (58) Alayash, A. I., Andersen, C. B., Moestrup, S. K., and Bulow, L. (2013) Haptoglobin: the hemoglobin detoxifier in plasma, *Trends Biotechnol* 31, 2-3.
- (59) Buehler, P. W., D'Agnillo, F., and Schaer, D. J. (2010) Hemoglobin-based oxygen carriers: From mechanisms of toxicity and clearance to rational drug design, *Trends Mol Med* 16, 447-457.
- (60) Schaer, D. J., Vinchi, F., Ingoglia, G., Tolosano, E., and Buehler, P. W. (2014) Haptoglobin, hemopexin, and related defense pathways-basic science, clinical perspectives, and drug development, *Front Physiol* 5, 415.
- (61) Thomsen, J. H., Etzerodt, A., Svendsen, P., and Moestrup, S. K. (2013) The haptoglobin-CD163-heme oxygenase-1 pathway for hemoglobin scavenging, *Oxid Med Cell Longev* 2013, 523652.
- (62) Griffith, W. P., and Kaltashov, I. A. (2003) Highly asymmetric interactions between globin chains during hemoglobin assembly revealed by electrospray ionization mass spectrometry, *Biochemistry* 42, 10024-10033.
- (63) Griffith, W. P. K., Igor A. (2006) Mass Spectrometry in the Study of Hemoglobin: from Covalent Structure to Higher Order Assembly, *Current Organic Chemistry* 10, 535-553.
- (64) Boys, B. L., Kuprowski, M. C., and Konermann, L. (2007) Symmetric behavior of hemoglobin alpha- and beta- subunits during acid-induced denaturation observed by electrospray mass spectrometry, *Biochemistry* 46, 10675-10684.
- (65) Knochel, J. P. (1982) Rhabdomyolysis and myoglobinuria, *Annu Rev Med* 33, 435-443.
- (66) Bosch, X., Poch, E., and Grau, J. M. (2009) Rhabdomyolysis and acute kidney injury, *N Engl J Med* 361, 62-72.
- (67) Reeder, B. J., Sharpe, M. A., Kay, A. D., Kerr, M., Moore, K., and Wilson, M. T. (2002) Toxicity of myoglobin and haemoglobin: oxidative stress in patients with rhabdomyolysis and subarachnoid haemorrhage, *Biochem Soc Trans* 30, 745-748.
- (68) Sakata, S., Yoshioka, N., and Atassi, M. Z. (1986) Human haptoglobin binds to human myoglobin, *Biochim Biophys Acta* 873, 312-315.
- (69) Javid, J., Fischer, D. S., and Spaet, T. H. (1959) Inability of haptoglobin to bind myoglobin, *Blood* 14, 683-687.

- (70) Loo, J. A. (1997) Studying noncovalent protein complexes by electrospray ionization mass spectrometry, *Mass Spectrom Rev* 16, 1-23.
- (71) Sharon, M., and Robinson, C. V. (2007) The role of mass spectrometry in structure elucidation of dynamic protein complexes, *Annu Rev Biochem* 76, 167-193.
- (72) Kaltashov, I. A., Bobst, C. E., and Abzalimov, R. R. (2013) Mass spectrometry-based methods to study protein architecture and dynamics, *Protein Sci* 22, 530-544.
- (73) Muneeruddin, K., Thomas, J. J., Salinas, P. A., and Kaltashov, I. A. (2014) Characterization of small protein aggregates and oligomers using size exclusion chromatography with online detection by native electrospray ionization mass spectrometry, *Anal Chem* 86, 10692-10699.
- (74) Pukala, T. L., Ruotolo, B. T., Zhou, M., Politis, A., Stefanescu, R., Leary, J. A., and Robinson, C. V. (2009) Subunit architecture of multiprotein assemblies determined using restraints from gas-phase measurements, *Structure* 17, 1235-1243.
- (75) Thompson, J. D., Gibson, T. J., and Higgins, D. G. (2002) Multiple sequence alignment using ClustalW and ClustalX, *Curr Protoc Bioinformatics Chapter 2*, Unit 2 3.
- (76) Mount, D. W. (2008) Using BLOSUM in Sequence Alignments, *CSH Protoc 2008*, pdb top39.
- (77) Eswar, N., Webb, B., Marti-Renom, M. A., Madhusudhan, M. S., Eramian, D., Shen, M. Y., Pieper, U., and Sali, A. (2006) Comparative protein structure modeling using Modeller, *Curr Protoc Bioinformatics Chapter 5*, Unit 5 6.
- (78) Pronk, S., Pall, S., Schulz, R., Larsson, P., Bjelkmar, P., Apostolov, R., Shirts, M. R., Smith, J. C., Kasson, P. M., van der Spoel, D., Hess, B., and Lindahl, E. (2013) GROMACS 4.5: a high-throughput and highly parallel open source molecular simulation toolkit, *Bioinformatics* 29, 845-854.
- (79) Stocker, U., and van Gunsteren, W. F. (2000) Molecular dynamics simulation of hen egg white lysozyme: a test of the GROMOS96 force field against nuclear magnetic resonance data, *Proteins* 40, 145-153.
- (80) Vangone, A., Spinelli, R., Scarano, V., Cavallo, L., and Oliva, R. (2011) COCOMAPS: a web application to analyze and visualize contacts at the interface of biomolecular complexes, *Bioinformatics* 27, 2915-2916.
- (81) Kruger, D. M., and Gohlke, H. (2010) DrugScorePPI webserver: fast and accurate in silico alanine scanning for scoring protein-protein interactions, *Nucleic Acids Res* 38, W480-486.

- (82) Nygaard, T. K., Liu, M., McClure, M. J., and Lei, B. (2006) Identification and characterization of the heme-binding proteins SeShp and SeHtsA of *Streptococcus equi* subspecies *equi*, *BMC Microbiol* 6, 82.
- (83) Gasteiger E., H. C., Gattiker A., Duvaud S., Wilkins M.R., Appel R.D., Bairoch A. (2005) Protein Identification and Analysis Tools on the ExPASy Server, In *The Proteomics Protocols Handbook*, Humana Press (Walker, J. M., Ed.), pp 571-607.
- (84) Benkert, P., Schwede, T., and Tosatto, S. C. (2009) QMEANclust: estimation of protein model quality by combining a composite scoring function with structural density information, *BMC Struct Biol* 9, 35.
- (85) Van den Oord, A. H., Wesdorp, J. J., Van Dam, A. F., and Verheij, J. A. (1969) Occurrence and nature of equine and bovine myoglobin dimers, *Eur J Biochem* 10, 140-145.
- (86) Adachi, K., Yang, Y., Lakka, V., Wehrli, S., Reddy, K. S., and Surrey, S. (2003) Significance of beta116 His (G18) at alpha1beta1 contact sites for alphabeta assembly and autoxidation of hemoglobin, *Biochemistry* 42, 10252-10259.
- (87) Li, L., Zhao, B., Cui, Z., Gan, J., Sakharkar, M. K., and Kanguane, P. (2006) Identification of hot spot residues at protein-protein interface, *Bioinformatics* 1, 121-126.
- (88) Gao, Y., Wang, R., and Lai, L. (2004) Structure-based method for analyzing protein-protein interfaces, *J. Mol. Model* 10, 44-54.
- (89) Malinoski, D. J., Slater, M. S., and Mullins, R. J. (2004) Crush injury and rhabdomyolysis, *Crit Care Clin* 20, 171-192.
- (90) Nicolis, S., Pennati, A., Perani, E., Monzani, E., Sanangelantoni, A. M., and Casella, L. (2006) Easy oxidation and nitration of human myoglobin by nitrite and hydrogen peroxide, *Chemistry* 12, 749-757.
- (91) Kristiansen, M., Graversen, J. H., Jacobsen, C., Sonne, O., Hoffman, H. J., Law, S. K., and Moestrup, S. K. (2001) Identification of the haemoglobin scavenger receptor, *Nature* 409, 198-201.
- (92) Nielsen, M. J., Petersen, S. V., Jacobsen, C., Thirup, S., Enghild, J. J., Graversen, J. H., and Moestrup, S. K. (2007) A unique loop extension in the serine protease domain of haptoglobin is essential for CD163 recognition of the haptoglobin-hemoglobin complex, *J Biol Chem* 282, 1072-1079.
- (93) Schaer, D. J., Schaer, C. A., Buehler, P. W., Boykins, R. A., Schoedon, G., Alayash, A. I., and Schaffner, A. (2006) CD163 is the macrophage

scavenger receptor for native and chemically modified hemoglobins in the absence of haptoglobin, *Blood* 107, 373-380.

- (94) Graversen, J. H., and Moestrup, S. K. (2015) Drug Trafficking into Macrophages via the Endocytotic Receptor CD163, *Membranes (Basel)* 5, 228-252.
- (95) Madsen, M., Moller, H. J., Nielsen, M. J., Jacobsen, C., Graversen, J. H., van den Berg, T., and Moestrup, S. K. (2004) Molecular characterization of the haptoglobin.hemoglobin receptor CD163. Ligand binding properties of the scavenger receptor cysteine-rich domain region, *J Biol Chem* 279, 51561-51567.
- (96) McWilliam, H., Li, W., Uludag, M., Squizzato, S., Park, Y. M., Buso, N., Cowley, A. P., and Lopez, R. (2013) Analysis Tool Web Services from the EMBL-EBI, *Nucleic Acids Res* 41, W597-600.
- (97) Eswar, N., Webb, B., Marti-Renom, M. A., Madhusudhan, M. S., Eramian, D., Shen, M. Y., Pieper, U., and Sali, A. (2007) Comparative protein structure modeling using MODELLER, *Curr Protoc Protein Sci Chapter 2*, Unit 2 9.
- (98) Shen, M. Y., and Sali, A. (2006) Statistical potential for assessment and prediction of protein structures, *Protein Sci* 15, 2507-2524.
- (99) Benkert, P., Tosatto, S. C., and Schwede, T. (2009) Global and local model quality estimation at CASP8 using the scoring functions QMEAN and QMEANclust, *Proteins* 77 Suppl 9, 173-180.
- (100) Berendsen, H. J. C. a. P., J. P. M. and van Gunsteren, W. F. and DiNola, A. and Haak, J. R., . (1984) Molecular dynamics with coupling to an external bath, *J Chem Phys* 81, 3684-3690.
- (101) Parrinello, M. a. R., A. (1981) Polymorphic transitions in single crystals: A new molecular dynamics method, *Journal of Applied Physics* 52, 7182-7190.
- (102) Verlet, L. (1967) Computer "Experiments" on Classical Fluids. I. Thermodynamical Properties of Lennard-Jones Molecules, *American Physical Society* 159.
- (103) Hess, B., Bekker, H., Berendsen, H. J. C., Fraaije, J. G. E. M. (1997) LINCS: A linear constraint solver for molecular simulations, *J Comput Chem* 18, 1463-1472.
- (104) Berliner, L. J. (2002) Electron magnetic resonance studies of calcium-binding proteins, *Methods Mol Biol* 173, 195-204.

- (105) McPhalen, C. A., Strynadka, N. C., and James, M. N. (1991) Calcium-binding sites in proteins: a structural perspective, *Adv Protein Chem* 42, 77-144.
- (106) Rigden, D. J., and Galperin, M. Y. (2004) The DxDxDG motif for calcium binding: multiple structural contexts and implications for evolution, *J Mol Biol* 343, 971-984.
- (107) Ahvazi, B., Boeshans, K. M., Idler, W., Baxa, U., and Steinert, P. M. (2003) Roles of calcium ions in the activation and activity of the transglutaminase 3 enzyme, *J Biol Chem* 278, 23834-23841.
- (108) Andersen, C. B., Madsen, M., Storm, T., Moestrup, S. K., and Andersen, G. R. (2010) Structural basis for receptor recognition of vitamin-B(12)-intrinsic factor complexes, *Nature* 464, 445-448.
- (109) Bottomley, M. J., Cirillo, A., Orsatti, L., Ruggeri, L., Fisher, T. S., Santoro, J. C., Cummings, R. T., Cubbon, R. M., Lo Surdo, P., Calzetta, A., Noto, A., Baysarowich, J., Mattu, M., Talamo, F., De Francesco, R., Sparrow, C. P., Sitlani, A., and Carfi, A. (2009) Structural and biochemical characterization of the wild type PCSK9-EGF(AB) complex and natural familial hypercholesterolemia mutants, *J Biol Chem* 284, 1313-1323.
- (110) Yasui, N., Nogi, T., and Takagi, J. (2010) Structural basis for specific recognition of reelin by its receptors, *Structure* 18, 320-331.
- (111) Nielsen, M. J., Petersen, S. V., Jacobsen, C., Oxvig, C., Rees, D., Moller, H. J., and Moestrup, S. K. (2006) Haptoglobin-related protein is a high-affinity hemoglobin-binding plasma protein, *Blood* 108, 2846-2849.